SUBCOMMISSION ON EUROPEAN QUATERNARY STRATIGRAPHY

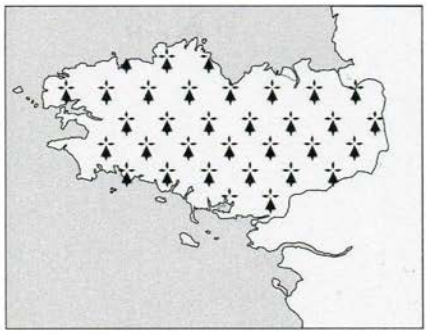

INQUA–
SEQS 2008

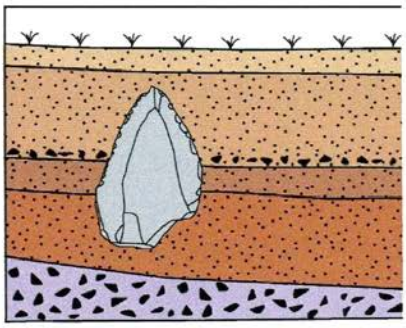

DIFFERENCES AND SIMILARITIES IN QUATERNARY STRATIGRAPHY BETWEEN ATLANTIC AND CONTINENTAL EUROPE

EXCURSION GUIDE BOOK

RENNES – 2008

INTERNATIONAL UNION FOR QUATERNARY RESEARCH
INQUA SUBCOMISSION ON EUROPEAN QUATERNARY STRATIGRAPHY
UNIVERSITY OF RENNES 1, FRANCE
NATIONAL SCIENTIFIC RESEARCH CENTRE
LABORATORY OF ARCHÉOSCIENCES (UMR 6566)

INQUA–SEQS 2008 Conference

22-27 September, 2008, Rennes, France

Differences and similarities in Quaternary Stratigraphy between Atlantic and continental Europe

Excursion Guide Book

Edited by J.-L. Monnier, J.-P. Lefort and G. Danukalova

Rennes – 2008

Excursion Guide Book. INQUA-SEQS, 22-27 September, 2008, Rennes, France. 68 pp.

This Excursion Guide Book has been compiled for the participants to the International INQUA-SEQS Conference held at the University of Rennes I (France) in September 2008 and titled "Differences and similiraities in Quaternary Stratigraphy between Atlantic and Continental Europe".

Guide compiled and edited by J.L. Monnier, J.P. Lefort and G. Danukalova

Scientific excursion 1: Southern Brittany.

Wednesday, 24 September 2008
Leader: Jean-Noël PROUST

Scientific excursion 2: Quaternary of Northern Brittany.

Thursday, 25 September 2008
Leader: Jean-Laurent MONNIER

Scientific excursion 3: Quaternary of Normandy.

Friday, 26 September 2008
Leaders: Dominique CLIQUET and Jean-Pierre LAUTRIDOU

ISBN: in progress

Travaux du Laboratoire d'anthropologie de Rennes № 45

ISSN 0768-3685

ORGANISERS:

University of Rennes 1.
National Scientific Research Centre.
Laboratory of Archéosciences (UMR 6566), University of Rennes 1, France.
INQUA, International Union for Quaternary Research.
INQUA – Subcommission on European Quaternary Stratigraphy (SEQS).
SEQS – EuroMam and EuroMal.

***PROGRAMME COMMITTEE*:**

Dr. Mauro Coltorti, Siena, Italy.
Dr. Guzel Danukalova, Insti tute of Geology USC Russian Academy of Sciences, Ufa, Russia.
Dr. Wim Westerhoff, Netherlands Institute of Applied Geosciences TNO, Utrecht, The Netherlands.

***ORGANISING COMMITTEE*:**

Dr. Jean-Laurent Monnier (UMR 6566), University of Rennes, President of the SEQS meeting.
Dr. Jean-Pierre Lefort (UMR 6566), University of Rennes, Secretary of the SEQS meeting.

***HONORARY COMMITTEE*:**

Cathelineau, President of the University of Rennes 1.
Patrick Saubost, Regional Delegate of CNRS.
Dominique Marguerie, UMR Director, University of Rennes 1.
Luc Aquilina, CAREN Director, University of Rennes 1.
Max Jonin, President of SGMB.

CONFERENCE AND FIELD TRIPS SPONSORED BY:

- DAY ONE -

Scientific excursion to Southern Brittany

Wednesday, 24 September 2008

Leader: Jean-Noël PROUST

Routes which will be followed between RENNES and PENESTIN

NOTICE

The text expected to illustrate the visit to Penestin region is actually missing because the former leader could not attend our meeting. This text is replaced by two published papers. One is in French with captions and abstract in English. The other is fully in English. They give two different views by different authors for this area. Doctor J.N PROUST who kindly accepted to lead this excursion will give all the necessary explanations in English.

Bull. Soc. géol. France, 2001, t. 172, n° 5, pp. 563-572

Le système fluvio-estuarien Pléistocène moyen-supérieur de Pénestin (Morbihan) : une paléo-Loire ?

NICOLAS BRAULT, FRANÇOIS GUILLOCHEAU, JEAN-NOËL PROUST, THIERRY NALPAS, JEAN-PIERRE BRUN, STÉPHANE BONNET et SYLVIE BOURQUIN[1]

Mots clés. – Massif armoricain, Pléistocène, Sédimentologie, Chenaux fluviatiles, Géomorphologie, Relations tectonique/sédimentation.

Résumé. – La formation de Pénestin (Pléistocène moyen-supérieur), dans le Morbihan, est un des rares témoins sédimentaires pléistocènes qui permettent, au travers de l'analyse sédimentologique et stratigraphique des sédiments préservés, de reconstituer l'évolution géomorphologique et tectonique récente du Massif armoricain. La formation de Pénestin, globalement fluviatile, comble un paléochenal érosif sur des micaschistes carbonifères et leurs formes d'altération. Elle comprend trois unités stratigraphiques. L'unité de base (unité I) correspond à un système en tresse proximal, l'unité intermédiaire (unité II) correspond à un système en tresse distal légèrement sinueux très bien préservé qui passe verticalement à un système estuarien interne et l'unité sommitale (unité III) correspond à un système en tresse distal à nombreuses évidences d'érosion / abandon (lacs temporaires). Ces trois unités s'enchaînent suivant deux cycles de chute et de montée du niveau de base (unités I et II, unité III). La formation de Pénestin est déformée pendant son dépôt par des plis en échelon associés à des décrochements du socle sous-jacent, expression d'une compression NNW-SSE.

L'analyse des paléocourants et de la pétrographie des galets de la formation de Pénestin montrent une discontinuité majeure entre les unités II et III qui se traduit par une inversion de la direction d'écoulement des chenaux, de N320 (unités I et II) à N135 et N180 (unité III). L'hypothèse proposée est que les unités I et II correspondraient à une paléo-Loire s'écoulant vers le NW alors que l'unité III serait le témoin d'une paléo-Vilaine s'écoulant vers le SSE.

Middle to Upper Pleistocene fluvio-estuarine system of Pénestin (Morbihan) : paleo-Loire river ?

Key words. – Armorican Massif, Pleistocene, Sedimentology, Fluvial Channels, Sedimentology, Tectonic/sedimentation relations.

Abstract. – In France, the basement domains are incised by large fluvial valley networks. Recent studies [Lefebvre *et al.*, 1994 ; Bonnet, 1998 ; Lautridou *et al.*, 1999 ; Antoine *et al.*, 2000 ; Bonnet *et al.*, 2000] show that these networks were cut during the Pleistocene in response to the uplift of western Europe combined with a fall of the base level [Haq *et al.*, 1987 ; Shackleton, 1987].

The aim of this article is to study one of the rare Pleistocene sedimentary accumulations preserved in the Armorican Massif, the Pénestin fluvial channel system in order to : (1) reconstitute the paleogeomorphological parameters and (2) discuss its relationships with recent tectonic movements.

The Pénestin fluvial system is localized at the top of the cliff of the Mine d'Or beach (west of Pénestin, south of the Vilaine estuary, fig. 1). The paleochannel cuts through the Carboniferous micaschists which pass laterally into Tertiary paleoweathering deposits. The paleochannel is deformed by folds and/or by strike-slipe faults. Three sectors are identified (fig. 2). Sector 1 : a northern undeformed sub-area ; sector 2 : an intermediate slightly folded sub-area ; sector 3 a southern folded and faulted sub-area. Three sedimentological units and seven associated facies are distinguished. Unit I (facies G), containing local matrix-dominated conglomerates characteristic of distal debris flows, suggests a proximal braided river environment, near the transition with alluvial fans [Blair and Mac Pherson, 1994]. Paleocurrent trends are directed toward N320 (fig. 3). Unit II (facies Sg, Sgm, Sf, Fb and T) is mainly dominated by sandy facies and corresponds to a more distal braided river flooded at the top by the sea (occurrence of inner estuarine deposits). The 2D and 3D megaripple cross-bedding structures indicate paleocurrents trending N320 (fig. 3). Unit III (facies G, Sg, Sgm and Fr) with multiple erosive channels is filled by braided river deposits (facies G, Sg and Sgm) or temporary lake sediments (facies Fr). The 2D and 3D megaripple cross-bedding structures indicate paleocurrents oriented N135 or N180 (fig. 3). Stratigraphically, these three units record two major base level cycles (fig. 6), in the sense of Wheeler [1958]. The first base level fall corresponds to the incision of the paleochannel. Unit I is amalgamated and was deposited during the beginning of the rise, while unit II corresponds to the maximal facies preservation during the maximum rate of rise. The erosion of unit II by unit III corresponds to a moderate base level fall followed by a small rise (little preservation of unit III).

The basement, the weathering deposits and the Quaternary sedimentary units are folded and faulted by N050 to N070 strike-slip faults (fig. 2). Two stages of deformation can be characterized. The first stage, taking place before the incision of the paleochannel, corresponds to a southward tilting of the weathering profile. The second stage took place during the paleochannel infilling, producing thickness variations of the bedsets within unit II. The amount of deforma-

[1] Géosciences Rennes, UMR 6118 du CNRS, Campus de Beaulieu, 35042 Rennes cedex, France.
Manuscrit déposé le 9 octobre 2000 ; accepté après révision le 3 mai 2001.

tion increased during deposition of unit III and is expressed by N050 to N070 strike-slip faults capped by unit III or by a topmost erosive surface. Fault orientation indicates a NNW-SSE compression (fig. 5) consistent with the stress field in northwestern Europe [Muller *et al.*, 1992 ; Zoback, 1992].

Paleocurrent directions in units I and II seem to indicate a southerly drainage basin. Today, the Vilaine river flows southward. The units I and II do not represent a paleo-Vilaine river, but since unit III shows paleocurrents similar to those of the present Vilaine river and contains red schists in its basin. It could represent a paleo-Vilaine river. Units I and II might represent a paleo-Loire river, the present Loire river following a curve as it passes over the South Armorican shear zone which reorientates it toward the N320 (fig. 7). Tourenq and Pomerol [1995] show that the Loire river was captured many times ago by the Seine river during the Pleistocene. In this way, when the paleo-Loire river was captured, the paleo-Vilaine river deposited unit III.

The Pénestin palaeochannel resulted from the fluviatile incision/filling of a braided river, which was temporarily overlain by estuarine deposits. The rivers filling this palaeochannel first flowed out to the north (flow of a paleo-Loire river : units I and II), and then to the south (flow of a paleo-Vilaine river : unit III).

The deformation is attributed to a N110 fault, to a set of N050 and N070 faults and to N050 folds.

INTRODUCTION

Les domaines de socle du territoire français sont incisés par de nombreux réseaux de vallées fluviatiles. Différentes études [Lefebvre *et al.*, 1994 ; Bonnet, 1998 ; Lautridou *et al.*, 1999 ; Antoine *et al.*, 2000 ; Bonnet *et al.*, 2000] tendent à montrer le caractère récent, Pléistocène, de cette incision, en réponse à une surrection de l'ouest européen qui se surimpose à la baisse généralisée du niveau de base suite au développement des glaciations quaternaires [Haq *et al.*, 1987 ; Shackleton, 1987].

La morphologie du Massif armoricain résulte de l'incision de surfaces d'aplanissement résiduelles par deux générations de réseaux hydrographiques : (1) un réseau miopliocène, avec des épandages de vastes cônes alluviaux en tresse passant à des réseaux de chenaux en tresse à faiblement sinueux épisodiquement ennoyés par la mer [Guillocheau *et al.*, 1998] et (2) un réseau initié au Pléistocène inférieur à moyen [Bonnet, 1998 ; Bonnet *et al.*, 2000].

Notre propos est d'étudier un des rares témoins sédimentaires du réseau pléistocène connu dans le Massif armoricain, le système fluviatile de Pénestin. L'objectif est double et s'attache à (1) cerner les paramètres paléogéomorphologiques qui ont participé à la mise en place de ce système fluviatile, et (2) discuter de l'importance des mouvements tectoniques récents dans sa préservation et de ses relations avec le réseau hydrographique actuel.

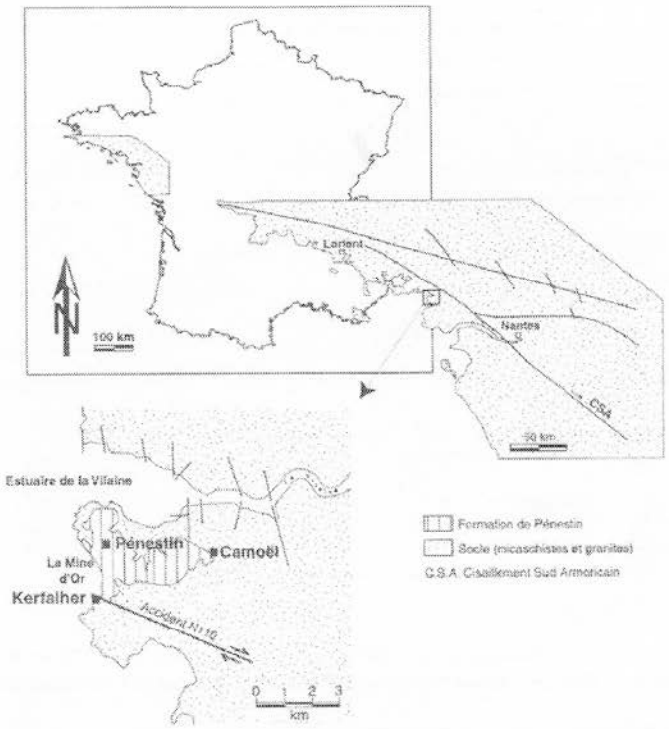

FIG. 1. – Cadre géologique de la région de Pénestin (modifié d'après la carte géologique au 1/50 000e n° 449).
FIG. 1. – *Geological framework of the studied area (modified after 1:50 000 geological map n° 449).*

CONTEXTE GÉOLOGIQUE ET TRAVAUX ANTÉRIEURS

Le système sédimentaire étudié se situe au sud de l'actuel estuaire de la Vilaine (Morbihan), immédiatement à l'ouest de Pénestin, dans les falaises de la plage de la Mine d'Or (fig. 1). Il est limité au nord par un « onlap » des sédiments sur le socle (fig. 2), et au sud par un décrochement majeur dextre de direction N110 (fig. 1).

Les sédiments reposent sur des micaschistes à muscovite, chlorite, albite et grenat, appartenant aux micaschistes de la Vilaine, une des trois unités métamorphiques de la Bretagne méridionale affectées par l'extension du Carbonifère de la chaîne hercynienne [Gapais *et al.*, 1993].

Ces sédiments ont d'abord été interprétés comme des témoins d'un paléo-estuaire de la Vilaine [Guilcher, 1948], sans précision d'âge. Durand et Milon [1955] les comparent aux sables rouges pliocènes d'origine marine de Kerfalher et de Quiberon et envisagent des phénomènes de solifluxion pour expliquer leur déformation. Rivière *et al.* [1963] soutiennent l'origine marine des dépôts mais attribuent en revanche les déformations à des pingos périglaciaires d'âge würmien. Van Vliet-Lanoë *et al.* [1997] rattachent ces mêmes sédiments à un complexe fluviatile et estuarien déposé au Pléistocène moyen, entre 600 000 ans B.P. à la base de la coupe et 300 000 ans B.P. au sommet (âges obtenus par résonance paramagnétique électronique ou R.P.E.) en précisant qu'ils auraient été déformés par des processus hydroplastiques de charge induits par des séismes en période d'englaciation.

Le milieu de dépôt de ces sédiments et le mode de déformation demeurent aujourd'hui encore sujets à discussions. En revanche, l'âge pléistocène proposé par Van

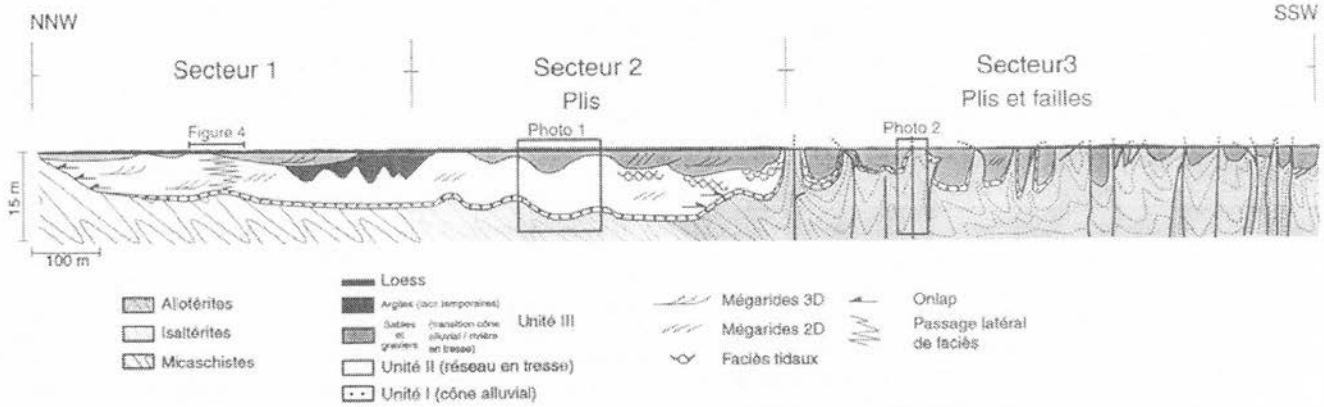

FIG. 2. – Coupe simplifiée de la falaise de la plage de la Mine d'Or montrant la géométrie des trois unités lithologiques et les déformations associées (failles décrochantes, plis et basculement du profil d'altération vers le sud).
FIG. 2. – *Simplified cross-section of the cliff of the « la Mine d'Or » showing the geometry of the three lithological units and the associated deformations (faults, folds and tilting of the weathering profil southward).*

Vliet-Lanoë *et al.* [1997] semble quant à lui confirmé par la présence de galets striés d'origine glaciaire trouvés dans un conglomérat à la base du comblement et qui pourraient être l'expression de l'une des glaciations quaternaires.

DESCRIPTION DE LA COUPE DE PÉNESTIN

La formation de Pénestin, visible sur une longueur d'environ 1800 mètres, présente une hauteur maximale d'affleurement de 8 mètres (fig. 2). Les sédiments reposent sur le substratum par l'intermédiaire d'une surface d'érosion correspondant à un paléochenal à fond plat, rempli en « onlap » sur les bordures. Le substratum est, du nord au sud, constitué de micaschistes sains à chlorite et albite qui passent latéralement vers le sud à leurs produits d'altération avec des isaltérites puis des allotérites riches en kaolinite et en quartz résiduel. Les isaltérites et les allotérites à kaolinite [Delvigne, 1998] proviennent en Bretagne des climats hydrolysants chauds et humides à saisons contrastées de la fin du Crétacé et du début du Tertiaire qui ont conduit au développement de grands profils d'altération météorique de type latéritique avec de grandes épaisseurs de kaolinite [Estéoule-Choux, 1967 ; Estéoule-Choux *et al.*, 1969 ; Thomas, 1999].

La formation de Pénestin est en partie déformée par des plis et/ou des failles qui permettent une subdivision en trois secteurs : (1) au nord, au niveau du socle sain, un secteur non déformé, (2) plus au sud, au niveau des isaltérites, un secteur affecté par des plis (photo 1) dont la longueur d'onde est d'environ 100 mètres et l'amplitude moyenne de 3 mètres et (3) au sud, au niveau des allotérites, un secteur caractérisé par des plis faillés (photo 2) dont la longueur d'onde est proche de 50 mètres et l'amplitude de 6 mètres. A l'extrême sud de la coupe, un décrochement N110 dextre marqué par des stries et des placages de quartz, parallèle au cisaillement sud armoricain, décale le tracé de la côte et limite les dépôts sédimentaires (fig. 1) pour ne laisser apparaître que le socle sain.

La coupe de Pénestin se subdivise en trois unités lithostratigraphiques (fig. 2) : (1) une unité basale conglomératique (unité I) datée à 600 000 ans B.P. [Van Vliet Lanoë *et al.*, 1997], (2) une unité médiane, passant de sables à gra-

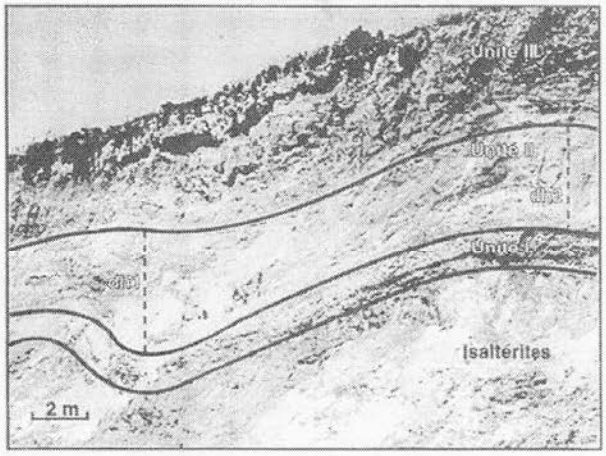

PHOTO 1. – Evidences de déformations syn-sédimentaires : variation d'épaisseur de l'unité II le long des plis (dh1 > dh2 : épaississement au cœur des synclinaux dans l'unité II).
PHOTO 1. – *Syn-sedimentary deformation evidences : thickness variation of unit II along the folds (dh1 > dh2 : thickening in the central part of synclines in the unit II).*

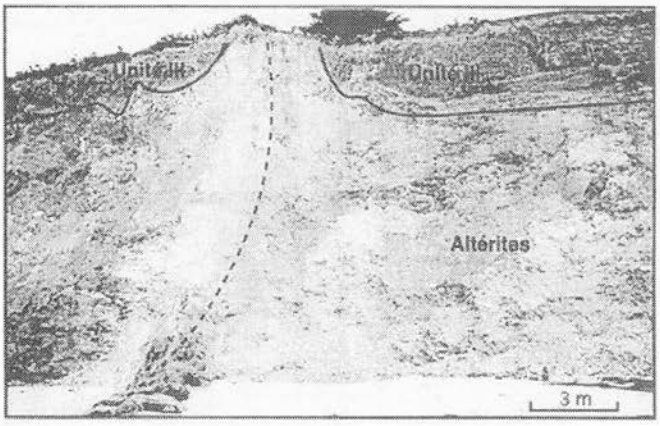

PHOTO 2. – En pointillés, faille recoupant le socle, les altérites et l'unité III.
PHOTO 2. – *Dotted lines, fault crossing the basement, the weathering rocks and unit III.*

viers au nord à des sables vers le sud (unité II) et (3) une unité sommitale érosive sur les unités I et II, argilo-silteuse ou sableuse à graviers et galets (unité III) datée à 300 000 ans B.P. [Van Vliet Lanoë *et al.*, 1997]. Ces unités présentent des épaisseurs variables, l'unité I possédant une épaisseur maximale de deux mètres, l'unité II de sept mètres et l'unité III de six mètres. Cette troisième unité est caractérisée par de nombreuses surfaces d'érosion correspondant à de petits chenaux dont l'extension latérale maximale est de 150 mètres. L'unité III tronque vers le sud (secteur 3) les unités II puis I pour directement reposer sur les allotérites (fig. 2). Les sables, en partie déformés, et le socle sont tronqués par une surface d'érosion horizontale (aplanissement) dont l'origine reste incertaine. Cette surface est recouverte par environ 60 cm de loess, probablement déposés au cours du dernier maximum glaciaire.

SÉDIMENTOLOGIE DE FACIÈS ET ARCHITECTURE SÉDIMENTAIRE

Lithofaciès et milieux de dépôts

Sept faciès élémentaires ont été identifiés (tabl. I). Ils sont essentiellement composés de sables mal classés, de galets de quartz et de quartzite, et épisodiquement de galets de granite ou de schistes rouges présents dans quelques niveaux conglomératiques. Les structures sédimentaires les plus fréquentes sont des mégarides de courant 2D et 3D, voire intermédiaires 2D-3D, des lamines planes subhorizontales et plus rarement des rides de courant. Les traces fossiles sont rares et limitées à quelques terriers horizontaux oligospécifiques.

L'absence des rides de vague et des HCS (« Hummocky Cross Stratification ») caractéristiques d'écoulements oscillatoires et unidirectionnels [Harms *et al.*, 1975 ; Dott et Bourgeois, 1982 ; Allen, 1985 ; Nøttvedt et Kreisa, 1987 ; Guillocheau et Hoffert, 1988], le caractère grossier et mal classé des sédiments à structures caractéristiques d'écoulement unidirectionnel, l'absence de macrofossiles, le caractère localisé et oligospécifique des traces fossiles limitées à quelques terriers horizontaux, indiquent un environnement principalement continental.

Unité I

L'unité I (fig. 2) est essentiellement formée par le faciès G, constitué de conglomérats à blocs, tantôt à matrice dominante, tantôt à mégarides frustres et à galets imbriqués selon le petit axe (tabl. I). Des niveaux de sables fins à litages obliques de courant, pouvant atteindre 50 cm d'épaisseur, sont intercalés entre les niveaux conglomératiques (tabl. I).

Le caractère localement dominant de la matrice, l'absence de granoclassement et la rareté des stratifications indiquent qu'il s'agit en partie d'écoulements de débris [Harms *et al.*, 1975 ; Miall, 1978]. Les litages de rides de courant exprimés dans les sables peuvent être interprétés, dans ce contexte conglomératique, comme des dépôts de crue en traction au toit des écoulements de débris à proximité d'un cône alluvial [Rust, 1978 ; Blair et Mac Pherson, 1994].

Les mesures de paléocourants, effectuées sur l'imbrication des galets, indiquent un écoulement prédominant vers le N315 (fig. 3).

Unité II

L'unité II (fig. 2) est formée des faciès Sg, Sgm, Sf, Fb et T. Le faciès Sg est localisé à l'extrémité nord du paléochenal où il repose en « onlap » sur les bordures. Il passe latéralement aux faciès Sgm et Sf (fig. 4) qui évoluent verticalement vers les faciès T et Fb. Les faciès Sg, Sgm et Sf sont constitués de sables grossiers (faciès Sg et Sgm) et de sables fins (faciès Sf) mal classés (tabl. I). Ces faciès présen-

TABL. I. – Faciès sédimentaires élémentaires : principales caractéristiques et interprétation.
TABLE I. – *Elementary sedimentary facies : principal characteristics and interpretation.*

Faciès	Description	Niveau stratigraphique	Hydrodynamisme - Milieu de sédimentation
G	Conglomérats à blocs et galets anguleux à subanguleux, hétérométriques (2 à 70 cm), localement à matrice dominante (sables grossiers) présentant parfois des évidences d'imbrications de galets et de litages obliques frustres de mégarides de courant Présence d'intercalations de 8 m de long et de 50 cm de haut de sables fins à rides de courant Epaisseur : 0,2 - 2,8 m	Unités I et III	Coulées de débris de faible densité dans l'unité I et épandages diffus dans l'unité III
Sg	Sables grossiers à graviers anguleux à subanguleux, mal classés à litages obliques de mégarides de courant 2D et 3D (parfois 2D-3D) Epaisseur : 0,2 - 2 m	Unités II et III	Ecoulements unidirectionnels dans le régime hydrodynamique inférieur Chenaux secondaires et barres losangiques de réseaux en tresse
Sgm	Sables moyens à grossiers, mal classés, à litages obliques de mégarides de courant 2D et 3D, parfois soulignés par des graviers et/ou des galets d'argile Epaisseur : 10 - 60 cm	Unités II et III	Ecoulements unidirectionnels dans le régime hydrodynamique inférieur Barres sableuses de réseaux en tresse évoluant vers le faiblement sinueux
Sf	Sables fins bien classés, à lamines planes subhorizontales ou à litages obliques de mégarides de courant 2D et 3D en traction ou chevauchantes ou à rides de courant en traction ou chevauchantes, ces litages étant parfois soulignés parfois sables grossiers et des galets d'argile Epaisseur : 20 - 60 cm	Unité II	Ecoulements unidirectionnels dans le régime hydrodynamique inférieur Barres sableuses de réseaux en tresse évoluant vers le faiblement sinueux
T	Alternances de strates de silts argileux et de sables silteux de 3 cm d'épaisseur moyenne Les strates de sables silteux possèdent des litages de rides de courant présentant des évidences d'écoulements de sens opposés L'épaisseur des strates varie verticalement d'une manière cyclique, l'épaisseur maximale étant de 6 cm Epaisseur moyenne : 80 cm	Unité II	Ecoulements unidirectionnels de sens opposé caractéristiques de courants de marées (cycles journaliers), les variations d'épaisseur des strates enregistrent les cycles lunaires Milieu estuarien interne
Fb	Argilites parfois silteuses, bioturbées horizontalement (*Planolites* ?) Epaisseur : 15 - 60 cm	Unité II	Toujours associé au faciès T Milieu estuarien interne
Fr	Argilites rouges à ocres, riches en silts, à traces de racines Surmonté parfois un niveau de galets de petites tailles Epaisseur : 0,2 - 2,4 m	Unité III	Lacs temporaires

tent des litages obliques de mégarides 2D (faciès Sg, Sgm et Sf), de mégarides 3D (faciès Sg, Sgm et Sf), voire de mégarides 2D-3D (faciès Sg), et quelques rides de courant en traction ou chevauchantes (faciès Sf). Le faciès T (tabl. I) est constitué de sables silteux à litages de rides de courants bi-directionnels parfois à doubles drapages argileux. Il présente des variations latérales régulières d'épaisseur des faisceaux de lamines et un mode de dépôt en accrétion verticale [Tessier, 1990]. Le faciès Fb est essentiellement constitué d'argilites bioturbées à terriers oligospécifiques horizontaux (tabl. I). Quand ce faciès est présent, il est toujours associé au faciès T.

La granulométrie grossière (des sables aux galets), les mégarides et les rides de courants unidirectionnels des faciès G, Sg, Sgm et Sf indiquent un transport en traction sur le fond du chenal [Germanoski et Schumm, 1993 ; Collinson, 1996 ; Todd 1996]. Ce type de transport est propre aux rivières en tresse ou aux rivières faiblement sinueuses [Miall, 1977 ; Cant, 1978 ; Cant et Walker, 1978 ; Schumm, 1981 ; Orton et Reading, 1993]. Le caractère purement tractif des faciès Sg, Sgm et Sf et les structures sédimentaires dominées par des mégarides 2D et 3D permettent de rattacher le faciès Sg à des barres sableuses de chenaux secondaires, et les faciès Sgm et Sf à des barres losangiques sableuses situées entre les chenaux secondaires [Miall, 1985 ; Miall, 1996]. L'absence de coulée de débris, la présence de chenaux secondaires, l'importance volumétrique des barres sableuses et l'association de mégarides 2D et 3D [Miall, 1977 ; Cant et Walker, 1978] montrent qu'il s'agit d'un réseau en tresse. La localisation préférentielle des chenaux secondaires au nord, et des faciès de barres sableuses au sud, suggère l'existence d'une légère sinuosité à grand rayon de courbure dans ce réseau en tresse [Miall, 1985].

L'association des doubles drapages argileux, des variations latérales d'épaisseur des faisceaux de lamines, des rides de courants bi-directionnels et du mode de dépôt en accrétion verticale du faciès T indique un environnement estuarien interne. Les doubles drapages argileux du faciès T sont interprétés comme les étales de haute et de basse mer [Visser, 1980] tandis que les variations latérales d'épaisseur des faisceaux de lamines sont l'expression des cycles lunaires [Allen et Homewood, 1984]. Ces critères s'expriment dans un milieu à faible diversité faunistique, marqué par les bioturbations rares et oligospécifiques du faciès Fb.

Les mesures de paléocourants, effectuées sur des mégarides 2D et 3D (galets dans les obliques) et sur des rides indiquent un écoulement globalement vers le N315 (fig. 3) avec un écoulement prédominant des rides vers le N210 in-

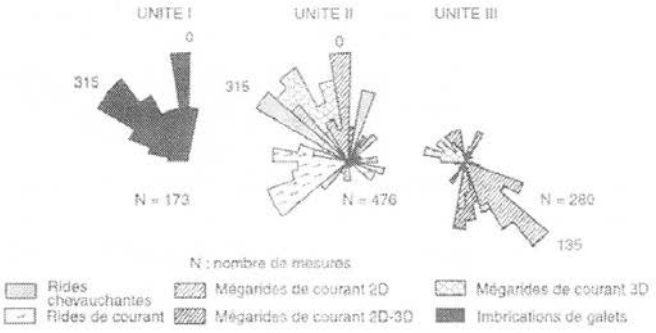

FIG. 3. – Mesures des paléocourants par unité lithologique et par type de structures sédimentaires.
FIG. 3. – *Representation of paleocurrent directions by lithological unit and by sedimentary structures.*

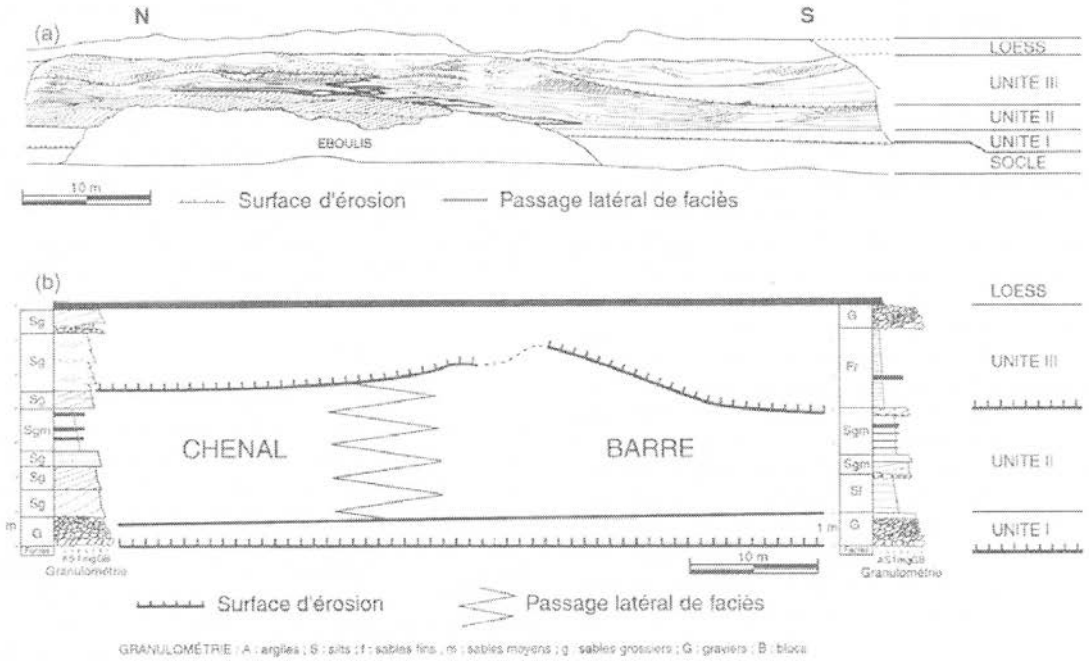

FIG. 4. – Passage latéral entre chenaux secondaires et barres losangiques du système de rivières en tresse de l'unité II : (a) coupe de la falaise, (b) interprétation à partir de deux logs. Le faciès G disparaît au profit des faciès Sgm et Sf.
FIG. 4. – *Lateral variation between secondary channels and losangic bars of the unit II braided river system : (a) cliff section, (b) interpretation from two logs. Facies G disappears laterally and passes to facies Sgm and Sf.*

terprété comme des figures de vidange des barres vers les chenaux secondaires.

Unité III

L'unité III (fig. 2) est composée des faciès G, Sg, Sgm et Fr. Les faciès G, Sg et Sgm (tabl. I) sont constitués de conglomérats à blocs (faciès G) et de sables grossiers (faciès Sgm et Sg) à graviers et à galets de schistes rouges (faciès Sg). Les structures sédimentaires sont représentées par des litages obliques de mégarides 2D et de mégarides 3D (faciès Sg et Sgm), voire à mégarides 2D-3D (faciès Sg). Le faciès Fr (tabl. I) est formé d'argilites rouges, riches en silts, à traces de racines.

L'unité III se caractérise par la présence de nombreuses surfaces d'érosion se recoupant les unes les autres et qui, de part leur morphologie concave, sont interprétées comme des chenaux. Ces chenaux sont comblés soit par l'association des faciès G, Sg et Sgm, soit par le faciès Fr.

Les structures sédimentaires exclusivement constituées de litages obliques de mégarides 2D et 3D et le caractère purement tractif des faciès Sg et Sgm permettent de rattacher ces faciès à des barres sableuses losangiques de chenaux secondaires [Miall, 1985 ; Miall, 1996]. La granulométrie grossière, le manque de granoclassement, le caractère localement dominant de la matrice et les quelques stratifications permettent de rattacher en partie le faciès G à des coulées de débris [Harms *et al.*, 1975 ; Miall, 1978]. L'association des faciès sableux à mégarides 2D et 3D avec des coulées de débris pourrait traduire un domaine de transition entre un cône alluvial dans lequel les écoulements de débris sont fréquents et un réseau en tresse dominé par les processus tractifs [Blair et Mac Pherson, 1994]. Le faciès Fr, qui comble une partie des chenaux au sommet de l'unité III, constitué d'argiles à racines, pourrait correspondre au remplissage de chenaux abandonnés à la faveur de lacs temporaires.

Les mesures de paléocourants, effectuées sur des mégarides 2D, 3D, et 2D-3D, indiquent un écoulement vers le N135 et plus épisodiquement vers le N180 (fig. 3). Les paléocourants dirigés vers le NW et vers le NE sont interprétés comme des courants de retour provoqués par des invaginations des berges du chenal [Rubin *et al.*, 1990].

La formation de Pénestin peut être interprétée comme un paléochenal érosif comblé par des dépôts essentiellement fluviatiles évoluant verticalement vers un estuaire interne.

Structures de déformation des sédiments

La formation de Pénestin est affectée par une déformation qui comprend des plis d'axe N050, avec dans le cœur des synclinaux une augmentation de l'épaisseur des faisceaux de mégarides de l'unité II (photo 1), et des failles décro-chevauchantes senestres de direction N050 à N070 (photo 2) qui recoupent le socle, les altérites et le corps sableux. Les failles sont soit scellées par l'unité III, soit scellées par la surface d'érosion sommitale. La déformation s'intensifie vers le sud, à l'approche d'un accident dextre de direction N110 (fig. 5), parallèle au cisaillement sud armoricain (fig. 1). L'évolution latérale de l'intensité de la déformation permet, comme nous l'avons déjà vu, d'individualiser du nord au sud trois secteurs (fig. 2 ; fig. 5) :

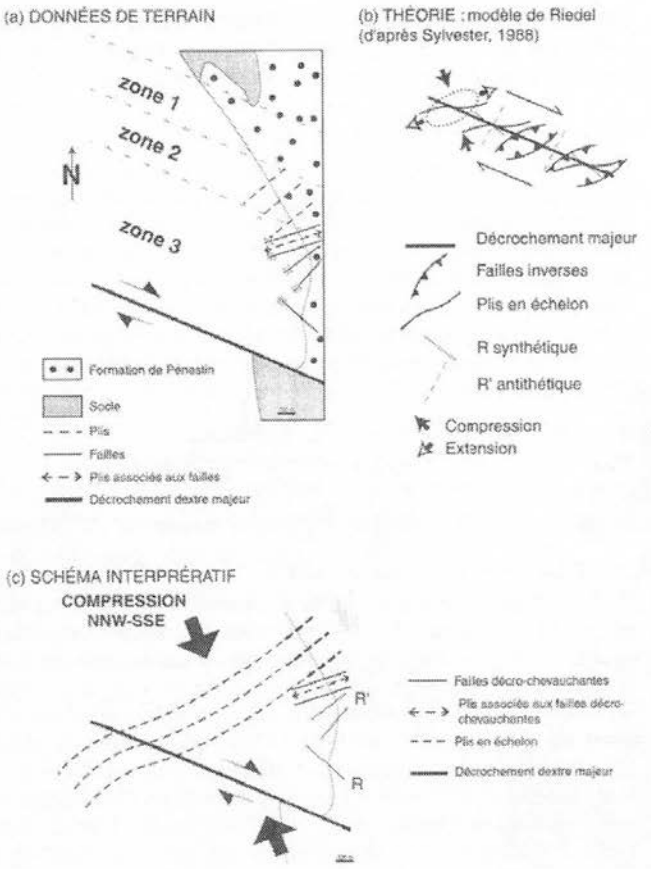

FIG. 5. – Les failles et les plis syn-sédimentaires de la formation de Pénestin : (a) carte simplifiée, (b) comparaison avec le modèle de Sylvester [1988] et (c) compatibilité avec une direction de raccourcissement NNW-SSE.

FIG. 5. – *Syn-sedimentary faults and folds of the Pénestin Formation : (a) simplified map, (b) comparison with the Sylvester's models [1988] and (c) compatibility with a NNW-SSE shortening direction.*

– un secteur nord sur socle non altéré non déformé (secteur 1, fig. 2) ;

– un secteur intermédiaire sur isaltérites déformé par des plis de direction N050 (secteur 2, fig. 2) dont la longueur d'onde est de 100 mètres et l'amplitude de 3 mètres ;

– un secteur sud sur allotérites, proche du décrochement dextre N110, déformé par des failles décro-chevauchantes de direction N050 et N070 qui traversent les micaschistes, les altérites puis partiellement ou totalement les sables pour donner des plis faillés (secteur 3, fig. 2) dont la longueur d'onde est de 50 mètres et l'amplitude de 6 mètres. Les anticlinaux sont systématiquement associés à des failles dans le socle sous-jacent. En passant du secteur 2 au secteur 3, l'amplification de l'amplitude des plis vers le sud est liée au rapprochement de l'accident dextre N110.

L'analyse des relations entre la géométrie de la formation sédimentaire, de la structure du socle et des structures tectoniques ont permis d'envisager deux étapes de déformation.

La première étape est marquée par la discordance du corps sableux à la fois sur le socle, sur les isaltérites et sur les allotérites. Cette disposition traduit un basculement d'un profil d'altération qui comprend verticalement et de

bas en haut, la roche saine, les isaltérites et les allotérites [Delvigne, 1998]. En effet, le développement des latérites requiert une topographie très peu pentée avec (1) des pentes faibles qui favorisent l'infiltration de l'eau et qui empêchent l'érosion du profil par ruissellement et (2) une altitude suffisante des reliefs par rapport au niveau de base pour permettre à l'eau de s'infiltrer [Wyns et Guillocheau, 1999]. A l'extrême sud, l'accident dextre N110 décale le socle verticalement avec, en relatif, un compartiment nord abaissé et un compartiment sud soulevé, ce qui est suggéré par la présence de socle sain et l'absence d'altérite au sud. Le jeu vertical sur l'accident N110 est vraisemblablement à l'origine du léger basculement vers le sud du profil d'altération et à l'origine de la discordance observée entre le corps sableux et le substratum. Ce basculement constitue la première étape de déformation, antérieure au comblement de la paléovallée. Les altérites de Pénestin ne sont pas datées. Cependant, l'essentiel des profils d'altération latéritique semble s'être formé en Bretagne de l'Yprésien supérieur au Lutétien [Estéoule-Choux, 1983]. Le basculement du profil d'altération n'a pu avoir lieu qu'entre l'Eocène moyen et le Quaternaire.

La deuxième étape, contemporaine du remplissage de la paléovallée, se traduit par (1) une variation d'épaisseur de l'unité II (photo 1) marquée par un épaississement des faisceaux de mégarides de l'unité II dans le cœur des synclinaux et (2) par l'apparition de failles pendant le dépôt de l'unité III qui sont pour certaines directement scellées par cette même unité, les autres étant scellées par la surface d'aplanissement sommitale.

L'augmentation d'épaisseur de l'unité II dans le cœur des synclinaux et les failles scellées par l'unité III témoignent d'une activité tectonique syn-sédimentaire d'âge quaternaire. L'augmentation de l'amplitude et la diminution de la longueur d'onde des plis affectant la formation de Pénestin, vers le décrochement N110 suggèrent un fonctionnement synchrone.

De plus, la disposition cartographique des failles décrochantes dextres de direction N110, des failles décrochantes senestres de direction N050 et N070 et des plis N050 sont compatibles avec un seul événement de déformation. Les failles correspondent à des Riedel R' (fig. 5) et/ou à la réactivation de failles de socle en décrochements conjugués associés au décrochement dextre N110. Les plis associés à ces décrochements conjugués accommodent une partie du raccourcissement dans la zone de décrochement (fig. 5). L'organisation cartographique de ces structures suggère une déformation transpressive avec une direction de compression NNW-SSE (fig. 5). Cette direction de raccourcissement NNW-SSE est en accord avec le champ de contrainte actuel en Europe nord-occidentale, de direction NW-SE, et dont la contrainte maximale est proche de l'horizontale [Muller *et al.*, 1992 ; Zoback, 1992].

Chronologiquement, deux hypothèses peuvent être envisagées : (1) le basculement se fait juste après la formation des altérites (Yprésien ou Lutétien), ou durant une des deux grandes étapes de déformation tertiaire décrites dans le Massif armoricain avec la distension est-ouest oligocène et la compression mio-pliocène [Thomas, 1999], ce qui implique un hiatus temporel important entre les deux étapes de déformation, ou (2) le basculement des altérites se produit juste avant le creusement du paléochenal, ce qui suggère un continuum de déformation entre les deux étapes, en accord avec les observations faites sur la compatibilité des structures tectoniques des secteurs 2 et 3 et du décrochement N110. C'est donc cette seconde hypothèse qui est retenue.

Le dépôt de la formation pléistocène de Pénestin est donc contemporain d'un régime compressif NNW-SSE qui s'exprime par des plis et des failles syn-sédimentaires qui pourraient être à l'origine de la préservation remarquable de l'unité II. Les déformations observées sur la plage de la Mine d'Or ont une origine purement tectonique et s'opposent aux déformations de type pingos proposées par Rivière *et al.* [1963] et aux processus hydroplastiques de charge induits par des séismes proposés par Van Vliet-Lanoë *et al.* [1997].

Modalités de préservation des dépôts

Un paysage sédimentaire peut être préservé sous trois états stratigraphiques différents [Allen et Posamentier, 1993], en sédimentation, en transit ou en érosion. En domaine continental, la préservation d'un milieu sédimentaire sous l'un de ces trois aspects est fonction des variations du niveau de base. Pour Wheeler [1958], le niveau de base correspond à une surface équipotentielle recoupant la topographie (profil longitudinal) et le long duquel le bilan érosion/sédimentation est nul (transit pur). C'est cette définition que nous retiendrons. Une montée du niveau de base se traduit par une préservation (sédimentation) des systèmes sédimentaires, une chute par une érosion de ces mêmes systèmes [Proust, 1990 ; Cross *et al.*, 1993 ; Proust, 1995].

La préservation peut être mesurée par la hauteur fossilisée d'un corps sédimentaire significatif du milieu, comme ici un chenal secondaire ou encore une barre sableuse. La principale difficulté est de séparer ce qui résulte d'un processus d'échelle locale, dit autocyclique (crues, avulsions), d'un processus d'échelle régionale, dit allocyclique. En conséquence, les mesures ont été effectuées à l'échelle de la falaise sur une section 2D et non sur une seule coupe 1D. La coupe 1D présentée (fig. 6) est la somme de mesures effectuées sur une trentaine de coupes 1D sur l'affleurement et qui présentent toutes le même type de variation verticale de préservation.

Deux cycles majeurs de variations du niveau de base peuvent être définis (fig. 6). La chute principale du niveau de base est à l'origine de l'incision du paléochenal dans le socle et les altérites. L'unité I, d'épaisseur réduite, marque le passage d'un état en transit à une faible préservation, donc le début d'une remontée. L'unité II, la plus épaisse et donc la mieux préservée, enregistre la remontée avec un ennoyage maximal marqué par les faciès d'estuaire interne. L'unité III, érosive sur l'unité II, débute par une nouvelle chute du niveau de base (base du deuxième cycle) suivie d'une légère remontée (préservation de l'unité III). Cette dernière présente plusieurs phases d'érosion et de remplissage qui, dans l'état actuel de nos connaissances, peuvent être soit autocycliques soit allocycliques et traduire les variations climatiques du Pléistocène moyen à supérieur.

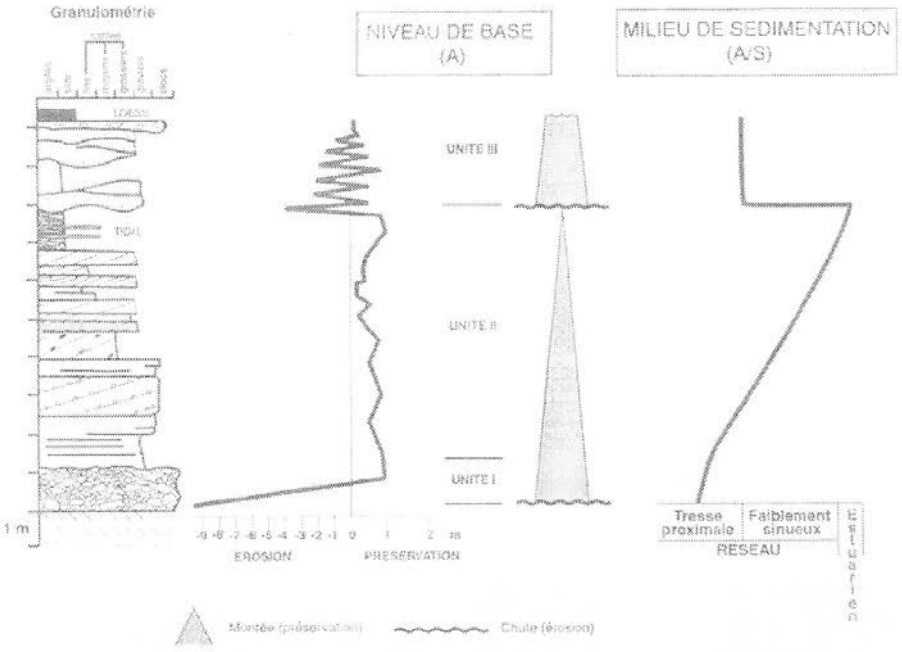

FIG. 6. – Variations verticales du niveau de base quantifiées à partir des épaisseurs préservées des faisceaux de litages obliques : définition de deux cycles de baisse-montée.
FIG. 6. – *Vertical variations of the base level quantified from the preserved thicknesses of the oblique lamina sets : definition of two fall-rise cycles.*

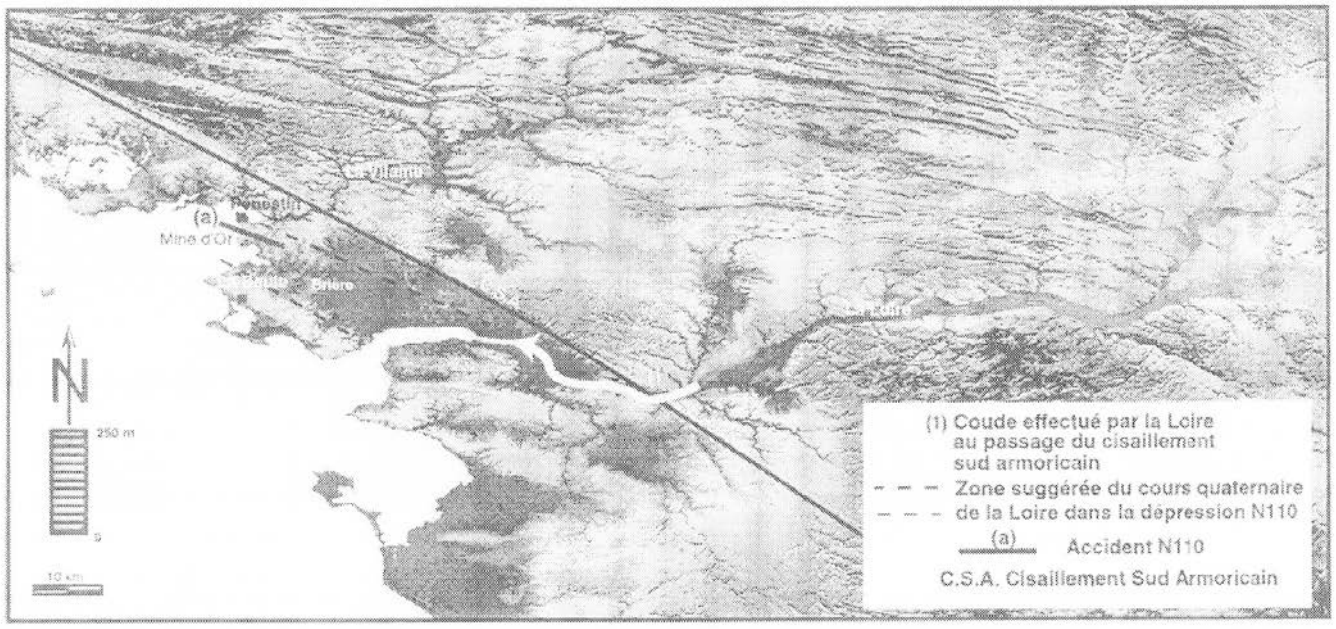

FIG. 7. – Tracé possible de la paléo-Loire au Pléistocène moyen-supérieur le long de la dépression de Brière.
FIG. 7. – *Possible path of the paleo-Loire river during Middle-Upper Pleistocene along the topographic depression of the Brière.*

ÉVOLUTION DU PALÉOCHENAL DE PÉNESTIN : IMPLICATIONS GÉOMORPHOLOGIQUES

Les mesures de paléocourants effectuées dans les unités I et II montrent une direction d'écoulement qui s'effectue vers le NNW (fig. 3). Cette direction n'est pas celle de la direction actuelle d'écoulement de la Vilaine qui se fait d'abord vers le sud puis vers le sud-ouest au niveau de l'embouchure (fig. 7). L'écoulement vers le N315 implique la présence d'un système fluviatile dont le bassin versant se situait au SE de la ville de Pénestin.

Le passage de l'unité II à l'unité III marque un changement de sens d'écoulement du système fluviatile (fig. 3), contemporain de la deuxième chute du niveau de base. A un écoulement vers le NNW (N315, unités I et II) succède un

écoulement vers le SSE (N140 à N180, unité III). L'unité III contient des galets de schistes rouges d'âge ordovicien reconnus dans la région des synclinaux, dits du Sud de Rennes, actuellement drainés par la Vilaine. Les directions d'écoulement dans cette unité et la présence des schistes rouges indiquent un bassin versant nord compatible avec celui de la Vilaine actuelle.

L'hypothèse la plus vraisemblable est que le réseau en tresse formant les unités I et II pourrait être le témoin d'une paléo-Loire. En effet, la Loire actuelle présente un coude au passage du cisaillement sud armoricain avec une réorientation suivant une direction NW (fig. 7), conforme avec l'orientation du réseau des unités I et II (fig. 3). Il existe, par ailleurs, une dépression topographique entre le cours actuel de la Loire et l'estuaire de la Vilaine (fig. 7), qui aurait pu être le passage privilégié de la paléo-Loire en direction de Pénestin (fig. 7).

Pour Bonnet [1998], l'écoulement de la paléo-Loire vers la Seine ou vers l'Atlantique durant le Pléistocène pourrait résulter de la formation d'une synforme d'axe E-W de longueur d'onde plurihectokilométrique, en relation avec un flambage d'échelle lithosphérique. Les unités I et II, qui semblent être les témoins d'une paléo-Loire, correspondraient à une période d'écoulement de cette paléo-Loire vers l'Atlantique. A titre d'hypothèse, la formation de la synforme d'axe E-W proposée par Bonnet [1998] pourrait être à l'origine de la destructuration du réseau fluviatile des unités I et II et aurait provoqué le détournement de la paléo-Loire vers son embouchure actuelle ou vers la Seine [Tourenq et Pomerol, 1995]. La Vilaine s'installe alors au droit de l'ancien cours de la paléo-Loire et dépose l'unité III.

CONCLUSIONS

Le paléochenal de Pénestin d'âge pléistocène moyen-supérieur résulte d'un creusement/remplissage fluviatile de type réseau en tresse proximal puis distal, temporairement ennoyé par la mer (faciès estuariens internes). Deux cycles stratigraphiques ont été définis. Le premier cycle débute par une surface d'érosion majeure qui correspond à l'incision du paléochenal. Le début de la remontée est enregistrée par l'unité I, mal préservée, le maximum d'inondation étant marqué par les faciès estuariens internes au sommet de l'unité II. Le deuxième cycle débute également par une chute du niveau de base. La remontée se traduit par la préservation de l'unité III.

Le fleuve comblant ce paléochenal s'écoulait tout d'abord vers le nord (écoulement d'une paléo-Loire : unités I et II) puis vers le sud (écoulement d'une paléo-Vilaine : unité III).

Le changement de direction de l'écoulement est contemporain de variations majeures du niveau de base probablement associées à des déformations sous forme de plis et de failles décrochantes d'âge pléistocène moyen-supérieur.

La validation de l'hypothèse d'une paléo-Loire préservée à Pénestin, suppose (1) de préciser les âges des trois unités définies sur la plage de la Mine d'Or mais également ceux des hautes à très hautes terrasses de la Loire et (2) de trouver d'autres témoins sédimentaires jalons entre la Loire et l'embouchure de la Vilaine, notamment dans les marais de Brière. Les acquisitions sismiques récentes, effectuées en mer au large de Pénestin (mission Géovil 1), ont montré l'existence de réseaux fluviatiles recouverts par des sédiments holocènes. La combinaison de ces deux conditions permettrait de reconstituer dans l'espace et dans le temps les différents réseaux hydrographiques successifs de la région. Ces réseaux étant sensibles à de faibles variations de pente régionale, la combinaison de toutes ces données pourrait alors permettre de caractériser plus précisément les mouvements tectoniques récents de ce domaine de socle.

Remerciements. – Les auteurs remercient les rapporteurs de ce manuscrit, B. Tessier et J.-P. Peulvast, pour leurs commentaires critiques et constructifs qui ont contribué à l'amélioration de cette note et M. Carpenter pour la révision de l'anglais.

Références

Allen P.A. (1985). – Hummocky cross-stratification is not produced purely under progressive gravity waves. – *Nature*, **313**, 562-564.

Allen P. & Homewood P. (1984). – Evolution and mechanics of a Miocene tidal sand-wave. – *Sedimentology*, **31**, 63-81.

Allen G.P. & Posamentier H.W. (1993). – Sequence stratigraphy and facies model of an incised valley fill : the Gironde estuary, France. – *J. Sediment. Petrol.*, **63**, 378-391.

Antoine P., Lautridou J.P. & Laurent M. (2000). – Long-term fluvial archives in NW France : response of the Seine and Somme rivers to tectonic movements, climatic variations and sea-level changes. – *Geomorphology*, **33**, 183-207.

Blair T.C. & McPherson J.G. (1994). – Alluvial fans and their natural distinction from rivers based on morphology, hydraulic processes, sedimentary processes, and facies assemblages. – *J. Sediment. Res.*, **A64**, 3, 450-489.

Bonnet S. (1998). – Tectonique et dynamique du relief : le socle armoricain au Pléistocène. – Thèse Doct., Univ. Rennes 1, 1997. – *Mém. Géosciences Rennes*, **86**, 352 p.

Bonnet S., Guillocheau F., Brun J.P. & Van Den Driessche J. (2000). – Large-scale relief development related to Quaternary tectonic uplift of a Proterozoic-Paleozoic basement : The Armorican Massif, NW France. – *J. Geophys. Res.*, **105**, B8, 19, 273-19, 288.

Cant D.J. (1978). – Development of a facies model for sandy braided river sedimentation : comparison of the south Saskatchewan river and the battery point bar formation. *In* : A.D. Miall, Eds., Fluvial sedimentology. – *Canad. Soc. Petrol. Geol., Mem.*, **5**, 627-639.

Cant D.J. & Walker R.G. (1978). – Fluvial processes and facies sequences in the sandy braided south Saskatchewan river, Canada. – *Sedimentology*, **25**, 625-648.

Collinson J.D. (1996). – Alluvial sediments. *In* : H.G. Reading, Ed., Sedimentary environments : processes, facies and stratigraphy. 3e éd. – Blackwell Science, Oxford, 37-82.

Cross T.A., Baker M.R., Chapin M.A., Clark M.S., Gardner M.H., Hanson M.S., Lessenger M.A., Little L.D., McDonough K.J., Sonnenfeld M.D., Valasek D.W., Williams M.R. & Witter D.N. (1993). – Applications of high-resolution sequence stratigraphy to reservoir analysis. *In* : R. Eschard & B. Doligez, Eds, Subsurface reservoir characterization from outcrop observations. – Technip Editions, Paris, 1993, 11-33.

DELVIGNE J.E. (1998). – Atlas of micromorphology of mineral alteration and weathering. – ORSTOM, Eds – *The Canad. Mineral., Spec. Publ.*, 495 p.

DOTT H.R. & BOURGEOIS J. (1982). – Hummocky stratification : significance of its variable bedding sequences. – *Geol. Soc. Amer. Bull.*, **93**, 663-680.

DURAND S. & MILON Y. (1955). – Le Pliocène de l'estuaire de la Vilaine. Etude des falaises de Pénestin (Morbihan). – *Bull. Soc. géol. minéral. Bretagne*, nouv. sér., **1**, 1-15.

ESTÉOULE-CHOUX J. (1967). – Contribution à l'étude des argiles du Massif armoricain. Argiles d'altération et argiles sédimentaires tertiaires. – Thèse, Rennes, 307 p.

ESTÉOULE-CHOUX J., ESTÉOULE J. & LOUAIL J. (1969). – Sur la présence d'un dépôt à kaolinite et gibbsite entre le Bajocien et le Cénomanien en Maine-et-Loire. – *C.R. Acad. Sci.*, Paris, **268**, 891-893.

ESTÉOULE-CHOUX J. (1983). – Altération et silicification au Tertiaire dans le Massif armoricain. – *Géol. Fr.*, **4**, (2), 345-352.

GAPAIS D., LAGARDE J.L., LE CORRE C., AUDREN C., JEGOUZO P., CASAS SAINZ A. & VAN DEN DRIESSCHE J. (1993). – La zone de cisaillement de Quiberon : témoin d'extension de la chaîne varisque en Bretagne méridionale au Carbonifère. – *C.R. Acad. Sci.*, Paris, **316**, sér. II, 1123-1129.

GERMANOSKI D. & SCHUMM S.A. (1993). – Changes in braided river morphology resulting from aggradation and degradation. – *J. Geol.*, **101**, 451-466.

GUILCHER A. (1948). – Le relief de la Bretagne méridionale de la baie de Douarnenez à la Vilaine. – Henry Potier, La Roche sur Yon, 682 p.

GUILLOCHEAU F. & HOFFERT M. (1988). – Zonation des dépôts de tempêtes en milieu de plate-forme : le modèle des plates-formes nord-gondwanienne et armoricaine à l'Ordovicien et au Dévonien. – *C.R. Acad. Sci.*, Paris, **307**, série II, 1909-1916.

GUILLOCHEAU F., BONNET S., BOURQUIN S., DABARD M-P., OUTIN J-M. & THOMAS E. (1998). – Mise en évidence d'un réseau de paléovallées ennoyées (paléorias) dans le Massif armoricain : une nouvelle interprétation des sables pliocènes armoricains. – *C.R. Acad. Sci.*, Paris, **327**, 237-243.

HAQ B.U., HARDENBOL J. & VAIL P.R. (1987). – Chronology of fluctuating sea levels since the Triassic. – *Science*, **235**, 1156-1166.

HARMS J.C., SOUTHARD J.B., SPEARING D.R. & WALKER R.G. (1975). – Depositional environments as interpreted from primary sedimentary structures and stratification sequences. – *Soc. Econ. Paleonto. Mineral., Short Course* n° 2, 161 p.

LAUTRIDOU J.P., AUFFRET J.P., BALTZER A., CLET M., LÉCOLLE F., LEFEBVRE D., LERICOLAIS G., ROBLIN-JOUVE A., BALESCU S., CARPENTIER G., DESCOMBES J.C., OCCHIETTI & ROUSSEAU D.D. (1999). – Le fleuve Seine, le fleuve Manche. – *Bull. Soc. géol. Fr.*, **170**, 4, 545-558.

LEFEBVRE D., ANTOINE P., AUFFRET J-P, LAUTRIDOU J-P & LECOLLE F. (1994). – Réponses de la Seine et de la Somme aux événements climatiques, eustatiques et tectoniques du Pléistocène moyen et récent : rythmes et taux d'érosion. – *Quaternaire*, **5**, (3-4), 165-172.

MIALL A.D. (1977). – A review of the braided-river depositional environment. – *Earth-Sci. Rev.*, **13**, 1-62.

MIALL A.D. (1978). – Lithofacies types and vertical profile models in braided river deposits : a summary. *In* : A.D. MIALL, Eds., Fluvial sedimentology. – *Canad. Soc. Petrol. Geol., Mem.*, **5**, 597-604.

MIALL A.D. (1985). – Architectural-element analysis : a new method of facies analysis applied to fluvial deposits. – *Earth-Science Rev.*, **22**, 261-308.

MIALL A.D. (1996). – The geology of fluvial deposits. Sedimentary facies, basin analysis and petroleum geology. – Springer Verlag, Berlin, Heidelberg, 582 p.

MULLER B., ZOBACK M.L., FUCHS K., MASTIN L.,GREGERSEN S., PAVONI N., STEPHANSSON O. & LJUNGGREN C. (1992). – Regional patterns of tectonic stress in Europe. – *J. Geophys. Res.*, **97**, 11783-11803.

NOTTVEDT A. & KREISA R.D. (1987). – Model for the combined-flow origin of hummocky cross-stratification. – *Geology*, **15**, 357-361.

ORTON G.J. & READING H.G. (1993). – Variability of deltaic processes in terms of sediment supply, with particular emphasis on grain size. – *Sedimentology*, **40**, 475-512.

PROUST J.N. (1990). – Expression sédimentologique et modélisation des fluctuations glaciaires. Exemple des dépôts du Protérozoïque terminal au Mali occidental. – Thèse, Univ. Louis Pasteur, Strasbourg, 165 p.

PROUST J.N. (1995). – Nature, géométrie et préservation des sédiments silicoclastiques dans les sytèmes de bas niveau des bassins de marge cratonique (Protérozoïque terminal ; Mali, Afrique de l'Ouest). – *Bull. Soc. géol. Fr.*, **166**, 6, 649-661.

RIVIÈRE A., VERNHET S., ARBEY F. & DESPRAIRIES A. (1963). – Le Pliocène et les accidents périglaciaires de la plage de la Mine d'Or à Pénestin (Morbihan). – *Bull. Soc. géol. Fr.*, (7), V, 1001-1011.

RUBIN D.M., SCHMIDT J.C. & MOORE J.N. (1990). – Origine, structure, and evolution of a reattachment bar, Colorado river, Grand Canyon, Arizona. – *J. Sediment. Petrol.*, **60**, 6, 982-991.

RUST B.R. (1978). – Depositional models for braided alluvium. *In* : A.D. MIALL, Eds., Fluvial sedimentology. – *Canad. Soc. Petrol. Geol., Mem.*, **5**, 605-625.

SCHUMM S.A. (1981). – Evolution and response of the fluvial system, sedimentologic implication. – *Soc. Econ. Petrol. Miner., Spec. Publ.*, **31**, 19-29.

SHACKLETON N.J. (1987). – Oxygen isotopes, ice volume and sea-level. – *Quat. Sci. Rev.*, **6**, 183-190.

SYLVESTER A.G. (1988). – Strike-slip faults. – *Geol. Soc. Amer. Bull.*, **100**, 1666-1703.

TESSIER B. (1990). – Enregistrement des cycles tidaux en accrétion verticale dans un milieu actuel (la baie du Mont-Saint-Michel) et dans une formation ancienne (la molasse marine miocène du bassin de Digne). Mesure du temps et application à la reconstitution des paléoenvironnements. – Thèse 3e Cycle Univ. Caen, 122 p.

THOMAS E. (1999). – Evolution cénozoïque d'un domaine de socle : le Massif armorician. Apport de la cartographie des formations superficielles. – Thèse 3e cycle Univ. Rennes, 148 p.

TODD S.P. (1996). – Process deduction from fluvial sedimentary structures. *In* : P.A. CARLING & M.R. DAWSON, Eds., Advances in fluvial dynamics and stratigraphy, 299-350.

TOURENQ J. & POMEROL C. (1995). – Mise en évidence, par la présence d'augite du Massif central, de l'existence d'une pré Loire-pré Seine coulant vers la Manche au Pléistocène. – *C.R. Acad. Sci.*, Paris, **320**, sér. IIa, 1163-1169.

VAN VLIET-LANOË B., BONNET S., HALLEGOUËT B. & LAURENT M. (1997). – Neotectonic and seismic activity in the Armorican and Cornubian massifs : regional stress field with glacio-isostatic influence ? – *J. Geodyn.*, **24**, 219-239.

VISSER M.J. (1980). – Near-spring cycles reflected in Holocene sub-tidal large-scale bedform deposits : a preliminary note. – *Geology*, **8**, 543-546.

WHEELER H.E. (1958). – Time-stratigraphy. – *AAPG Bull.*, **42**, 1047-1063.

WYNS R. & GUILLOCHEAU F. (1999). – Géomorphologie grande longueur d'onde, altération, érosion et bassins épicontinentaux. *In* : Colloque Géofrance 3D. Résultats et perspectives. – *Doc. BRGM*, **293**, 103-108.

ZOBACK M.L. (1992). – First- and second-order patterns of stress in the lithosphere : the world stress map project. – *J. Geophys. Res.*, **97**, 11703-11728.

Int J Earth Sci (Geol Rundsch)
DOI 10.1007/s00531-007-0295-7

ORIGINAL PAPER

Seismically induced shale diapirism: the Mine d'Or section, Vilaine estuary, Southern Brittany

B. Van Vliet-Lanoe · C. Hibsch · L. Csontos · S. Jegouzo · B. Hallégouët · M. Laurent · A. Maygari · D. Mercier · P. Voinchet

Received: 6 February 2007 / Accepted: 19 December 2007

Abstract The Pénestin section (southern Brittany) presents large regular undulations, commonly interpreted as evidence of periglacial pingos. It is an upper Neogene palaeoestuary of the Vilaine River reactivated during the middle Quaternary (middle terrace). It is incised into a thick kaolinitic saprolite and deformed by saprolite diapirs. This paper presents the arguments leading to a mechanistic interpretation of the deformations at Pénestin. Neither recent transpressive tectonics nor diagnostic evidence of periglacial pingo have been found despite evidence for a late paleo-permafrost. The major deformational process is shale diapirism, initially triggered by co-seismic water supply, with further loading and lateral spreading on an already deformed and deeply weathered basement, which allowed the shale diapirism to develop. Deformations are favoured by the liquefaction of the saprolite and a seaward mass movement and recorded, rather distant, effects of an earthquake (c. 280 ka B.P.) resulting from the progressive subsidence of the southern Armorican margin. These deformations triggered by an earthquake are similar to those induced by classical shale diapirism. They are probably common in tectonically active continental environments with shallow water table.

Keywords Shale diapirism · Earthquake · Saprolite · Periglacial · Neotectonics · Brittany

Introduction

The recognition of neotectonic activity is important for seismic hazard assessment, especially in relation to Quaternary deposits. Classical features used for the recognition of tectonic activity include geomorphological evidence of recent fault displacements such as enhanced subsidence or

B. Van Vliet Lanoe (✉)
UMR 6538 Domaines Océaniques,
IUEM & Université de Bretagne Occidentale,
29280 Plouzané, France
e-mail: brigitte.vanvlietlanoe@univ-brest.fr,
brigitte.van-vliet-lanoe@univ-lille1.fr

C. Hibsch
G2R, Nancy Université, CNRS, Boulevard des Aiguillettes,
B.P. 239, 54506 Vandoeuvre lès Nancy, France
e-mail: Christian.Hibsch@g2r.uhp-nancy.fr

L. Csontos
Department of Geology,
University L. Eotvos, 1117 Budapest, Hungary
e-mail: csontos@ludens.elte.hu

S. Jegouzo
SAGE Vie et Jaunay, 11 rue du Bourg, 85800 Givrand, France
e-mail: sage.vieetjaunay@wanadoo.fr

B. Hallégouët
Department of Géographie,
Université de Bretagne Occidentale,
29238 Brest Cedex 3, France
e-mail: bernard.hallegouet@univ-brest.fr

M. Laurent · P. Voinchet
Department of Geochronology, Muséum National d'Histoire Naturelles, 1 rue Panhard, 75005 Paris, France
e-mail: pvoinch@mnhn.fr

A. Maygari
Hungarian Geological Survey (MAFI), Stefánia út. 14,
1143 Budapest, Hungary
e-mail: magyari@mafi.hu

D. Mercier
Ecole des Mines Paris Fontainebleau, 35 rue St Honoré,
77305 Fontainbleau Cedex, France
e-mail: daniel.mercier@ensmp.fr

tilting, river incision or deviation, and enhanced denudation. These features are usually difficult to attribute to an accurate stratigraphic position. Synsedimentary deformation features are attributed to specific events acting in a narrow time span and specific palaeoclimatic conditions. In former periglacial areas of potentially seismically active regions, it is important to distinguish between deformational processes induced by tectonic, possibly co-seismic, activity and periglacial ones.

With regard to these deformational processes, we shall analyse whether "fold" succession in soft sediments can be related to tectonics, periglacial forms or to seismically induced soft-sediment flows. Converging morphologies with those induced by diapirism is often indicated. Such examples exist in the southern Pénestin section (Van Vliet-Lanoë et al. 1997a, b; Brittany, N.W. France, Figs. 1, 2a, b) and the Bovey Tracey basin (Devon, UK; Fig. 2c) where they were first interpreted either as pingo scars (Jenkins and Vincent 1981; Rivière and Vernhet 1962) or as more complex features attributed to permafrost by Eisseman (1981) and Strunk (1983). More recently it has been suggested that these "fold trains" could be interpreted as induced by seismic shaking (Van Vliet-Lanoë et al. 1997a, 2004) or as Quaternary synsedimentary tectonic folding (Brault et al. 2001).

The section of the Mine d'Or, at the SW of Pénestin city, is located south of the Vilaine estuary. The studied section crops out at the shore cliff, which has been rapidly eroded since 1950 (Fig. 3). It corresponds to an upper Neogene (lowstand) palaeoestuary of the Vilaine river (southern Brittany), reactivated and deformed during the middle quaternary and forming today the middle terrace of the river. The topographical slope at the top of the section is 0.5% to the north but 1% to the west (seaward), explaining winter seepage along the cliff.

This paper presents the tectonic, petrographic and stratigraphic arguments leading to the mechanistic interpretation of the quaternary deformation processes at Pénestin. The morphologic convergence with classical deep-seated shale diapirism will be explained on the basis of earthquake-induced transient transformation of local saprolite. Altitudes are given in NGF, the French Ordnance Survey.

Geology

The section of the Mine d'Or corresponds to a fluvio-marine terrace complex (Fig. 4), located at circa 15 m above the Hercynian basement, which is faulted in several compartments (Fig. 5) and deeply weathered (kaolinitic

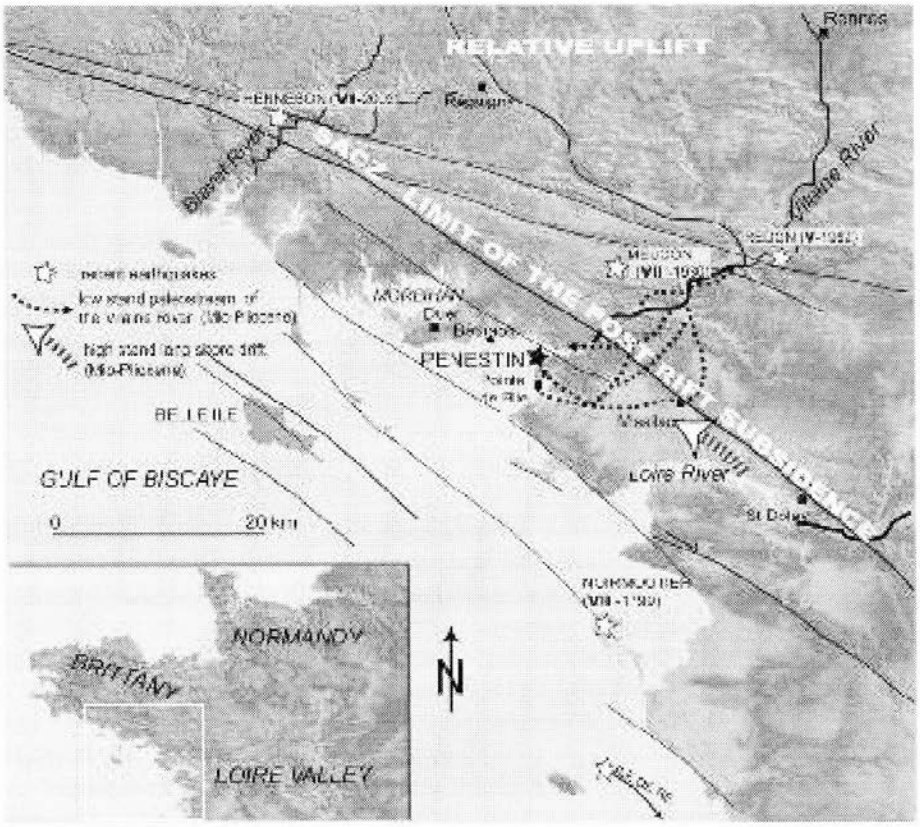

Fig. 1 Geographical location of the site with the main faultlines and recent earthquakes. *SASZ* Southern Armorican Shearing Zone

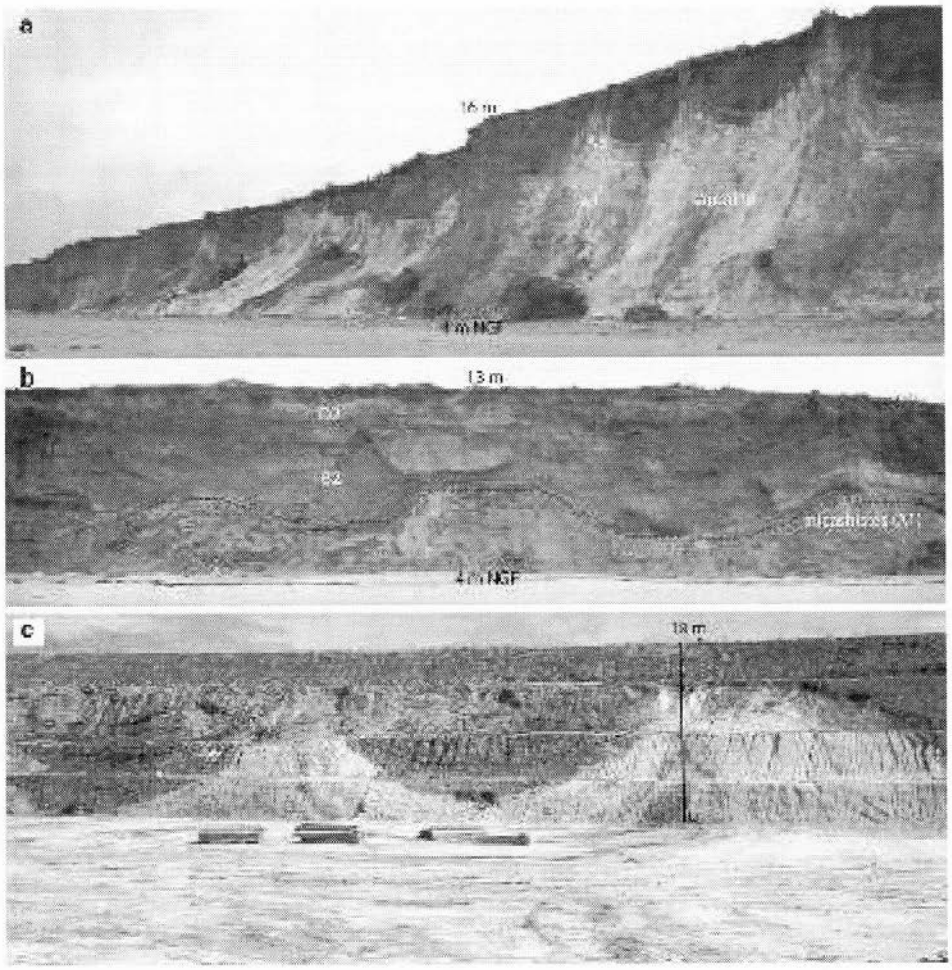

Fig. 2 Large "fold" trains in the Channel region: a Pénestin, southern section, Brittany; b Pénestin northern section; c Bovey Tracey china clay pit, with "bowls" consisting of lignite (base, *dotted lines*) and Quaternary conglomerate (*top*); note the china clay diapirs (Devon, GB). Lettering corresponds to the stratigraphical units described in the text

saprolite). A water table is commonly perched above it. The section is oriented roughly north–south and is rapidly eroding as a result of water seepage at the contact between the saprolite and the fluvio-marine complex. Detailed sedimentological descriptions were provided by Guillaume-Bruno (1972), Van Vliet-Lanoë et al. (1997b) and Brault et al. (2001). Initial interpretations of the deformation were provided by Durand (1960) and Guillaume-Bruno (1972).

Pénestin is located close to a southern branch of the South Armorican Shear Zone (SASZ, Fig. 1). This structure is one of the major Variscan dextral strike-slip faults of the European plate (Gapais et al. 1993). It has been truncated by a post-Hercynian palaeosurface (de Martonne 1907), often supporting deep weathering as commonly reported (e.g. Klein 1996; Wyns 1991). This SASZ zone was reactivated during the opening of the Gulf of Biscay and probably from the Turonian like most of the tectonic zones in the Western Approaches of the Channel (Ziegler 1992), in connection with the displacement of the Iberian and African plates. Up to the Messinian, it controlled the formation of small pull-aparts and horsts along the southern Brittany coast (synthesis in Proust et al. 2001). Presently, the seismicity is moderately active (Levret et al. 1994), as shown by the 2003 Hennebon seism (magnitude 5.5) and cluster of events around the Isle of Ré in 2005 (Fig. 1). MSK intensities can reach values of VII, as during the Meucon earthquake (Landes de Lanvaux) in 1930 or even VII–VIII, as at Noirmoutier, in 1799 (SIRENE data base, Fig. 1).

The basement is weathered along most of the cliff but with the highest intensity at La mine d'or. To the north, from the Pointe de Lomer (Fig. 3), the basement consists of Palaeozoic muscovite-rich micaschists; south of this point, it consists of gneisses with quartz nodules. The geometry of the weathered basement (Fig. 4) has been interpreted as a northward tilting of the block north of the Kerfalher fault, which would have also tilted the palaeo-weathering profile (Brault et al. 2001).

The basement constitutes Unit A: south of La Source (Figs. 4, 5), weathered shales can be subdivided into three sub-units: (1) A1: weathered coherent shales, dark grey or

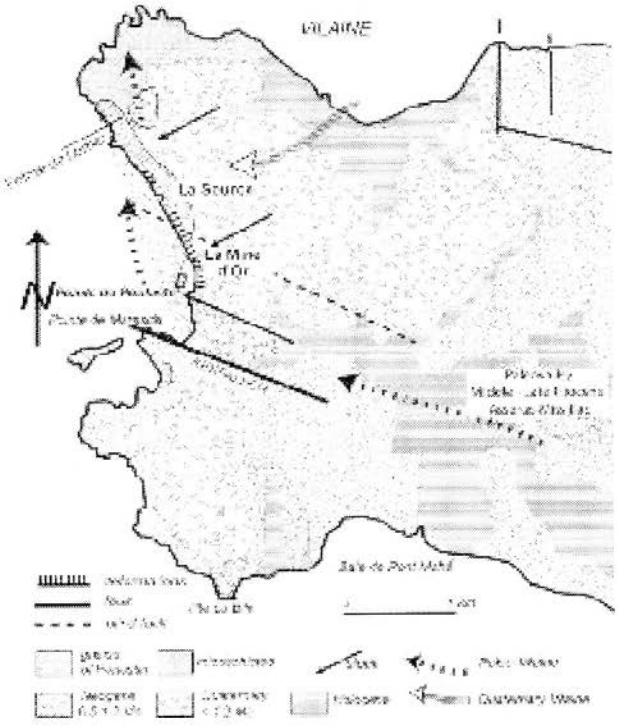

Fig. 3 Geology of the Pénerf peninsula

oxidized in colour, (2) A2: soft grey to white weathered shales, with preserved fabric, and highly susceptible to slumping, (3) A3: compact grey to white weathered shales, with disturbed petrofabric. All the A units are "isalterites", a saprolite with or partialy preserved rock petrofabric. Contrary to the statement of Brault et al. (2001), no alloterite, a saprolite with fully pedogenetically transformed petrofabric, has ever been observed in the present study. The palaeosurface truncating the saprolite rises thus from +8 m at La Source (Figs. 4, 5) to +15 m NGF at Kerfalher. The presence of soft, unconsolidated grey to white weathered shales along the section corresponds to collapsed compartments limited by normal faults in the A1 and A2 units (Fig. 5). No prolongation of these normal faults has been observed in unit A3.

Sedimentological data and stratigraphy

The sedimentary succession resting on the saprolite corresponds to:

Unit B: scattered blocks of possible Eocene quartzitic sandstones ("Grès Ladères") observed at the contact between the saprolite and the fluvio-marine levels (Figs. 4, 5). Laterally to the south, some quartzite sandy gravel with a white kaolinitic matrix crops directly out at the top of the saprolite. In Brittany, such gravel is generally attributed to Eocene or Oligocene deposition (Durand 1969; Estéoule-Choux 1983). Late Oligocene is the most probable age. The geometry of the section reveals a palaeosurface (Fig. 5) at A3-B interface, shaped at least since the Oligocene (unit B) and further incised by four successive channel generations (units C1, C2, D1 and D2), without glacial influence. This is a significant difference from Brault et al.'s interpretations.

Fig. 4 Composite stratigraphical log of the cliff section

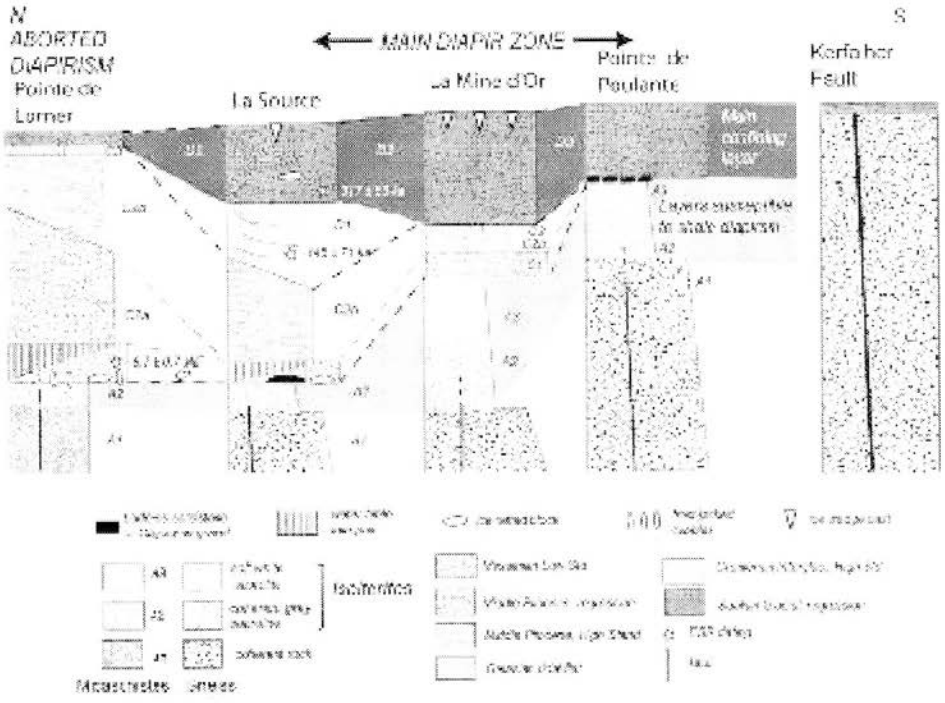

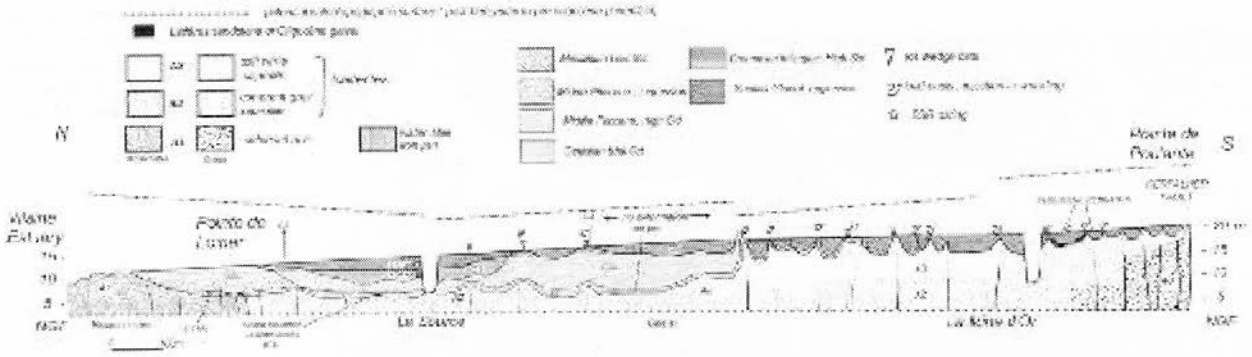

Fig. 5 Sketch section of La mine d'Or cliff

Unit C1: a basal conglomerate, prograding from the south (*unit I* from Brault et al. 2001). This unit is initially attributed by Brault et al. (2001) to fluviatile deposition, owing to an imbricate cobble fabric (base of *unit I* of Brault et al. 2001). The sandy matrix is well sorted, with shiny polish of marine origin. The dominant imbricate fabric of the conglomerate is related to a swash-stacking of cobbles in the form of large, faintly stratified bodies: it attests to a longshore transit towards the NW (N-315E to N-350E), which is similar to the present one. At its base, it includes flat-lying blocks of quartzitic sandstones ("Grès Laderes") and vertical frost-jacked cobbles (frost jacking) stacked into the saprolite forming cryogenic pattern ground interpreted as the result of a longshore transportation by anchored ice rafting (Van Vliet-Lanoë et al. 1997a, 2002). It is also characterized by a variegated petrographic composition common for anchored ice-rafting drift. The truncation as well as of soft as of coherent saprolite, with absence of scouring, also argues for a shore face deposition under a cold climate (Van Vliet-Lanoë 2005). This unit yields an age of 6.7 ± 0.7 Ma by ESR in agreement with previously supposed ages (Van Vliet-Lanoë et al. 2002). It is further locally consolidated by a hydromorphic goethite hard pan, which could be interpreted as a tropical ferricrete (Schwartz 1994), in agreement with the Lower Pliocene climate (Zagwijn 1989) but could also correspond to an aged podsolic iron pan (Al-goethite), in low topographic position. The goethitic hard pan has a major impact on the deformations throughout the section, by modifying the permeability and the rheology above the saprolite. The age of c. 6.7 Ma for a lowstand shoreline implies a subsidence of 50 m, based on the eustatic curve of Hardenboll et al. (1998).

Units C2 and C3: Unit C2, a prograding coarse sandy unit with an increasing charge of angular rock fragments (*unit II* of Brault et al. 2001) constitutes an estuarine progradation, river dominated, clearly coming from the south (Brault et al. 2001). This orange–brown unit is strongly rubified close to the surface by pedogenesis with some violet–reddish mottling and manganese precipitation at the base. It is covered by rhythmic red and grey silty clays (unit C2b), often wrinkled. It is lapped further on by unit D2, which is in contrast to the description of Brault et al. (2001). Unit C2a is characterized by a mineralogy, which consists of 60% illite and 40% kaolinite with minor reworked red schists from the Rennes basin (Guillaume-Bruno 1972). Unit C21 also reworks minerals from the Loire River (Esteoule-Choux 1983), inherited from longshore palæodrift from the St Dolay formation (Missillac outcrop; Fig. 1), which contains fauna Lower Pliocene in age. This unit has been initially attributed to the Pliocene "red sands" (Durand 1960), but further on to the Quaternary (Guillaume-Bruno 1972). In contrast with the interpretation of Brault et al. (2001), the C2 unit represents a Middle Pliocene estuarine progradation coming from Missillac via Asserac (Fig. 3; Van Vliet-Lanoë et al. 2002): it probably corresponds to a complex estuary, with rocks and inlets separated by channels and dominated by fluvial clast-rich sedimentation. It corresponds to the top of an estuarine braided fan formed during a major regression and fed by clasts produced by increasing frost shattering. The upper tidalites, C3 represent the Gelasian—Pre-Tiglian highstand (Van Vliet-Lanoë et al. 2002; +50 m NGF, Hardenboll et al. 1998). It attests to a local subsidence of at least 35 m since 2.4 Ma.

Unit D1: the C2 unit is eroded by an estuarine channel from the Vilaine River (unit III of Brault et al. 2001), consisting of fine grained sands and clays, lacking frost perturbation. It represents an interglacial complex. Mineralogy belongs to the Vilaine watershed, with occurrence of about 20% smectite and 60% kaolinite (Guillaume-Bruno 1972). This estuarine material is dated at 445 ± 71 ka by ESR (Marine Isotope Stage 13 = MIS 13) (Laurent 1993). The extent of the sands is visible at the base of the large "bowls" up to 200 m of the southern access to the beach. Sediment facies attests a sea level normally close to +30 m NGF (Van Vliet-Lanoë et al. 2000), and thus a global subsidence of circa 15 m since 400 ka. This unit is

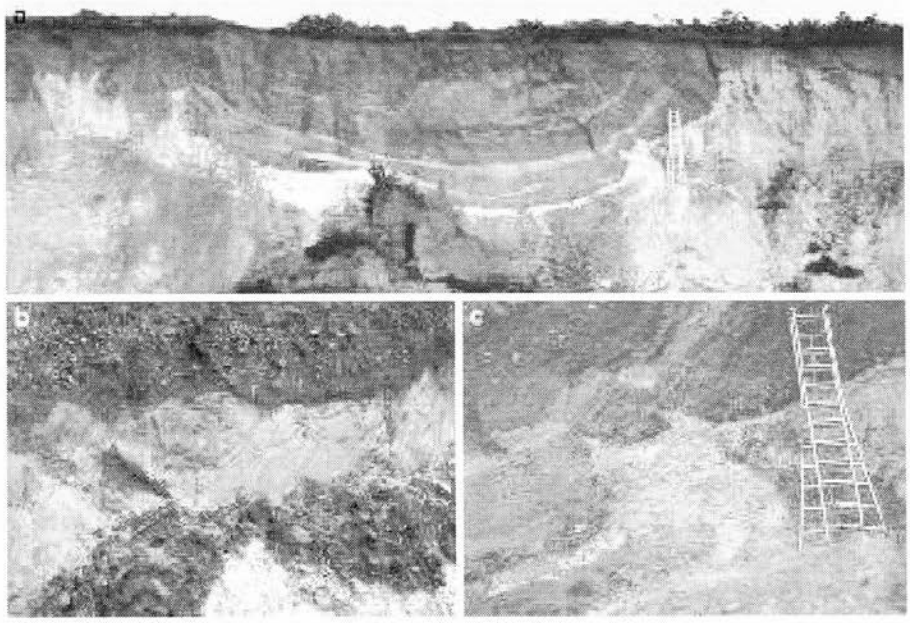

Fig. 6 Bowl deformation of D2 and C2a sediments between two diapirs. Note the stretching in C2a sands (b), and the mud injection on tension gashes (c)

practically never deformed when it is thick (La Source), but is susceptible to stretching when it is thin (to the south) and sometimes faulted (Fig. 6b).

Unit D2: this sandy gravel belongs to a braided river system with large ice-rafted blocks from paleozoic sandstone and vein quartz; it covers most of the section, except the northern part (*unit IV* from Brault et al. 2001). This periglacial river corresponds to the Middle Pleistocene "middle" terrace of the Vilaine and is further weathered by a polygenetic red yellow podsolic soil. It as been dated at 317 ± 53 ka (MIS 9c) by ESR (Laurent 1993).

Locally, unit E1 appears. It is a loess-like kaki silt infilling ice-wedge casts, which post-date unit D2 and the large "fold train" deformations. Casts develop in specific tensional position related with saprolite diapirs (Van Vliet-Lanoë et al. 1997a). These ice-wedge casts are truncated by an erosion surface, some recent loesses and periglacial slope deposits (unit E2), and by recent dune sands (unit F), Holocene in age. Those features are not represented on Figs. 4 and 5.

Further to the south, at Kerfalher, the conglomerates from unit B are cemented by goethite and immediately covered by a perched mudflat accumulation, reaching +10 m NGF, and by younger periglacial slope deposits. Unit C2a crops out at 1 km to the south, with some shore ice-rafted blocks at the base.

C1 crops out as a marine strand flat, corresponding to a yet cold lowstand, Upper Miocene in age. C2 is a temperate tidal channel, ending by a mud flat and coming from the south, Middle to Upper Pliocene in age. D1 is a younger temperate tidal channel, c.420 ka in age. D2 is a conglomerate with more sandy layers, corresponding to a periglacial braided river, c.307 ka in age: it deposited prior to the fold-like deformations.

From this interpretation, total subsidence yields 15 m since c.400 ka, 35 m since 2.5 Ma and 50 m since 6.5 Ma. These subsidence rates follow the evolution of the margin of the Gulf of Biscay (200 m since the Eocene; Sibuet 1972). Nevertheless this side of the Vilaine estuary seems to have suffered less subsidence than the Morbihan Gulf.

Basement and tectonics

This stratigraphic interpretation makes possible to define the age range of the basement's deformations. To the north of the bay, the weathered substratum of oxidized micaschists with quartz nodules and preserved petrofabric is truncated by a marine abrasion reaching 8 m NGF. The Pointe de Lomer corresponds to a tectonic contact of probable Hercynian age between micaschists and gneiss but may have been reactivated more recently (Figs. 3, 5). South of the Pointe de Lomer, the substratum is often deeply weathered in bleached soft clayish silt. Owing to continuous water seepage, in the middle part of the cliff, La Source dell develops above a blind fault. The main Kerfalher fault is located further south of the Pointe de Maresele. A secondary fault of the SASZ (Fig. 1) fault bundle outcrops at the Pointe de Poulante (Fig. 3) at the end of La Mine d'or cliff, separated from the main fault by a wide erosional depression. Its orientation is roughly N120°E. Previously interpreted as a Quaternary fault

(Durand, 1960), this fault at this point does not seem in fact to have suffered recent tectonic rupture reaching the surface. No clear fault scarp morphology is noticeable and the contact with the Neogene and Quaternary sediments is rather a marine palaeo-valley filled by solifluected schist blocks, conglomerates and estuarine sediments than a tectonic contact.

Pre-quaternary faulting

In detail, abrupt transitions of sub-units into the saprolite suggest pre-quaternary differential normal displacements of basement compartments, which lead to different interpretations. First, if the weathering profile was horizontal, it could have been faulted in at least four compartments prior to the Messinian as proposed in Fig. 5 and not only as a single tilted block as stressed by Brault et al. (2001). A second hypothesis should be to consider a heterogeneous palaeo-weathering profile in previously faulted rocks more susceptible to weathering into kaolinite owing to higher feldspar content. Both hypotheses are difficult to demonstrate. The intense weathering, which occurred during the whole Palaeogene has certainly provided thick argillaceous saprolite (Wyns 1991). Nevertheless, sandy kaolinitic clays with pyrite nodules, Upper Cretaceous in age, are found in eastern Morbihan in coring a micro-basin at the Pointe de Duer (Fig. 1). It attests to a pre-existing deep weathering of this post-Hercynian palaeosurface. This suggests much older deep weathering in a faulted zone where some of these faults may have acted later as water drains favouring potential fold-like deformations. Moreover kaolinitic clays may shrink 30% in volume from pronounced consolidation or desiccation, leading to self-polygonal faulting of the saprolite as described for marine clays by Henriet et al. (1992). Desiccation or frost usually exploit pre-existing failures.

Quaternary faulting

The wavy contact (fold-like deformation train) between the weathered bedrock and the sedimentary units (Figs. 2b, 5) has been interpreted as evidence of Quaternary strike-slip faulting of the Kerfalher fault system (Brault et al. 2001). According to Brault et al., the right-lateral activation of the N110°E Kerfalher fault would have induced a Riedel pattern controlled by a NNW–SSE shortening suggested to be compatible with the present-day NW–SE direction of shortening. This pattern would present NW–SE right-lateral *R* faults, N50°E en echelon folds and N50 to N70°E left-lateral *R'* faults. For these latest the angle with the supposed horizontal shortening (reaching 90°) seems too wide and even overpasses the angle between the supposed σ1 and the proposed fold axes. Such supposed *R'* faults are drawn with a NNE–SSW to NE–SW direction (i.e. Fig. 5 in Brault et al. 2001), which directions appear theoretically more compatible but in strong contradiction of the descriptions. Deformations do not present a regular wavelength. Some sectors are devoid of them though others close to the Pointe de Poulante are smaller and more clustered. Our observations rather suggest a strong link between the strike of the "saprolite upbursting" and the strikes of the inherited faults which have been previously interpreted as *R'* faults. We consider those faults to have acted as specific water pathways during deformations. The fault pattern described by Brault et al. (NW–SE right-lateral and NE–SW to ENE–WSW left-lateral) on the contrary seems to be very compatible with the N–S to NNE–SSW horizontal shortening related to the Pyrenean event of Eocene age (Ziegler 1992) and may have been coeval with the strong weathering of the micaschists during the same period.

As previously mentioned (Van Vliet-Lanoë et al. 1997a; Brault et al. 2001), it seems clear that the more intense deformation features almost always developed above a fault affecting the basement, which fault is frequently outlined by specific grey argillaceous rocks. Few striations were observed on these grey clays. The slip movements N62°E–80°N rake-50°W and N43°E–76°W rake-64°S revealed normal-sinistral kinematics, compatible with a sliding towards the seaside and incompatible with the supposed positive flower structure (Fig. 7a). Pre-existing faults controlled water migration as well as during seismic pumping or during active weathering.

Mechanical properties and deformations

For an understanding of the mechanical comportment along the La mine d'Or section, the mechanical properties of the saprolite and the sediments must be known. Deformations mostly develop in thick bleached saprolite. These are much less intense when the preserved overburden sedimentary thickness is large (at least 10 m of coarse sand, 1–2 m of conglomerate) and is more permeable (interstitial porosity of sands and conglomerates). No deformation develops when the conglomerate C1 is cemented with goethite. The D1 sands and conglomerates are infiltrated by pedogenetic clay illuviation and present nowadays a low porosity. The deformations are smoother and "longer" in wavelength when the saprolite is moderately weathered (A2 facies), larger and stronger for A3 facies and smaller but strong when the alluvial complex is thin (Fig. 4). Deformations are thus controlled by (1) the pre-existing faults, (2) the overburden sedimentary load,

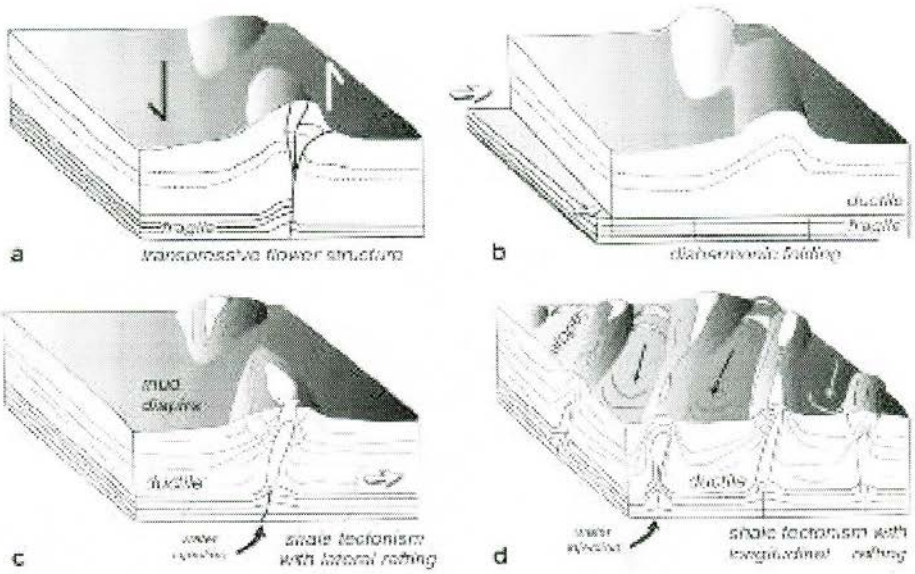

Fig. 7 Different hypotheses (*A–B–C-D*) of deformation's dynamic suspected of developing the structures at Bénest m. *D* is the most probable dynamic

(3) the characteristic of its porosity and (4) the mechanical properties of the saprolite.

At the north of the section, the unit C1 is locally deformed by the moderate upbursting of the A2 saprolite above pre-existing normal faults. It only occurs when the C1 conglomerate is not consolidated by the goethite. Metric scale upbursting of the saprolite induced for a few metres a collapse in fabric inside the basal conglomerate. It generates large, asymmetric "bowls", up to 50 m in length in units C2 and D1 (Fig. 2b). In association with limited upbursting, decimetric wrinkling develops in unit C2b immediately south of the saprolite bursting; neither load cast nor other liquefaction structures are observed in this location. It also induces further metric-scale normal faulting in the deformed beds, followed by soil bleaching, especially immediately north of La Source. Locally to the north, the beds simulate to accommodate the deformation, as for synsedimentary folding.

South of La Source, the deformation style changes drastically. The geometry of the deformations is more or less continuous and elongated roughly N60°E as are the faults observed in the weathered basement (Fig. 8a). Upbursting evolve into diapirs with some lateral metric injection of kaolinitic mud separated by asymetric "bowls", up to 35 m in length in units C2 and D1–2. The successive pictures taken since 1985 do not show any clear meandering of the injection features despite an average retreat of the cliff of about 1 m/year since that time (Jegouzo 2001). This trend is clearly controlled by the main fracture network in the Palaeozoic substratum. Short, often asymmetric, irregular "bowls" developed, thanks to the presence of the thick white saprolite below unit D1 (residual gravel and sandy layer) and mostly below unit D2 (Fig. 5). Usually 2–3 m below the base of D1, the saprolite is undisturbed and porous. The wavelength of the deformation is much shorter, about 20 m. No synsedimentary adaptations of the deposits were observed, such as fan-shaped features, despite the affirmations of Brault et al. (2001). Liquefaction can develop in clayish sands (Ruxton 2004) allowing an incipient doming which stretches the overburden sandy cover (Powley 1999), and pinches out the flanking sandy units (Fig. 7c), comparable with synsedimentary deformation. When present, the D1 sandy unit presents evidence of stretching with listric microfaults and bending (Fig. 6b). At the level of the maximal curvature of the extrados, tension gashes are injected with liquefied kaolinitic silts, revealing tension at the sedimentary interface (Fig. 6c). Moreover, at the level of the saprolite out-bursting, load casts deform the extruded saprolite mass, sometimes associated with a lateral shortening inducing wrinkling. These features are interpreted as to the result of the interaction of surface P and Rayleigh waves on uncompressible fluid (Van Vliet-Lanoë et al. 2004). In the section, ice-wedge casts filled with kaki loesses (unit E1) develop specifically in zones of saprolite upward injection, concentred on tension bulges created by the large undulations (Fig. 5). Post-deformation thermal cracking re-used pre-existing failures or mechanical discontinuities during MIS 8. These casts are later deformed by cryoturbation. On such highly frost-susceptible soils as the silty saprolite, differential frost heave can partly deform the structures afterwards (Van Vliet-Lanoë et al. 2004). To the south, at the level of the Poulante Point, the coherent weathered gneiss (A1) outcrops at 15 m above nearly unweathered rock.

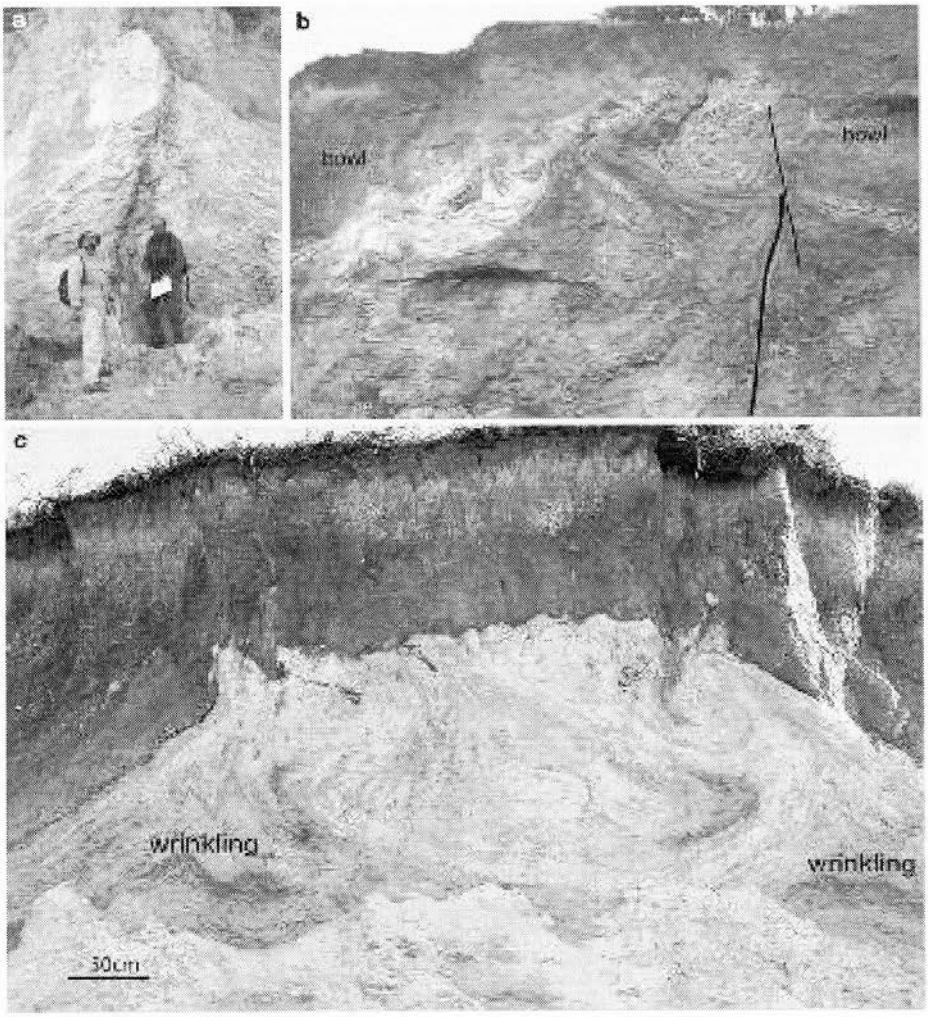

Fig. 8 a Normal fault in the saprolite; b loads on upwards-injected saprolite at the apex of a normal fault; c giant load with lateral wrinkling in the whitish saprolite A3 (angular microfolding). Note the undulating contact with the alluvial dark member D2

Mechanical properties

The clay fraction consists essentially of authigenic, silt-sized kaolinite with about 10% of illite (Guillaume-Bruno 1972), leading to a low density and a high porosity in the undisturbed saprolite (Fig. 9a). Such material has a much lower plasticity index than the other clay minerals (Skempton 1953). According to our laboratory measurement, the winter water content of unremoulded saprolite is around 23%, a little above the water content at Atterberg plastic limit (20%, Cassagrande methodology). Liquefaction occurs above 30% in unremoulded sediment (28% at Atterberg liquid limit) when the water table seeps along most of the cliff. Today, shocks induced by storm waves can easily bring about the collapse of the original porous fabric of the saprolite, the expulsion of excess water and further mass wasting.

The wet and dry density of the saprolite increases towards the surface. The undisturbed dark grey saprolite (unit A2) yields a 1.3 g/cm^3 dry bulk density, while when slightly disturbed it rises to 1.6 g/cm^3 and for white (unit A3), fully disturbed saprolite density rises to 1.9 g/cm^3. The deformation cannot be related to the sedimentary aggradations and load as the sediments deposited on a long time span (Neogene to middle Quaternary), the overburden often being deposited after phases of desiccation/consolidation of the substratum, normally reducing its liquefaction susceptibility. The dry bulk density of the coarse sands is about 1.9 g/cm^3 and circa 2.0 g/cm^3 from the conglomerates. The overburden load (c. 8 m) on the saprolite at the Pointe de Lomer can thus be estimated at 24 t/m^2 at water saturation. At the Mine d'Or, outside the injection features, the overburden (c. 5 m) represents circa 15 t/m^2 at water saturation and the winter water content close to saturation in the unremoulded saprolite reaches 23% (unit A3). To reach the liquid limit (30%) and equilibrate the pressure induced by the overburden conglomerates, we need to remould the original porous fabric of the "light" saprolite

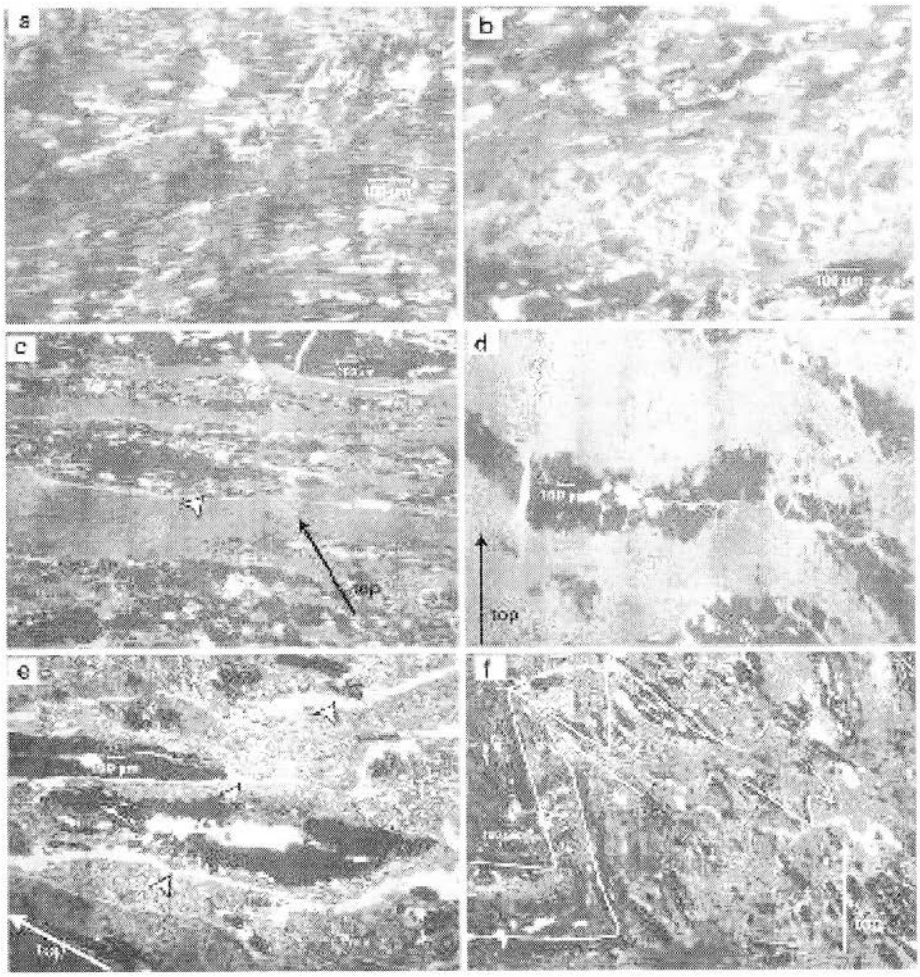

Fig. 9 Petrographic investigation of the saprolite (impregnation with plastic under vacuum, stained with a fluorescent dye (reflected UV light); the porosity is *white to light grey*, quartz are *black*; vertical thin sections excepted when top is mentioned. a, b Undisturbed rock fabric with authigenic kaolinite; c slightly disturbed and densified saprolite with shearing plane (*small arrows*); d remoulded dense saprolite; e slickenside shearing planes (*small arrows*) in a disturbed saprolite; f macroscopic wrinkling

to reach 23% of water in the collapsed silt and to add a minimum 7% of water without possibility of water escape. The origin of this supplementary water supply is clearly connected to the basement faults. Gravel-supported conglomerates usually behave as cohesive and are resistant to liquefaction, especially when they are further partly consolidated by clay illuviation. Cohesive kaolinitic silts are hard to liquefy in normal conditions (Skempton 1953; Lawrence 1980); to destroy the fabric, we need an external trigger to induce liquefaction. To induce mass movement, water needs to be confined in excess within the liquefied saprolite and the oversaturation of the saprolite needs to be continued for some days.

Close to the Pointe de Poulante, the truncation of the saprolite (Fig. 4) by the thin porous D1 conglomerate seriously limits the direct rise in overburden pressure. South of the Pointe de Lomer, its truncation by the thick C2a sandy unit provides a potential overburden pressure, which is immediately limited by the potential evacuation of the water in excess.

Petrography

The petrographic analysis of the saprolite reveals the state of perturbation of the original fabric (Fig. 9). Oriented thin sections impregnated under vacuum by fluorescent polyester resin (dye: UVITEX POB) were manufactured from undisturbed samples.

The horizon with a low-bulk density (A2) does not show any petrographic change from an undisturbed and porous saprolite (crystallographic-preferred orientation and spatial organization of the polymineralic aggregate, Fig. 9a, b, c). The anisotropy driven by a wavy-foliated organization of the residual micas flakes and elongated quartzite bodies is evident; interstitial porosity developed by feldspar solution and also authigenic kaolinite crystallization (Fig. 9b).

On the contrary, the material with an unpreserved petrofabric and a high bulk density (A3) in the field shows distinct massive isotropic fabric at microscopic scale, consisting of fragmented kaolinite crystals, slightly oriented in section with fractured quartz bodies (Fig. 9d).

Moreover, the higher dry bulk density of the disturbed saprolite is related to the collapse of the original interstitial porosity (Fig. 9d).

The material with a partly disturbed petrofabric preserves most initial anisotropy and porosity, but is deformed at microscopic scale by micro-wrinkling (Fig. 9f), folding or even jigsaw fabric, attesting strain and lateral mass displacement and retraction fissures. The fine kaolinitic matrix is partly crushed. At the contact of the D1 unit, the saprolite presents internal sliding planes up to 30 cm from D1 contact, confirmed in thin section by a stretched jigsaw fabric, smoothed sliding planar fissures, attesting to a lateral movement of the saprolite mass compared with the alluvial D1–D2 mass (Fig. 9e).

Other units, such as C2b and D2, present late traces of well developed ice-lensing (palaeo-permafrost), cross-cutting orignal petrofabric in association with illuvial clay skins fragmentation. This fragmentation may occur as well with frost activity, but also fragment rotation, which is also indicative of seismic activity and local liquefaction (Van Vliet-Lanoë et al. 2004). Frost-induced porosity usually promotes lateral drainage.

Discussion

Liquefaction

In the southern section, liquefaction is evident by injections and the global geometry of the deposits reveals mostly a positive gradient of density where light unconsolidated saprolite is overlaid by dense gravelly sedimentary units. But the coarse-grained D2 unit revealed mostly brittle behaviour and the sandy basal layer from D1 is stretched with brittle fracturing, in agreement with the observation in parallel of sliding planes close to the contact of the deformed saprolite. The occurrence of subsurface overconsolidation of the saprolite at Pénestin, with reduction of the intersticial porosity, thin mud injection and fabric wrinkling, suggests rapid deformation (Van Vliet-Lanoë et al. 1997a) but the development of the large deformations with larger injection seems related to a slower motion over several days.

Liquefaction susceptibility reflects the relative resistance of soils to loss of strength when subjected to ground shaking. Primarily, physical properties and soil conditions such as sediment grain-size distribution, compaction, saturation, and depth govern the degree of resistance. Cohesive soils such as clays or silts are generally considered poorly susceptible to liquefaction. Soils resistant to liquefaction include all sediments that are dry or consolidated (Ruxton 2004). In the USA most geotechnical studies take into account liquefaction susceptibility for saprolite (Ruxton 2004; Derakhshandi et al. 2007).

Co-seismic liquefaction is always associated with water-saturated sediments (Seed and Idris 1971)—with moist, coherent and porous sediments able to reach oversaturation by fabric collapse or with sediments oversaturated by co-seismic water supply (Sibson et al. 1975; Sibson 1981; Muir-Wood and King 1993). Co-seismic liquefaction also leads to overconsolidated sediments at shallow depth although the superficial layers are liquefied. The effect of plastic fines (kaolinite) on pore pressure generation in saturated sands reveals that specimens with up to 20% plastic fines content generated larger values of pore water pressure than clean sand specimens but the excess pore water pressure at 30% fines content decreased below that of clean sand (Derakhshandi et al. 2007). It means that liquefaction is highly dependent on the local composition of the saprolite and the alluvial sands.

At Pénestin we interpret evidence of liquefaction and overconsolidation in normally cohesive sediment as a result of fabric collapse and supplementary transient water supply. An external trigger for liquefaction and a complementary water supply were obviously needed here to explain it. As water is a non-compressible fluid, the alternating squeezing and suction from the local water table in the faulted basement that were caused by vibrations rise in excess pore water pressure (Woith et al. 2003). This advective overpressure with subsequent liquefaction needed to reach a minimum 1.5 bar (overburden weight) in the overlying saprolite. This is probably the result of surface seismic waves propagation perpendicular to the main fault system, simple compressive P waves and squeezing by peristaltism Rayleigh waves. At Pénestin an oversaturation in sediments raised by fabric collapse and by co-seismic water supply can lead to mud escape towards the surface, as apparently visible in the southern part of the section (south, Pointe de Poulante). This ejection of mud is normally locked by overburden sediments. Here the overburden weight is limited by erosional truncation and mud ejection was made easier. D2 unit setting is associated with a sea level probably close to c.4 m NGF (present HWM) but the regional water table could have been relatively higher, as discussed further (see Reconstruction).

When saturated silty deposits are subjected to earthquake-induced shaking, pore water pressure progressively builds up, leading to loss of soil strength and liquefaction or even fluidization (Sibson et al. 1975; Sibson 1981; Muir-Wood and King 1993). An earthquake of strong magnitude can liquefy various cohesive sediments. Above 15% of clay, the viscosity of the mud may be reduced from 10^5 poises to 10^3 poises (Ruxton 1985), which is already enough to permit motion.

Youd et al. (2004) have observed on instrumented liquefaction sites that soil-softening led to lengthening of period of ground motion and to the amplification of the long period, owing to a liquefaction-transmitted ground oscillation. The main point made by Youd et al. (2004) is that ground oscillation led to a continued rise of pore water pressures after ground-shaking ceased. The generated overpressure is confined at depth in the regional water table contained in a fractured substratum with low conductivity (Montgomery and Manga 2003). During past years major earthquakes that have occurred, such as that in 1964 in Anchorage Alaska, have demonstrated the effects of soil liquefaction on silty soils. Observation during this seism showed the development of a self-consolidation polygonal pattern in silty depressions with mud expulsion in nodal position (Grantz et al. 1964). Liquefaction was very important even on gentle slopes at the foot of the Turnagain hills, with lateral spreading and sliding of a rafted suburb of Anchorage (Martirosyan et al. 2002). A similar situation was described concerning saprolite in Puerto Rico (Santiago and Larsen 2001) but also in Brittany for palaeo-earthquakes in poorly-drained sands in Upper Pliocene position (Reguigny, Henanbihan; Van Vliet-Lanoë et al. 2004).

Periglacial deformation or shale diapirism?

The Pénestin deformations are firstly interpreted by Rivière and Vernhet (1962) as pingo scars, an ice hydrolaccolith relative to continuous permafrost, as evidenced in the form of ice-wedge casts, but the clustered deformations do not fit the cone-in-cone internal fabric related to the ice-body collapse (thermokarstic depression formed by the fusion of ice accumulation) observed by De Gans (1988) and the isolated occurrence of such structures. Other periglacial mounds, known as palsa and formed by the accumulation of ice lenses in the ground, could correspond to these deformations, as they occur in clustered locations, on wet silty or clayish surfaces, sloppy or not. Hereto, the observed deformations do not fit those described on sections by Pissart (1983). In scars of pingo and of palsa, regular layers overturning is observed into the rims of the scar, sometimes disrupted by normal faults (pingo) and a lacustrine sedimentation or peat usually develops within the central depression (Van Vliet-Lanoë et al. 2004). Another situation can induce diapirs at shallow depth as a residual thick icecap decaying on oversaturated subglacial sediment such as glacio-marine or glacio-lacustrine silts and clays (Brodzikowski and Van Loon 1980; Schwan et al. 1980). This process is far from the Pénestin palaeo-climatic context, as the site is located at least 800 km of the southernmost extent of the British ice-sheet (Clarck et al. 2004). The remaining possible mechanisms for macroscopic deformations are thus shale diapirism or synsedimentary folding.

Diapirs

If often converging in morphology with folding (Powley 1999), shale diapirism usually develops in marine basins in association with fast sedimentation, strong sedimentary overburden leading to water overpressure in unconsolidated sediments. Active shale diapirism occurs when the overburden layer is thinned by tension and the mobilized shales are pushed upward in response to the rise in internal pressure (Vendeville and Jackson 1992a; Van Rensbergen et al. 1999). During burial, dewatering and compaction at the shale/overburden contact builds a permeability barrier which prevents further drainage and may induce overpressuring within the shale unit, even at shallow burial depths (e.g. 150 m, in the southern North Sea, Henriet et al. 1991). A clay with a high interstitial water pressure behaves cohesively but when the water pressure rises, it behaves as a fluid, with a very low dynamical viscosity, inducing buoyancy forces and hydraulic fracturing in the confining layer, with differential loading (Bolton and Maltman 1998). The initial diapir shape is modified by lateral or oblique upward migration of fluidized shales and may generate a network of clay dykes and sills. They usually develop in the form of ring or conic faults, which help the rise of the diapir. When the hydraulic pressure is lowered, the shale diapirism normally stops, followed by drainage and consolidation (Vendeville and Jackson 1992b; Powley 1999) followed by a later normal collapse, inducing conic faulting.

Folding

Another hypothesis for the macroscopic deformations could be late disharmonic surface folding of an unconsolidated surface in response to the plastic behaviour of the unconsolidated surface material on a deforming basement (Fig. 7b). This situation, on similar lithologies, is common in the Pannonian Basin (Magyari et al. 2005) but difficult to apply to the geometry of deformation at Pénestin, which is clearly connected with the apex of basement faults. Before the Pénestin event, the water table was high, allowing folding, and the saprolite was coherent but porous. After the deformation, the whole system has been truncated by a late erosion surface related to the periglacial regime of MIS 8 and MIS 6, without younger evidence of "folding". Tectonic transpressive folding hypotheses thus do not fit the observations in both the north and the south of Pénestin section, as discussed previously.

Shale diapirism triggered by earthquake

At Pénestin there is no evidence of thick overburden sediments to justify confining, since alluvial sedimentation stopped at about 300 ka BP, prior to the main deformation. D1–D2 units consist mostly of dense gravels occluded by clay illuviation (paleosol), behaving as a limited confining system for the saturated saprolite in accordance with the observed mud injection (Fig. 6e). An extra pore-fluid was produced locally to trigger the diapiric motion and may be explained by seismic-induced water supply along the normal faults observed in the basement, as discussed earlier. This localized overpressure source induced a metric swell or bulge of the saprolite at the apex of the injection point, resulting in the rigid confining alluvial system in tension gashes development also close to its apex. During the fracturing process, an inner hydraulic pressure gradient was probably involved in fracture opening, as stressed by Levi et al. (2006b) for hydrofracturing process forming clastic dykes. Nevertheless, it is difficult to assess whether that fracturing and fluidization were synchronous, but tension gashes were apparently rapidly injected by the fluidized saprolite (see petrography) and mud masses locally extruded to the surface. Russian geologists have observed this phenomenon in the region of the Caspian Sea after an earthquake (A.A. Vassiliev, personal communication). The conic faulting further developed, marked and eased by injections of fluidized saprolite on the side of the diapirs. It is this fracture geometry, which has been confused with flower structures owing to transpressive shear (Figs. 6b, 7a,). More specifically, at microscopic scale, the laminated pattern of the undisturbed saprolite and the rise in internal water pressure resulting from the earthquake have helped the shearing-sliding between the kaolinite flakes, detached in water as platy sands and loams. It mostly formed a cohesive fluid promoting the shale diapirism. To conclude, shale diapirism should explain most but not all the mesoscopic deformational structures such as stretching in sands and sliding planes developed in the saprolite observed at the base of the bowl-like structures (Fig. 6b, e).

Shale diapirism associated with rafting

These mechanisms, co-seismic fluidization and diapiric motion, do not perfectly explain the elongation of the observed macroscopic patterns and their higher frequency close to the summit of the Poulante Point. The elongation develops in parallel with the main slope (E–W 1%) of the Pénestin peninsula. During the Anchorage earthquake discussed previously, the sliding of the whole liquefied saprolite mass induced buoyancy and also the rafting of sedimentary bodies (Seed and Wilson 1967). For Pénestin, alternative raft models can be proposed. On the first one, the sliding is perpendicular to the positive ridges that correspond to local mud diapirs in stretched areas (Fig. 7e). On the second model, the raft structures are groove-shaped and each raft is separated by and striking along mud diapirs (Fig. 7d). This last model is in accordance with the topographic slope towards the sea (marine lowstand at the time of the deformation) and also with normal-sinistral kinematics observed on NE-SW slickensides in the deformed saprolite which can be coeval with apparent "transpressive faulting" along the sides of the rafted alluvial bodies. This could have stretched the inter-injection bodies by rafting along slope just like periglacial stripe pattern ground (Van Vliet-Lanoë 1998), fitting our earlier observations. Upslope, the stretching and/or thinning of the overburden alluvial body limits the confining and facilitates the upward migration of the saprolite diapir. In downslope, the accumulation by mass wasting or rafting of the alluvial body will limit the extrusion of the saprolite by thickening the confining overburden.

Reconstruction of the Pénestin event: a combination of seismogenic liquefaction, shale diapirism and lateral spreading

With this succession of mechanisms, nearly synchronic, we are now able to reconstitute the whole story. A major earthquake may have occurred around 280–290 ka when the climate was already periglacial and the braided fan of the Vilaine River was prograding from the onset of the MIS 8 regression. The sea level was not yet too low, the regional water table still high and the permafrost still absent. During the earthquake, the water was supplied by the fractured weathered substratum, fluids probably escaping along basement fault nets, bulging the saprolite locally and consequently weakening the rigid confining alluvial body. When the basal conglomerate is consolidated by goethite and not permeable, no shale diapirism developed in the saprolite. The bulging saprolite went over the plastic limit and in the upper layer (unit A3), the liquid limit; then it began to rise, deforming rapidly the base of the C2b, D1 and D2 deposits. Conical to wedge-like tension fractures developed in the wall of the alluvium and were immediately filled with injected kaolinite mud (Fig. 4e). The rising interstitial pressure helped the extrusion of the diapirs. This process probably continued to evolve with the continuing rise of pore water pressures after ground shaking ceased. The diapir movement probably persisted for several hours after the seism and generated lateral spreading. The mass displacement may have been mostly south-westward, following the main slope. The sliding was groove-shaped by differential loading of the D1 gravels, parallel to the diapirs

separating the various corrugations. Such displacement appears to be in accordance with palaeo-slopes deduced from sedimentological data (original setting of unit D2) and with normal-sinistral kinematics measured on sheared saprolite along the faults just below the ENE–WSW striking mud diapirs.

The question remains only partly open regarding the "folds" in the northern part of the section. The change in style of deformation is clearly related to the change in lithology and to the intensity of the weathering of the basement. The weathered micaschists (unit A2 only) remain brittle. Co-seismic water supply from the faults was direct. Here, the discontinued nature of the preserved tidalite clay at the top of the section did not allowed the confining of the hydrostatic pressure, limiting in consequence the potential development of the deformation. Moreover, the alluvial sands, porous even enriched in illuvial clays, did not allowed the rise of important pore overpressure, as demonstrated experimentally by Derakhshandi et al. (2007). The "folds" in the northern part of the section thus reflect an aborted shale diapirism.

Significance in terms of regional geodynamics

The present-day estuary of the Vilaine is located at the east of the subsiding block of the Morbihan on an important secondary fault of the SASZ fault bundle (Fig. 1). The palaeosurface truncating the saprolite is old, probably late Eocene to Oligocene, and was reactivated during a Messinian lowstand. The tilting of the blocks is probably pre-Oligocene or even much older, with the discrete subsidence of the southern coast of Brittany since the early Cretaceous. Similar deformational structures, possibly synchronous, were observed at Bétahon (Fig. 1) in tidal clays but are larger in size on the other side of the present-day Vilaine estuary (Guillaume-Bruno 1972). The date of the palaeo-earthquake roughly signalled the onset of a regional relaxation event after a regional compressional event (circa 430–280 ka) with some additional disturbances by the building of major ice sheets in Britain (MIS 12 and 10; Van Vliet-Lanoë et al. 1997a, 2002). After this event, the saprolite probably desiccated during the Saalian I (MIS 8; 280–240 ka) by segregated ice development into the permafrost associated with the development of ice-wedges and by subsequent drainage of the alluvial body when permafrost thawed. Today a superficial water table is perched on the saprolite A3 consolidated by co-seismic liquefaction.

Evidence of strong tectonic activity was also recognized at 280 ka in many places at that time in Western Europe (Van Vliet-Lanoë et al. 2002). Former major tectonic events are usually closer to 1,000–800 ka (Van Vliet-Lanoë et al. 2002), a fact that should perhaps imply a period of relative quiescence from circa 800 to 300 ka. Tectonic movements are still recorded by change in channel position by the Vilaine River between the two periods. At the time of the earthquake, between 317 and 280 ka, the sea level was low at −50 m based on $\delta^{18}O$ (curve by Funnel 1995), but from dated coastal sites in the English Channel and Brittany, it was usually very close to the present-day sea-level, under control of basement buckling deformation (Van Vliet-Lanoë et al. 2000). The regional water table was thus shallow at that time and probably at least brackish or even marine as presently in the granite of Ploemeur-Bodou, a condition which favours the peptization by Na^+ of the kaolinite, also lowering its bearing capacity, enabling fluidization.

Significance in terms of geodynamics

Such development in tectonically active regions is thus basically linked to the occurrence of an unconsolidated clay body (sedimentary or saprolite). It is also linked to the presence of a rather shallow water table and a confining surface layer such as consolidated clayish conglomerate or even a lodgement till. In formerly glacierized regions, it can trace the normal load of dead ice bodies on unconsolidated mud (Brodzikowki and Van Loon 1980) but also seismic activity induced by glacio-isostatic rebound (Hasegawa and Basham 1989). Outside the glacial limits, so-called "periglacial" diapirs in sectors like the Rhine Graben (Strunk 1983) or in basins like the Bovey Tracey one (Devon), are more likely induced by seismically induced shale diapirism or by disharmonic surface folding. In the Bovey Tracey basin we had the chance to observe classical diapirs in an abandoned clay-pit next to the main china-clay pit described by Jenkins and Vincent (1981). This should also justify our interpretation.

Conclusion

The deformations observed along the Mine d'Or section at Pénestin represent the evidence of successive mechanism triggered by an earthquake linked to the discrete subsidence of the Southern Armorican margin. These events are recorded on an already deformed and deeply weathered basement that allowed the shale diapirism to develop. They are probably more or less synchronic with other regional events at the onset of MIS 8. The major deformational process is shale diapirism, initially triggered by co-seismic water supply, loading and lateral rafting, favoured by the liquefaction of the saprolite. High and saline water table (saline marine water wedge) at the time of the earthquake eased the fluidization. No quaternary transpressive

tectonics are evidenced at this precise site which registered distant effects of an earthquake, as no local rupture is evidenced in the field. Neither traces of periglacial pingo nor palsa are observed at Pénestin, despite the presence of a palaeo-permafrost. During the seismic after-shock the shale diapirism probably developed further on. This whole process resulted, especially at the Mine d'Or, in a liquefied mud, which led to a local mega-load cast on top of the saprolite and burst out onto the surface, with lateral shortening induced by pulsated motion (wrinkling). Post-seismic relaxation, drainage and normal collapse of the stretched saprolite allowed some normal tension faults to develop, probably also related to the mass wasting, especially near La Source. Diapir motion probably persisted at much lower rates for a few days or weeks, controlled by the main topographic slope, explaining the bulging of some of the diapirs exploited on tension zones by younger ice-wedges (c. 260 ka, MIS 8), when permafrost developed and definitively stopped the motion by free drainage induced by cryogenic residual porosity.

Seismically induced shale diapirism seems to be frequent in active continental basins, when a shallow water table is available to promote liquefaction of non-consolidated shales.

Acknowledgments This paper Contribution No. 1046 of the IUEM, European Institute for Marine Studies (Brest, France).

References

Bolton A, Maltman A (1998) Fluid-flow pathways in actively deforming sediments: the role of pore fluid pressure and volume change. Mar Petr Geol 15:281–297

Brault N, Guillocheau F, Proust J-N, Nalpas T, Brun J-P, Bonnet S, Bourquin S (2001) Le système fluvio-estuarien Pléistocène moyen-supérieur de Pénestin (Morbihan): une Paléo-Loire ? Bull Soc Geol France 172:563–572

Brodzikowski K, Van Loon AJ (1980) Sedimentary Deformations in Saalian Glaciolimnic Deposits near Wlostow (Zary area, Western Poland). Geol Mijnb 59:250–272

Clark CD, Gibbard PL, Rose J (2004) Pleistocene glacial limits in England, Scotland and Wales. In: Ehlers J, Gibbard PL (eds) Quaternary glaciations: extent and chronology, Part I: Europe. Developments in quaternary science. Elsevier, London, pp 47–82

De Gans W (1988) Pingo scars and their identification. In: Clark MJ (ed) Advances in periglacial geomorphology. Wiley, London, pp 299–322

Derakhshandi M, Rathje EE, Hazirbaba K, Mirhosseini SM (2007) The effect of plastic fines on the pore pressure generation characteristics of saturated sands. Soil Dyn. Earthquake Engine. Corrected Proof, Available online 2 August 2007 (in press)

Durand S (1960) Le Tertiaire de Bretagne. Etude stratigraphique, sédimentologique et tectonique. Mém Soc Géol Min Bretagne 1, 389p

Eissmann L (1981) Periglaziäre Prozesse und Permafroststrukturen aus sechs Kaltzeiten des Quartärs. Altenberger Naturwis. Forsch 1, 171p

Estéoule-Choux J (1983) Altérations et silicifications au tertiaire dans le Massif Armoricain. Géol. France 4:345–352

Funnell BM (1995) Global sea-level and the (pen)insularity of late Cenozoic Britain. In: Preece RC (eds) Island Britain: a quaternary perspective, vol 96. Geological Society, London, Special Publ, pp 3–13

Grantz A, Plafker G, Kachadorian R (1964) Alaska's good friday earthquake, March 17, 1964. A preliminary geologic evolution. Geol Surv Circular 491

Gapais D, Lagarde J-L, Le Corre C, Audren C, Jegouzo P, Casas Sainz A, Van Den Driessche J (1993) La zone de cisaillement de Quiberon. Témoin d'extension de la Chaîne Varisque en Bretagne méridionale au Carbonifère. CR Acad Sci Ser II 316:1123–1129

Guillaume-Bruno S (1972) Le Plio-Quaternaire des Côtes du Morbihan.Etude sédimentologique et stratigraphique. Université d'Orsay, Thèse III cycle (PhD), 110p

Hardenbol J, Thierry J, Farley MB, Jaquin T, de Graciansky PC, Vail P (1998) Mesozoic and Cenozoic Sequence Chronostratigraphic chart. In: Mesozoic and Cenozoic Sequence Stratigraphy of European basins, SEPM spec. public., 60

Hasegawa HS, Basham PW (1989) Spatial correlation between seismicity and postglacial rebound in Eastern Canada. In: Gregersen S, Basham PW (eds) Earthquakes at North-Atlantic Passive Margins: Neotectonics and Postglacial Rebound, Kluwer, Dordrecht, pp 483–500

Henriet JP, De Batist M, Verschuren M (1991) Early fracturing of Palaeogene clays, southernmost North Sea: relevance to mechanisms of primary hydrocarbon migration. In: Spencer AM (ed) Generation, accumulation and production of Europe's hydrocarbons (Spec. pub.). Eur Ass Petrol Geosci 1:217–227

Jégouzo S (2001) Analyse du recul de la falaise littorale de la mine d'Or. Applied Mast. Th. Géode, Lille 1 University, 90 p

Jenkins DG, Vincent A (1981) Periglacial features in the Bovey basin, south Devon. Proc Ussher Soc 5:201–205

Klein C (1996) Du polycyclisme à l'acyclisme en géomorphologie. Ophrys, Paris, 299 pp

Laurent M (1993) Datation de quartz de formation quaternaires, comparaison avec le paléomagnétisme. Thèse Muséum d'Histoire Naturelle, Paris, 104 pp

Lawrence D (1980) Some properties associated with kaolinitic soils. Geotechnical Group, PhD thesis, Cambridge University, 67 pp

Levret A, Backe JC, Cushing M (1994) Atlas of macroseismic maps for french earthquakes with their principal characteristics. Nat Hazards 10:19–46

Magyari Á, Muszbz B, Csontos L, Unger Z, Van Vliet-Lanoë B (2005) Late quaternary neotectonics south of Lake Balaton (Somogy Hills), SW Hungary—evidence from field observations. Tectonophysics 410:43–62

Martirosyan A, Dutta U, Biswas N, Papageorgiou A, Combellick R (2002) Determination of site response in Anchorage, Alaska on the basis of spectral ratio methods. Earthq Spectra 18:85–104

Muir-Wood R, King GCP (1993) Hydrologic signatures of earthquake strain. J Geophys Res 98:22035–22068

Montgomery DR, Manga M (2003) Streamflow and water well responses to earthquakes. Science 300:2047–2049

Obermeier SF (1996) Using liquefaction—induced features for paleoseismic analysis. In: McCalpin J (ed) Paleoseismology, Academic Press, London, pp 331–396

Pissart A (1983) Remnants of periglacial mounds in the Hautes Fagnes, Belgique; structure and age of the ramparts. Geol Mijnb 62:551–555

Powley DE (1999) Shale Domes Search and Discovery Article #60001, Amoco Production Company web report

Proust JN, Menier D, Guillocheau F, Guennoc P, Bonnet S (2001) Les vallées fossiles de la Baie de la Vilaine: Nature et évolution du

prisme transgressif du Pléistocène armoricain. Bull Soc Geol France 172:733–749
Rivière A, Vernhet S (1962) Accidents périglaciaires dans la région de Pénestin, (Morbihan). CR Acad Sci Paris 255:744–746
Ruxton BP (1985) The structure of some debris flows in Hong Kong. Geol Soc Hong Kong Bull 2:105–111
Ruxton BP (2004) Contrasting regolith structures: hydroplastic undulations or fluidised piercement giving megaboles. In: Roach IC (ed) Regolith. CRC LEME, pp 311–315
Santiago M, Lanzen MC (2001) Earthquake induced landslide susceptibility in the San Juan Metropolitan Area, Puerto Rico: US Geological Survey, Open file Rep 01–39, 1 CD
Schwan J, Van Loon AJ, Steenbeek R, Van Der Gaauw P (1980) Intraformational clay diapirism and extrusion in weichselian sediments at Omehuj (Funen, Denmark). Geol Mijnb 59:241–250
Schwarz T (1994) Ferricrete formation and relief inversion: an example from Central Sudan. In: Schwarz T, Germann K (eds) Lateritization processes and supergene ore formation. Catena 21:257–268
Seed HB, Idriss IM (1971) Simplified procedure for evaluating soil liquefaction potential. J Soil Mech Found Div Proc Am Soc Civil Eng 97:1249–1273
Seed HB, Wilson SD (1967) The turnagain heights landslide, Anchorage, Alaska. J Soil Mech Found Div ASCE 93:325–353
Sibson RH (1981) Fluid flow accompanying faulting: field evidence and models. In: Simpson DW, Richards PG (eds) Earthquake prediction: an international review, vol 4. Maurice Ewing Ser., Washington DC, pp 593–603
Sibson RH, Moore J, Rankin RH (1975) Seismic pumping—a hydrothermal fluid transport mechanism. J Geol Soc Lond 131:653–659
Sibuet JC (1972) Histoire structurale du Golfe de Gascogne. PhD Thesis, Orsay University, 175 p
SISFRANCE (1996) Base de la macrosismicité française. CEA-IRSN-BRGM
Skempton AW (1953) The colloidal activity of clays. In: Proceedings of the 3rd international conference on soil mechanism and foundation engineering, Switzerland, vol 1, pp 57–61
Schunk H (1983) Pleistocene diapiric upturnings of lignites and clayey sediments as periglacial phenomena in central Europe. 4th Intern. Permafrost Conf. Proc., Nat. Academic Press, Washington DC, 1:1200–1204
Van Rensbergen P, Morley CK, Ang DW, Hoan TQ, Lam NT (1999) Structural evolution of shale diapirs from reactive rise to mud volcanism; 3D seismic data from the Baram Delta, offshore Brunei Darussalam. J Geol Soc 156:633–650
Van Vliet-Lanoë B (1998) Frost and soils: implications for paleosols, paleo-climates and stratigraphy. Catena 34:157–183
Van Vliet-Lanoë B (2005) LA PLANETE DES GLACES. Histoire et environnements de notre ère glaciaire. Vuibert, Paris, 430 p
Van Vliet-Lanoë B, Bonnet S, Hallégouët B, Laurent M (1997a) Neotectonic and seismic activity in the Armorican and Cornubian Massifs: regional stress field with glacio-isostatic influence? J Q Geodyn 24:219–239
Van Vliet-Lanoë B, Hallégouët B, Monnier JL (eds) 1997b The Quaternary of Brittany. Rev. Archeol. Prehist. No. spec. University of Rennes 1:153 pp
Van Vliet-Lanoë B, Laurent M, Baleriaux S, Baham JL, Falguères C, Field M, Keen D, Hallégouët B (2000) Middle Pleistocene raised beaches anomalies, English Channel and Dover Strait. Regional and Global Stratigraphic Implications. J Q Geodyn 29:5–41
Van Vliet-Lanoë B, Meilliez F, Maygari A (2004) Distinguishing between tectonic and periglacial deformations of Quaternary continental deposits in Europe. Glob Planet Ch 43:103–127
Van Vliet-Lanoë B, Vandenberghe N, Laignel B, Laurent M, Laridon A, Louwye S, Manry JL, Meilliez F, Mercier D, Hallégouët B, Lacquement F, Michel Y, Mogueded G (2002) Paleogeographic evolution of Northwestern Europe during the upper Cenozoic. Geodiversitas 24:511–541
Vendeville BC, Jackson MPA (1992a) The rise of diapirs during thin-skinned extension. Mar Petr Geol 9:331–353
Vendeville BC, Jackson MPA (1992b) The fall of diapirs during thin-skinned extension. Mar Petr Geol 9:354–371
Wozh H, Wang R, Milkereit C, Zschau J, Milwald U, Pelidoger A (2003) Heterogenous response of hydrogeological systems to the Izmit and Düzce (Turkey) earthquakes of 1999. Hydrol J 11:113–121
Wyns R (1991) Evolution tectonique du bâti armoricain oriental au Cénozoïque d'après l'analyse des paléosurfaces continentales et des formations géologiques associées. Géol de la France 3:11–42
Youd TL, Steidl JH, Nigbor RL (2004) Lessons learned and need for instrumented liquefaction sites. In: Soil Dynamics and Earthquake Engineering, vol 24. Elsevier, Amsterdam, pp 639–646
Zagwijn WH (1989) The Netherland during the tertiary and the quaternary: a case history of coastal lowland evolution. Geol Mijnb 68:107–120
Ziegler PA (1992) European cenozoic rift system. Tectonophysics 208:91–11

- DAY TWO -

Scientific excursion to the Quaternary of Northern Brittany

Thursday, 25 September 2008

Leader: Jean-Laurent MONNIER

Routes which will be followed between RENNES and ST BRIEUC BAY.

Note the stop at MONT ST MICHEL and the night in St LO.

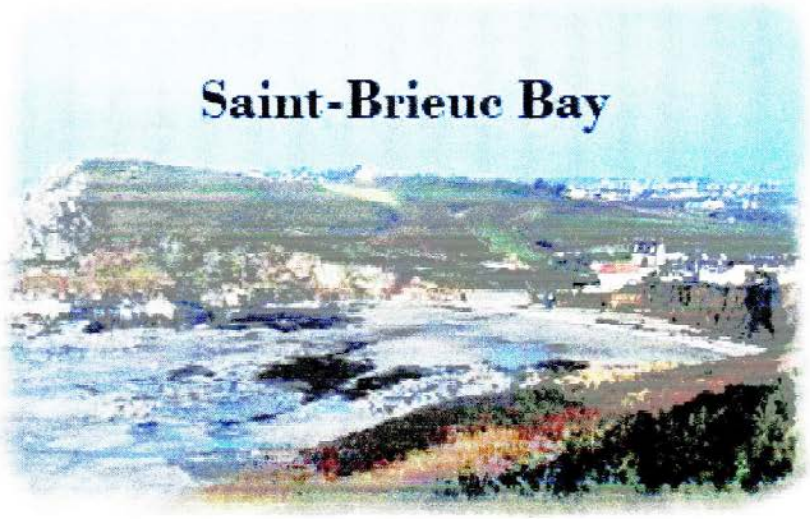

Centre de Recherche en Archéologie Archéosciences Histoire

UMR 6566

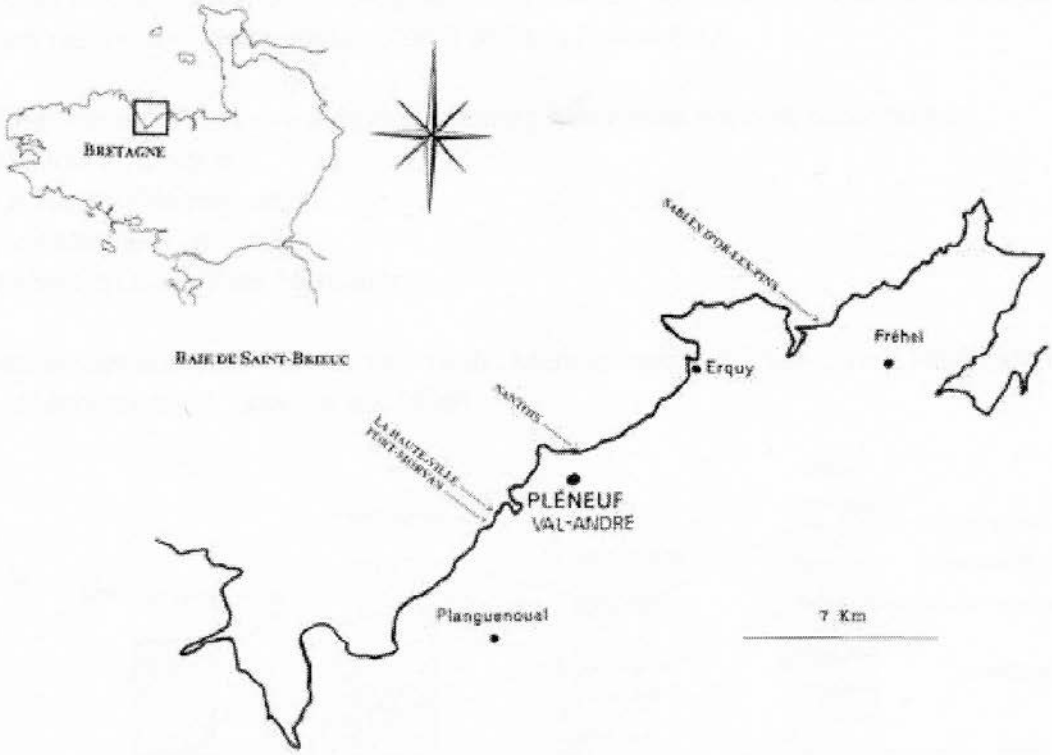

Fig. 1: Carte de localisation de la coupe de Nantois.
Fig. 1: Location map of the Nantois section.

General considerations

The stratigraphy of the Pleistocene deposits of Northern Brittany is mainly based on the study of sections of marine cliffs showing sediments trapped by coastal depressions (river beds or valley slopes).The previous valleys cut in the hard rocks are consequently often "fossilized" by periglacial loam deposits actually in "balcony" position because they were latter cut by the actual marine erosion.
The sediments can be characterized as loess, sandy loams deposited either by the wind or the running waters, slope crumbled rocks, head deposits incorporating various types of stones and dunes or old beaches, marine boulder bars ; sometimes interbedded by more or less developed "paleo-soils".

Study of the numerous sections known all along the Northern coast of Brittany permitted, by successive correlations (and taking account of the gaps), to establish a chronostratigraphic reference scale.

The periglacial loess does not reach any significant development inside Brittany, when compared with the sediment infilling of the coastal depressions that now form the cliffs.

The Northern coast of Brittany displays an important development of the loams of the second half of the Middle Pleistocene and of the Upper Pleistocene. Four formations, in the geological sense of the term, have been recognized in the eastern coast of Saint Brieuc Bay.

In the Pleneuf-Val-André area the following formations are now recognized:
- Nantois Formation.
- La Haute-Ville Formation.
- Port Morvan Formation.
- Sables-d'Or-les-Pins Formation.

(Hallégouet and Van-Vliet-Lanoê, 1986 ; Monnier and Van Vliet-Lanoê,1996 ; Monnier and Bigot,1987; Bigot and Monnier,1987, Loyer *et al.*, 1995).

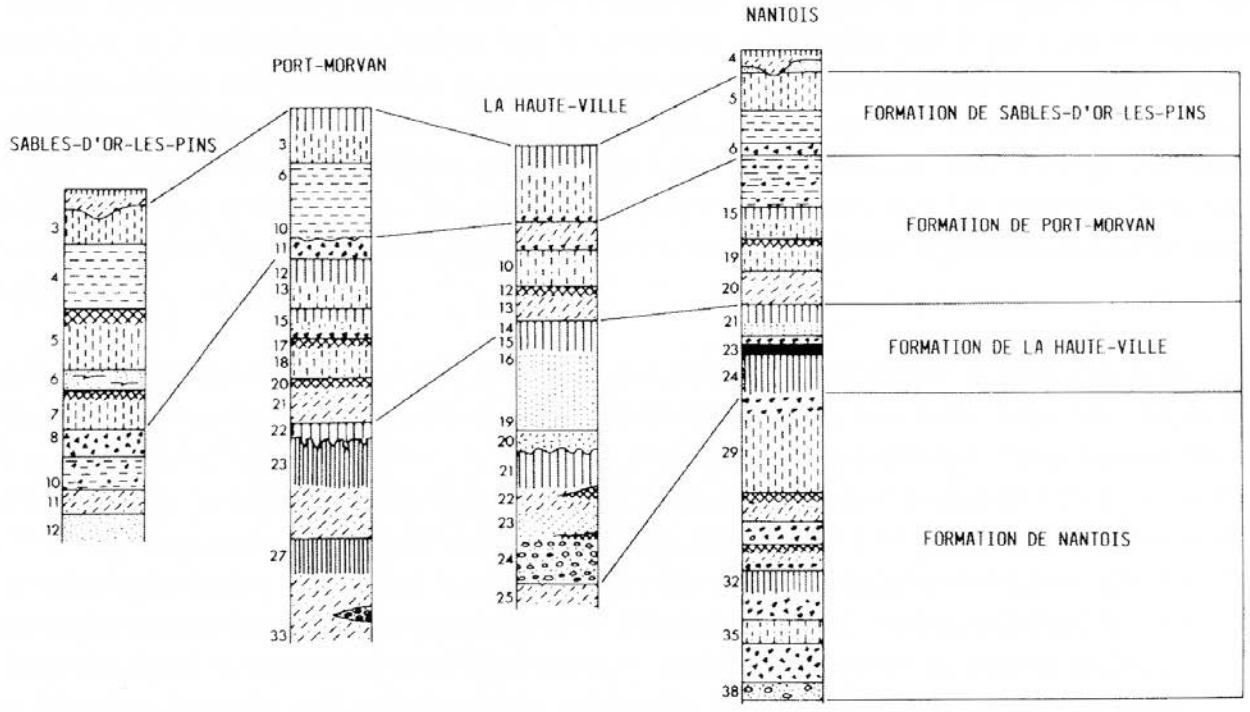

Fig. 10. — Schéma récapitulatif de la lithostratigraphie et des formations définies.
(La Formation de Nantois sera ultérieurement révisée).

Fig. 10. — Recapitulative diagram of the lithostratigraphy and of the defined formations.
(The Nantois Formation will be ulteriorly revised).

loess massif horizon oxydé loess à lits sableux sol isohumique loess massif sable fin lité loess grossier massif	FORMATION DE SABLES-D'OR-LES-PINS
head (lité) sol brun calcique limon sableux carbonaté sol brun calcique limon sableux carbonaté cailloutis sol isohumique sable limoneux carbonaté sol isohumique dune carbonatée colluvions sableuses	FORMATION DE PORT-MORVAN
sol lessivé dune fluée dune décarbonatée sol lessivé head limoneux sable dunaire flué ranker plage ancienne	FORMATION DE LA HAUTE-VILLE
loess, head et paléosols	FORMATION DE NANTOIS

The Nantois formation is made of thick deposits resulting from a strong sedimentary activity (cryoclastic blocks layers, clayish and sandy loams, loess with carbonated concretions). It also exists some interbedded sands of marine or coastal origin as well as layers made from of old soils, which are used as markers. This formation corresponds with two different glacial/interglacial cycles (isotopic stage 6 to 9) which precedes the last stage (5 to 2). There is consequently here, during three different periods of time (between about 330 000 and 125 000 years) evidences of mild interglacial stages where the sea level was close to nowadays and the forest landscape more or less similar. The carbonated part of the loess's and other sandy loams cannot originate in the English Channel, which suggests, at some moments, large regressive episodes and widely open surfaces open to wind activity.

La Haute-Ville Formation is, in opposition, characterized by a low sedimentary activity, that is to say that erosions and pedologic horizons are very important respect with the loamy sedimentation. This is at the origin of large gapes in the stratigraphic successions. It witnesses the existence of a complex interglacial dynamics which can be approximately correlated with the isotopic stage 5 (between 125 000 and 75 000 years). This formation incorporates boulder bars (with boulders mixed with sands), loam layers with stony blocks emplaced by gravity sliding (sol fluxion and colluvioning), well-established paleo-soils. The Haute-Ville formation evidences consequently the presence of an interglacial climatic optimum (raised beaches in the lower part or brownish washed paleosoils) where the sea level was close to the actual level or perhaps slightly above. Two cold episodes occurred, one after the other, followed by two mild periods (about 110 000 and about 90 000 years). During these oscillations we suspect that the marine coastline could have changed between -70 and - 10m.When pollens are preserved we can establish that the vegetation was first marked by oaks groves mixed with aune and hazel trees (climatic optimum) followed during intermediate stages by their regression and the development of birches and pines (taiga). The cooler oscillations developed open landscapes dominated by herbaceous species with, by places, in deep valleys, oak groves, aulne, hazels, willows and ashes. Deposits

gathered in Haute-Ville provided the largest number of old traces of human occupation in northern Brittany. This is clearly related with geology, paleoclimates and paleogeography.

Port-Morvan Formation corresponds approximately with stage 4 and the beginning of stage 3, that is to say between 75 000 and 40 000 years. It comprises colluviums, more or less loamy and carbonated sands, and on top with sheeted loams (related with the segregation of ice and characteristic of paleo-soils). Small humus rich soils are inter-sliced in the sandy loams, witnessing the existence of short phases of climatic stability in an environment certainly more open and occupied by an herbaceous vegetation. The last paleo-soil (brown and calcareous) is well marked and represents a marker ("interpleniglacial "). Study of continental mollusk shells evidences from the bottom to the top of a drier and cooler climate, cut in places by milder climate. Port-Morvan Formation shows that more rigorous conditions developed ("pleniglacial") associated with a rare vegetation dominated by herbaceous species. The coastal domain is at that time characterized by more or less reworked elements (sand grains, shells) deposited by wind. This is contemporaneous with a marine regression and true loess conditions.
A study made in Cotentin area shows that the period running between 115 000 and 45 000 years is characterized by mixed cool-temperate forests with marine sea level close to the actual time evolving towards boreal/arctic landscapes with tundra and steppe. The latter being widespread over the littoral plain now devoid of water.

The Sable-d'Or-les-Pins Formation represents the "Upper Pleniglacial" characterized by a major loess sedimentation .After the isotopic curves it broadly corresponds with the second half of stage 3 and stage 2, that is to say between 40 000 and 15 000 years. At that time there was a strong lowering of the sea, which corresponds, with the "continentalisation" of very large surfaces of the English Channel, thus, favoring the effect of winds and loess transportation. At the beginning loess alternate with multiple sandy layers deposited by running waters, then the sandy sediments become thinner and thinner because the far origin of the sources, the dryer climate, the stronger regression). Erosion slopes sometimes separate the different layers. Paleo-soils are rare and poorly developed (tundra soils). Marks of freezing and other periglacial phenomena are well developed (syngenetic cryoturbation responsible for cracks and undulations). The rare malacologic remains confirm the cold climate. The more recent loess which only appears as thin sheets in the interior of Brittany is often eroded. They participate to the agricultural "Golden belt" of this region.
The climatic curve of Sables-d'Or-les-Pins Formation relies on the interpretation of pedogenetic remains, cryoturbation and the granulometry of loess. The general tendency is towards the development of a more sever cold episode cut by a warmer period. Some horizons witness the existence of a tundra landscape. Three important climatic breaks separate four loess sedimentary units.
The field trip will show you various sections, from West to East, in the oriental side of the St Brieuc Bay, on Pléneuf-Val-André area.

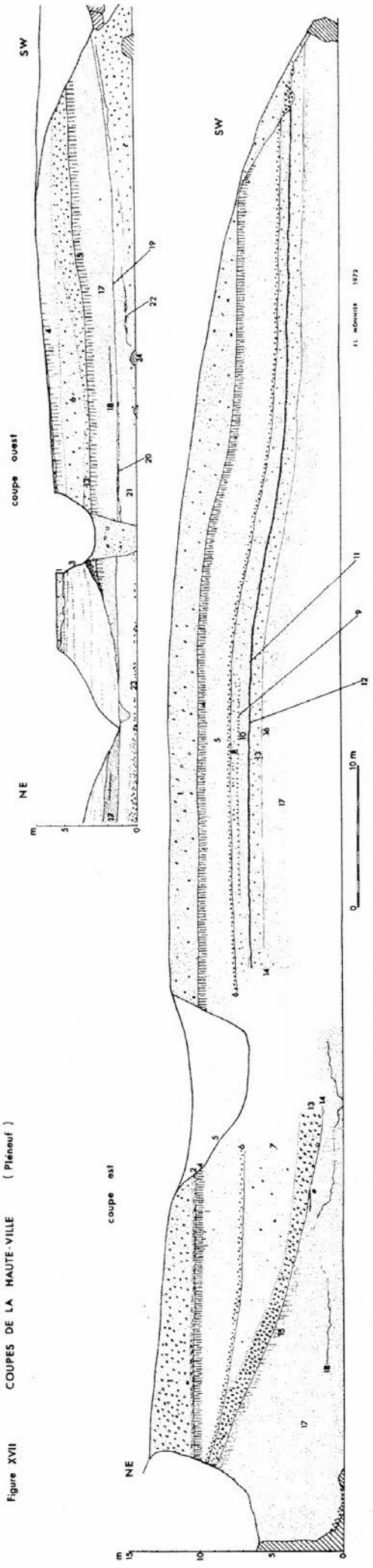

Figure XVII COUPES DE LA HAUTE-VILLE (Pléneuf)

First stop.

La haute-Ville cliffs (stratotype of the La Haute-Ville Formation).

A rocky outcrop representing without doubts an old reef, is now attached to the mainland thanks to loam deposits actually eroded by the sea. Two little bays are recognized. One in the East and the other in the West. On the western side a little brook cut across the soft sediments. In the East in contrary there no running water but the continuous crumbling of the cliff is associated with surface action of the rains. There, the erosion is very rapid.

Layers 1 and 2: loamy colluvium (post-glacial)
Layer 3 : (only western section) sandy loam with stony layers
Layer 4: compact and "prismatic" brown loam, illuviated (post-glacial forest soil)
Layer 5: calcareous yellow loess; mollusc shells (*Pupilla muscorum*)
Layer 6: stony and loamy layer
Layer 7: brown loess with calcareous nodules ; polyhedral structure (old soil)
Layer 8: sandy loam, calcareous, with mollusc shells
Layer 9: stony layer
Layer 10: sandy loam, calcareous, mollusc shells (*Cepaea sp., Vallonia pulchella, Pupilla muscorum, Trichia hispida, Cochlicopa lubrica...)*
Layer 11: sandy loam, calcareous, terrestrial mollusc shells, also broken marine chells
Layer 12: dark brown loamy humic sand (small palaeosoil)
Layer 13: brown loamy sand with rotten gravels
Layer 14 : loamy brown sand with clay, polyhedral structure (upper part of an old colluviated soil)
Layer 15: clayed brown sand with "prismatic" structure (illuviated old soil on a dune)
Layers 16 to 19: brown sand (dune)
Layer 20: loamy-clayed sand, gley
Layer 21: sandy-clayed loam, yellow-brown, polyhedral structure
Layer 22: loamy-clayed sand extended into head; presence of a small isohumic soil

Layer 23: clayed sand wit-h (at the western end of the section) of a small humic soil (ranker)
Layer 24: coarse clayed sand with marine pebbles (old beach).

In some place, this pebble beach layer is above old loams and head (MIS 6) witch have been eroded by marine erosion.

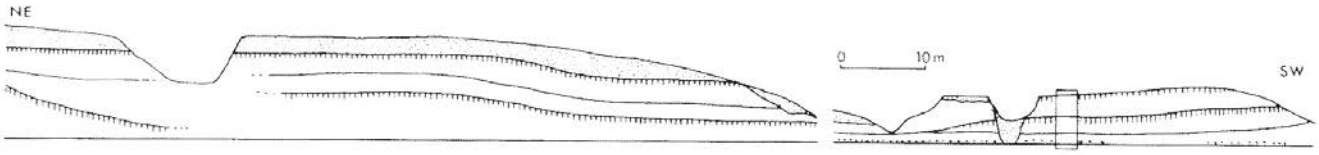

Fig. 6. — Profil général de la falaise de La Haute-Ville et localisation du stratotype sur la coupe sud-ouest.

Fig. 6. — General contour of the cliff of La Haute-Ville and localization of the stratotype on the south-western section.

The La Haute-Ville Formation corresponds to layers 24-14. It reflects the end of an interglacial series of events that took place in a littoral environment open to the effects of the west winds at the end of the last interglacial (Eemian s.s.). The interglacial optimum (i.e. MIS 5e) is represented by the pebble beach (Layer 24). Probably layers 20 to 23 represent the first cold event (MIS 5d) and the soil above is a correlative of MIS 5c. Erosion and the gleying process can correspond to MIS 5b. The dune deposit and the main palaeosoil above (layers 15 to 19) can correspond to MIS 5a.

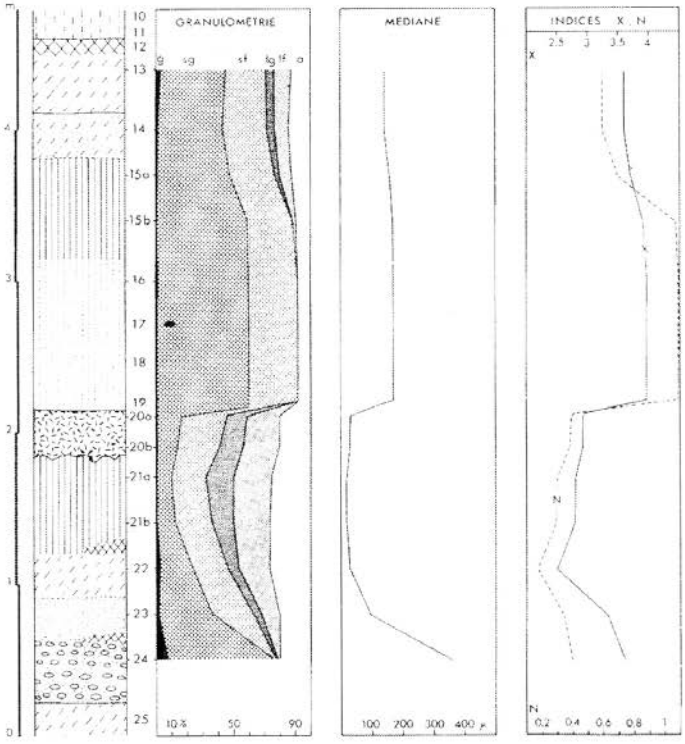

Fig. 8. — Formation de La Haute-Ville : diagrammes granulométriques.

g = graviers, sg = sable grossier, sf = sable fin, lg = limon grossier, lf = limon fin, a = argile.

Fig. 8. — Formation of La Haute-Ville : granulometric diagrams.

g = gravels, sg = coarse sand, sf = fine sand, lg = coarse loam, lf = fine loam, a = clay.

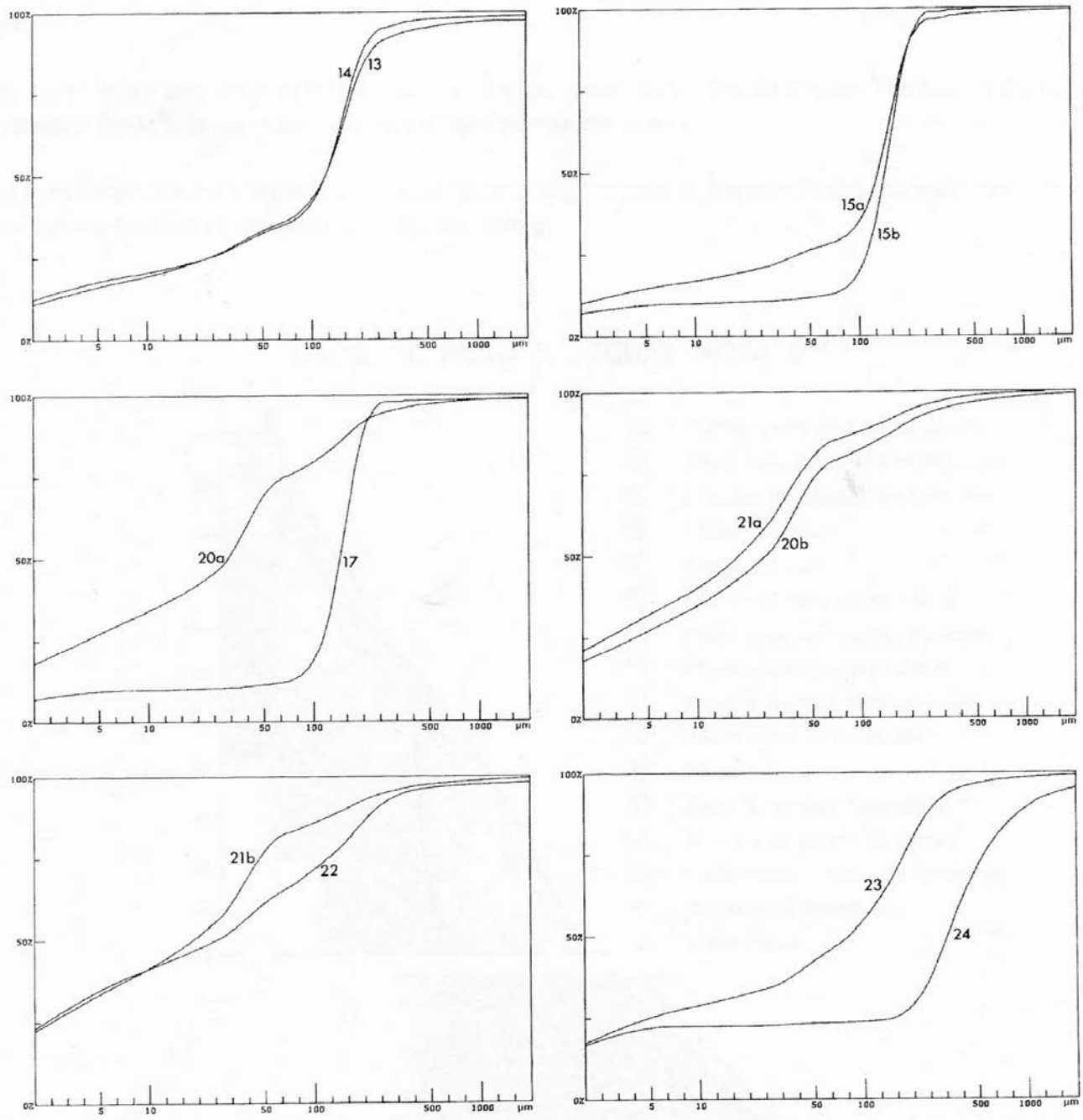

Fig. 9. — Formation de La Haute-Ville : courbes granulométriques cumulatives semi-logarithmiques.
(Pipette d'Andreasen + tamisages). Les numéros renvoient aux couches décrites.

Fig. 9. — Formation of La Haute-Ville : semi-logarithmic, cumulative granulometric curves.
(Pipette of Andreasen + sifting). The numbers refer of the described layers.

Second stop.

Piégu.

Piégu is a Middle Palaeolithic settlement which was excavated during the 1987 year. The face of the site had been strengthened with concrete. So, we cannot see now the layers.

Piégu is important for the knowledge of neandertalian occupations in Western France. Correlations with cliffs of Les Vallées-Nantois (Third stop) are very interesting.

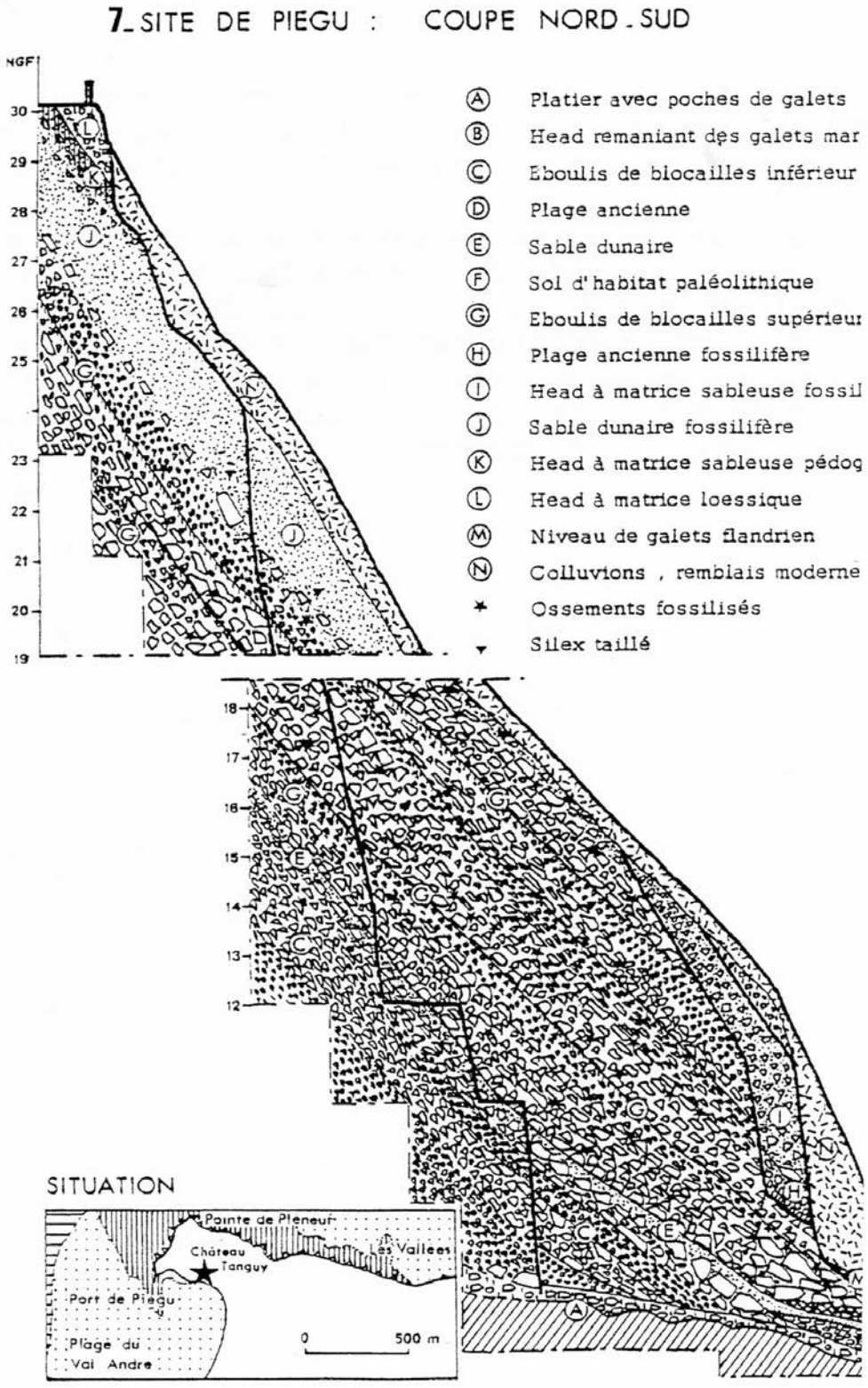

Section from the top:

L : head with loessic matrix;
K : head with a sandy matrix and presence of a "brown soil";
J : dune sand, calcareous;
I : sandy head, fossiliferous;
H : fossiliferous beach;
G : upper screes ; blocks with infiltration of sand from the above dune and containing numerous bones;
F : Neandertalian living floor;
E : dune sand (decalcified but with rare marine shells);
D : fossil beach (pebbles);
C : lower screes;
B : head with marine pebbles;
A : bed-rock.

The Piégu excavation exhibited fossiliferous beds into periglacial and coastal deposits leaned against an old cliff. At least 3 palaeolithic occupations have been found : the first (a small handaxe made from flint) in the layer B ; the second is on the fossil beach (layer F). The third is in the upper screes (layer G).

In layer B, it is only the indication of an old presence of Palaeolithic (Lower Palaeolithic ?) on the oldest marine platform, à the bottom of the cliff. The flint industry from layer F has also been found on the actual beach, after marine erosion. Its main features is a Levalloisian technique. The distinctive Levalloisian facies with numerous Levallois points includes well made side-scrapers. Upper screes (layer G) contains many faunal remains and some flint flakes. It was probably a collapsed butchery station which was at the origin at the top of the cliff. Fauna is represented by Cervus (85 %), the Auroch, Horse, Wolf, Rhinoceros, Roe deer, Wild boar, Megaloceros. Geological correlations and radiometric datations indicate an age about MIS 6 or 7 for the main occupations.

Les Vallées - Nantois

Le Vauclair sections

The large beach of Les Vallées spreads between Pléneuf in the East and an other cape located at the eastern side of the Nantois brook. Two depressions correspond with the mouth of two brooks, the Vauclair brook and the Nantois brook. The loamy formations are caked on the slopes and are mainly developed on both sides of the rocky spur which separate the two brooks. Here the so called "Vauclair section" incorporates observations made on both sides of this brook.

History.

The west Vauclair section is very interesting because it contains mammals remnants (Leclerc and Milon, 1925). The following species have been found:
-Equus caballus (L.)
-Canis vulpes (L.)
It has also been found many teeth of bull or bison, pieces of bones (perhaps of badgers) and above all many remnants of a fossil elephant (*Elephas).*
The stratigraphic position of the fossils indicate a deposition between the lower marine level and the head formations. There is no sorting and grains are almost no eroded; many pieces of shells, more or less eroded, ostracods shells and foraminifera are also found in this outcrop which has been interpreted as a marine and fluviatile deposit (Leclerc and Milon, 1925).
After Giot (1968b) pieces of molar teeth of mammoths also exist at the lower part of the head formations, on top of sandy beach or dune deposits, then considered to be of Riss-Wurm age.

Stratigraphic description:

- Western part of the section :

Layer 1: colluvium (holocene)
Layer 2: residual loess
Layer 3: head with loamy matrix
Layer 4: head with blocks, cryoturbation features
Layer 5: very loamy head, laminated, with scattered blocks
Layer 6: head with big blocks and stones
Layer 7: loamy head, slightly laminated
Layer 8: head with many blocks, gelifluxion mudslide features
Layer 9: laminated loamy sand with stones and gravels
Layer 10: head with big blocks
Layer 11: slightly laminated brown sand
Layer 12: calcareous sand, very crumbly, with terrestrial molluscs

Third stop.

Les Vallées – Nantois

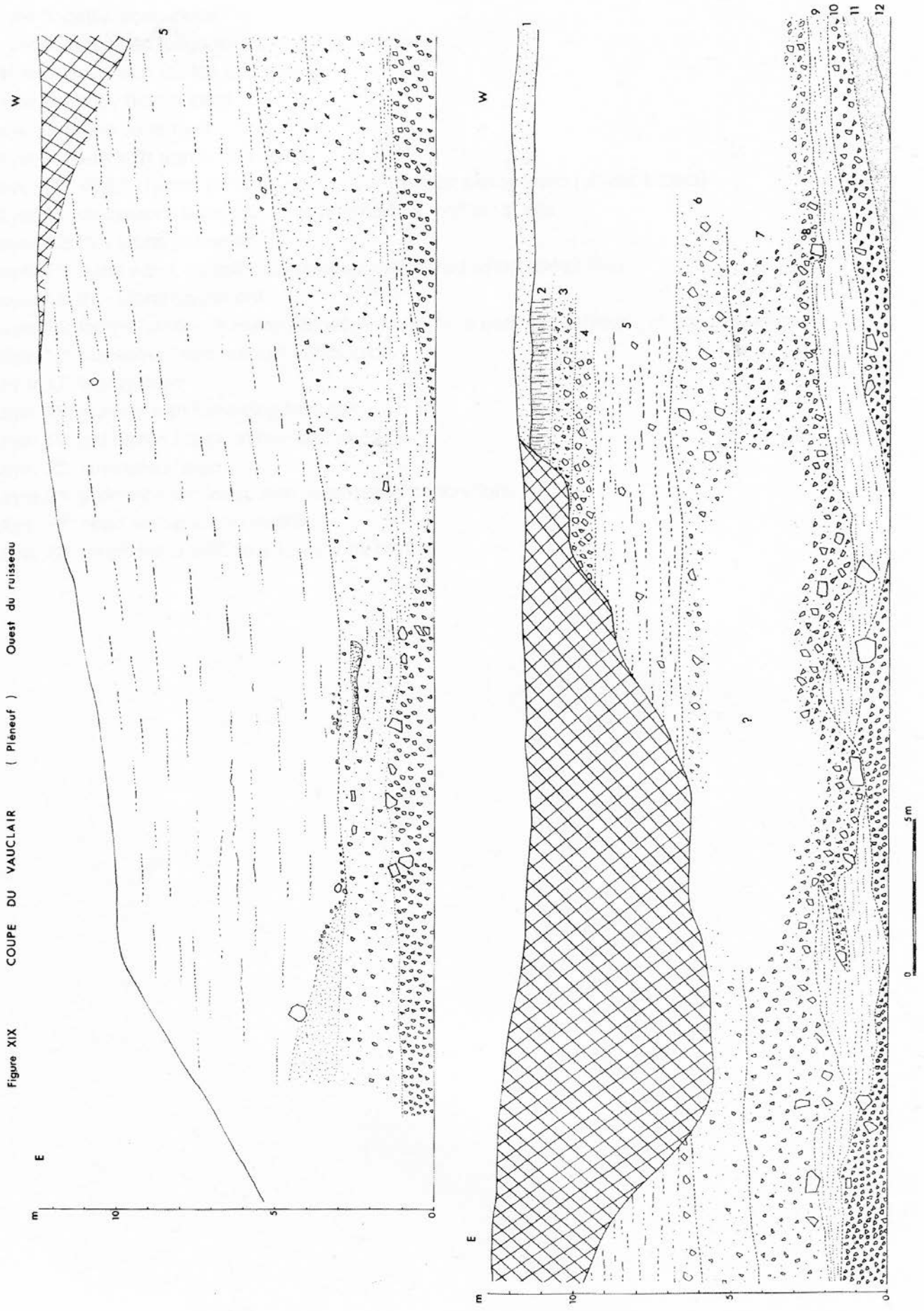

Figure XIX COUPE DU VAUCLAIR (Pléneuf) Ouest du ruisseau

- Eastern part of the section:

Layer 1 : loamy colluvium
Layers 2 & 3: Postglacial soil at the top of the loessic deposits
Layer 4: calcareous loess
Layer 5: laminated loess with gravel fine layers
Layer 6: head with stones and gravels
Layer 7: lumpy brown loam
Layer 8: stone pavement
Layer 9: loam with gravel fine layers
Layer 10: slightly humic horizon, on a decarbonated sandy loam (yellow-brown)
Layer 11: calcareous sandy loam with terrestrial mollusc shells
Layer 12: thin stone pavement
Layer 13: dune sand, partially calcareous, yellow red when decalcified
Layer 14: thin stone pavement
Layer 15: loamy head with many stones, less or more bedded; polyedric structure (paleosoil)
Layer 16: the same head without pedological
Layer 17: loamy head
Layer 18: gravels with furrowing features
Layer 19: old brown loess, micro-laminated
Layer 20: laminated head
Layer 21: yellow-brown loess with carbonated concretions
Layer 22: head with a loamy matrix
Layer 23: rough head with very few loamy matrix

Figure XX

COUPE DU VAUCLAIR (Pléneuf) Est du ruisseau

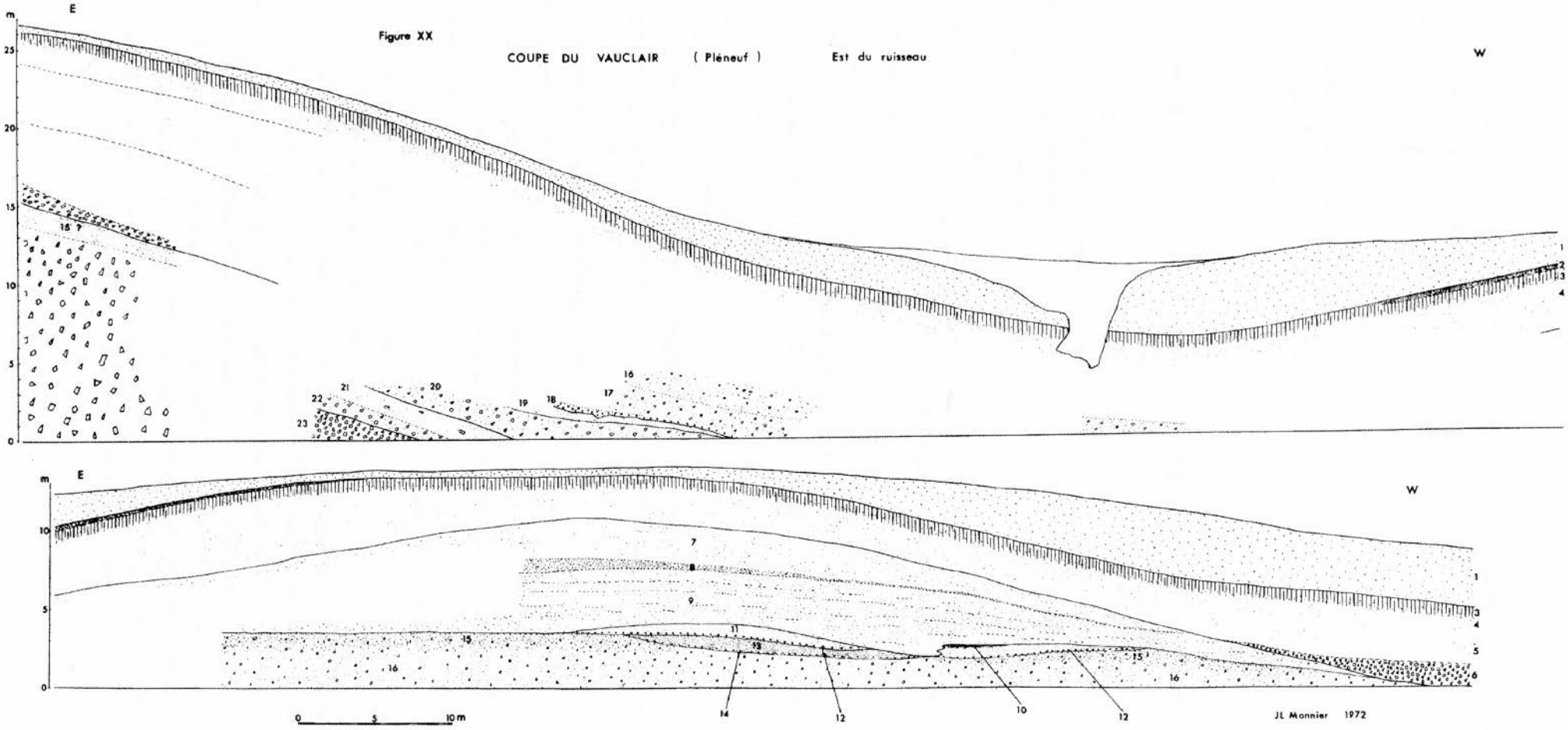

Nantois section

Location.
We are dealing here with a large marine cliff cut in the glacial deposits and located in a long slope oriented to the east-northeast. The valley open to the North.
The section shows a series of ancient and recent loams, which display a step dip.

Layer 1: actual soil
Layer 2: Holocene dune sand
Layers 3 & 4: post-glacial soil (brown illuviated soil)
Layer 5: calcareous loess
Layer 6: a bed of angular gravels
Layer 7: laminated lumpy brown loam, with gravels
Layer 8: bedded yellow-brown loam, laminated (segregation ice, pergelisol features)
Layer 9: stone pavement
Layer 10: laminated loam with gravels, slightly lumpy
Layer 11: slightly laminated loam, lumpy
Layer 12: stone pavement
Layer 13: loam with gravels
Layer 14: gravel bed
Layer 15: lumpy loam
Layer 16: calcareous yellow-brown loam, terrestrial mollusc shells
Layer 17: stone bed
Layer 18: humic horizon (paleosoil)
Layer 19: brown loam, slightly bedded at the base of the layer
Layer 20: sandy loam with reddened-spoiled stones and gravels (colluvium)
Layer 21: red sand (old dune)
Layer 22: loamy stone bed
Layer 23: black clay (marsh mud)
Layer 24: clayey loam, polyedric structure, hydromorphic features at the bottom of the slope under the marsh (greenish gley soil); orange brown at upper positions on the slope (Interglacial illuviated brown soil)
Layer 25: stone bed
Layer 26: clayed loam with bedded stones
Layer 27: loamy head
Layer 28: calcareous loam with stones beds
Layer 29: calcareous yellow-brown loam, slightly laminated (cf. "doublets"); contain very big calcareous concretions (cf. "poupées de loess")
Layer 30: calcareous loam with stones-gravels beds and sandy beds
Layer 31: head with small angular packed stones
Layer 32: sandy loam with angular gravels and stones
Layer 33: rounded and reddened-spoiled packed gravels, clayed-sandy matrix
Layer 34: laminated loamy yellow-brown sand, with angular gravels and stones
Layer 35: calcareous loamy sand with concretions, thinly bedded (broken terrestrial mollusc shells)
Layer 36: head with packed blocks and stones, very few matrix
Layer 37: angular small stones (gelifracts), without matrix (slope fallen rocks)
Layer 38: big blocks and stones with a sandy matrix; some marine pebbles
Layer 39: coarse slope fallen rocks (gelifracts) with very big angular blocks, on contact with the rocky cliff ; presence of some marine pebbles at the base (not actually visible)

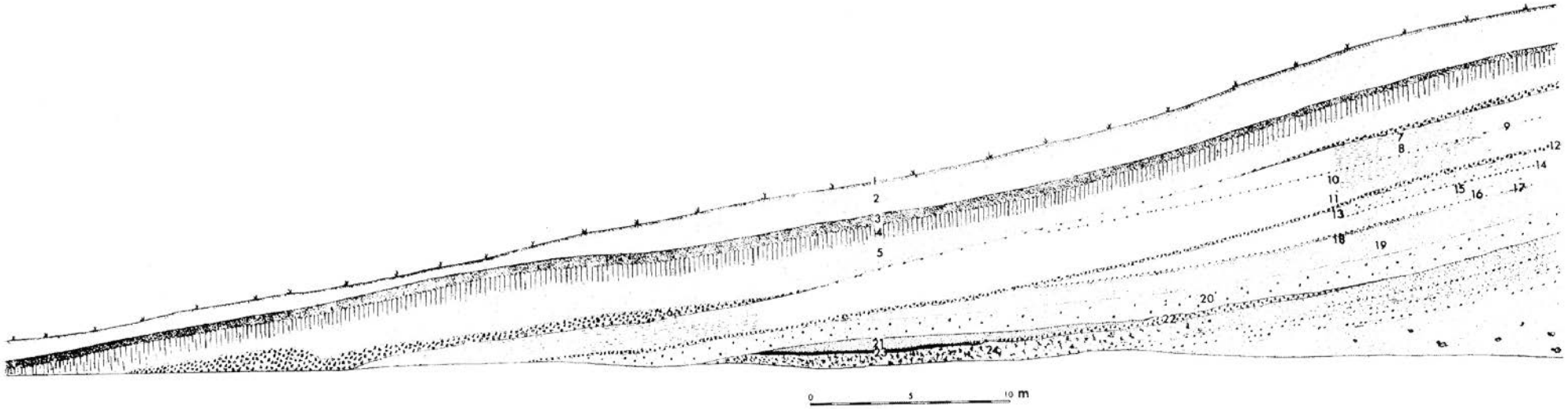
0 5 10 m

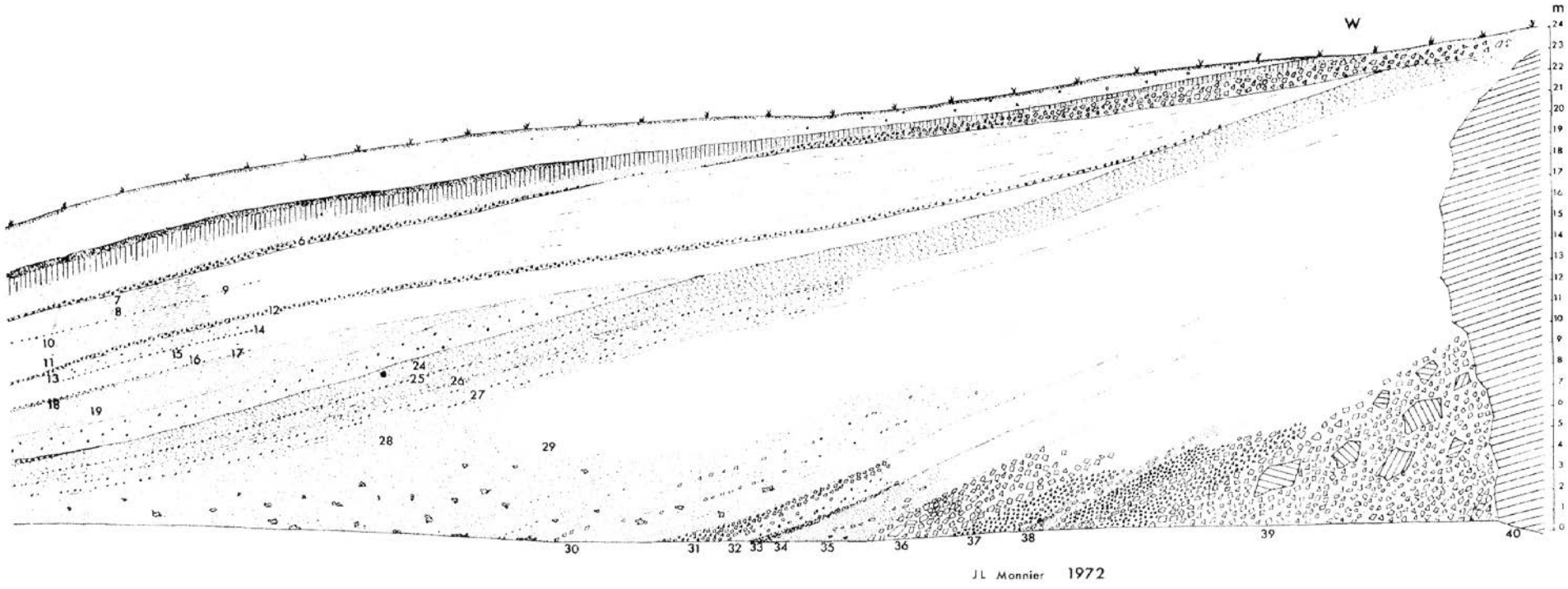
W
m
JL Monnier 1972

From the bottom to the top (that is to say, when one moves from the right to the left) at the foot of the cliff, two main head and loam formations separated by a large pedo-complex can be observed. The lower sequence itself can be separated in two parts:

- in the lower part, blocks of rocks and a head formation reworking the remnants of an old beach (layer 38), incorporating partly carbonated muddy sands (layer 35), can be seen. The loam formation and the overlying head are themselves associated with a pedo-complex (layers 33 and 34).
-on top, well-developed (layers 28 and 29) carbonated loess are covered by a layered loamy head and by the pedo-complex (washed soils) including a dune (layers 21 to 27).
The Upper sequence includes:

-sandy colluviums (layer 20)
-Carbonated sandy loams with continental mollusk fauna, and showing pedogenetic horizons (layers 13 to 19).
-layered loams with head (layers 6 to 12).
-recent loess similar to the Sables-d'or–les-Pins formation but with an incomplete series (layer 5).
-thin sands and reworked loams infilling eroded surfaces cut in washed loess and brownish washed old soils (layer 4)
-humus-rich soils and dune of post-glacial age (layers 1 to 3).

The base of the of the upper sequence (lithostratigraphy, sedimentology and pedology).
The decarbonated old beach (layer 38) is formed by well-sorted thin sands (median=220 microns). And poorly polished (the sampling corresponds with a sol fluxed layer).
The lower pedo-complex (figure 2) developed above head formations and loamy sands rest above a layered calcareous loamy sand, partly decarbonated. This sediment is thin (median=88 microns) and well sorted. It corresponds originally with a marine sediment (relatively large number of smoothed grains) probably reworked by the wind.
The dune formation was stabilized and partly alterated before the sol fluxion stage. The pedo-complex itself developed in the old dune which is more and more polluted by loams towards the top with a concomitant decarbonation.It corresponds with a brownish washed soil characterized by thin clayish layered of brownish-yellowish color illuvions ; Only the lower horizons (B3t to C2) are preserved. This soil is cut by a head formation made of loam and stones affected itself by a small brown soil more or less washed, which displays polyedric structures partly angular with thin clay-humus coating. This second soil pass towards the top to a coarser head with loamy matrix partly humus-rich and gelifluxed reworking the lower horizons; it probably corresponds with an old forest soil poorly transformed.
It exists consequently a climatic succession which was divided in two phases ranging between a temperate to cold temperate climate separated by a short cold period reworking a marine sediment.

The old loess (lithostratigraphy and sedimentology).

They are typical loess (12,5% carbonated) with big loess puppets. The layering is not well established (granulometry shows a part of sand). Sorting is good. Median being 35 microns. From a sedimentological point of view those loess are equivalent to loess of the Upper Pleniglacial.
The mean pedocomplex (lithostratigraphy, sedimentology and pedology) Figure3, levels 1 to 6.

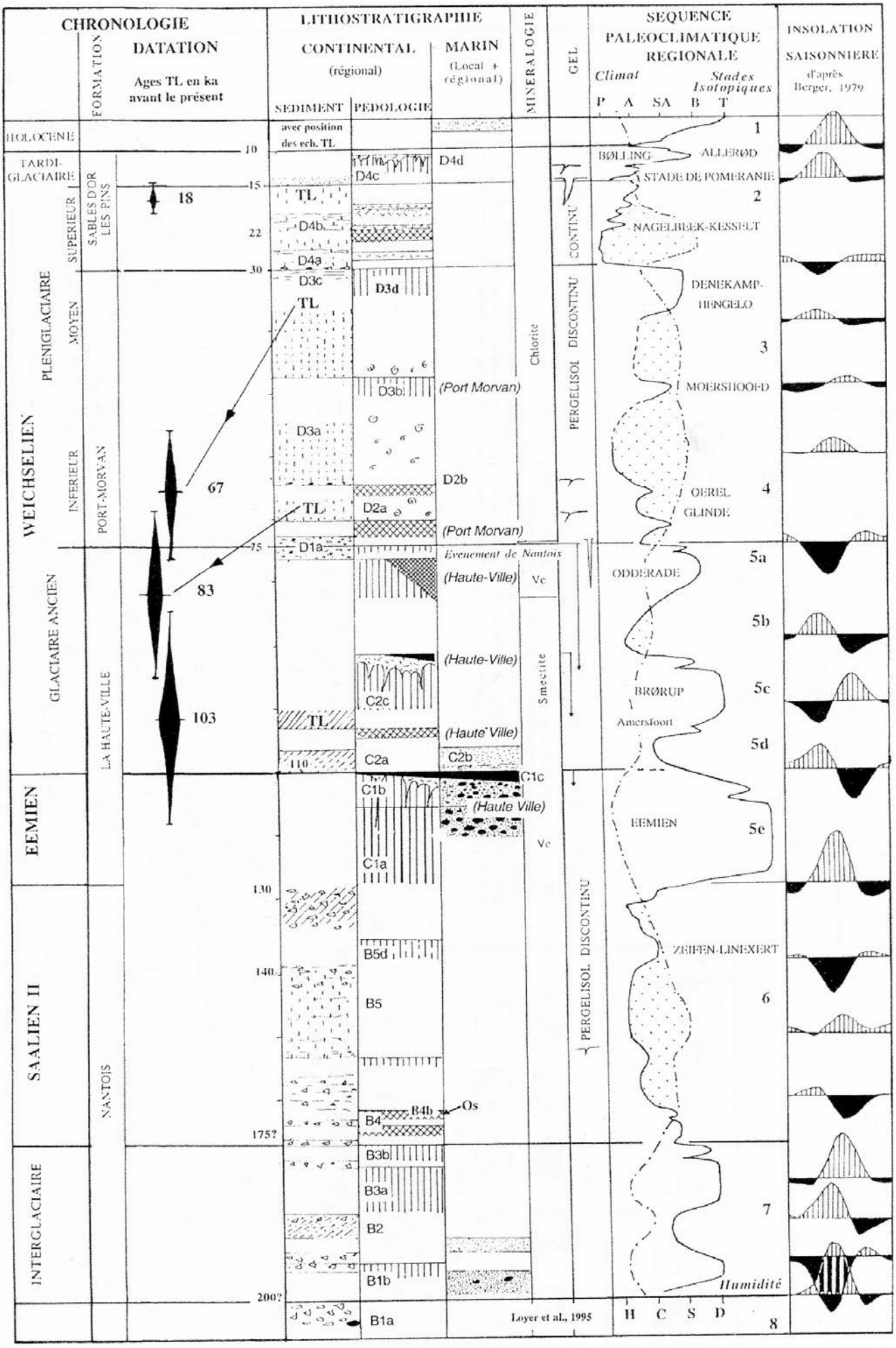

Fig. 2: Synthèse chronostratigraphique et paléoenvironmentale de la coupe de Nantois (légende : voir fig. 3).
Fig. 2: Chronostratigraphy and palaeoenvironmental synthesis of the Nantois section (legend : see fig. 3).

D'après Loyer et al. 1995

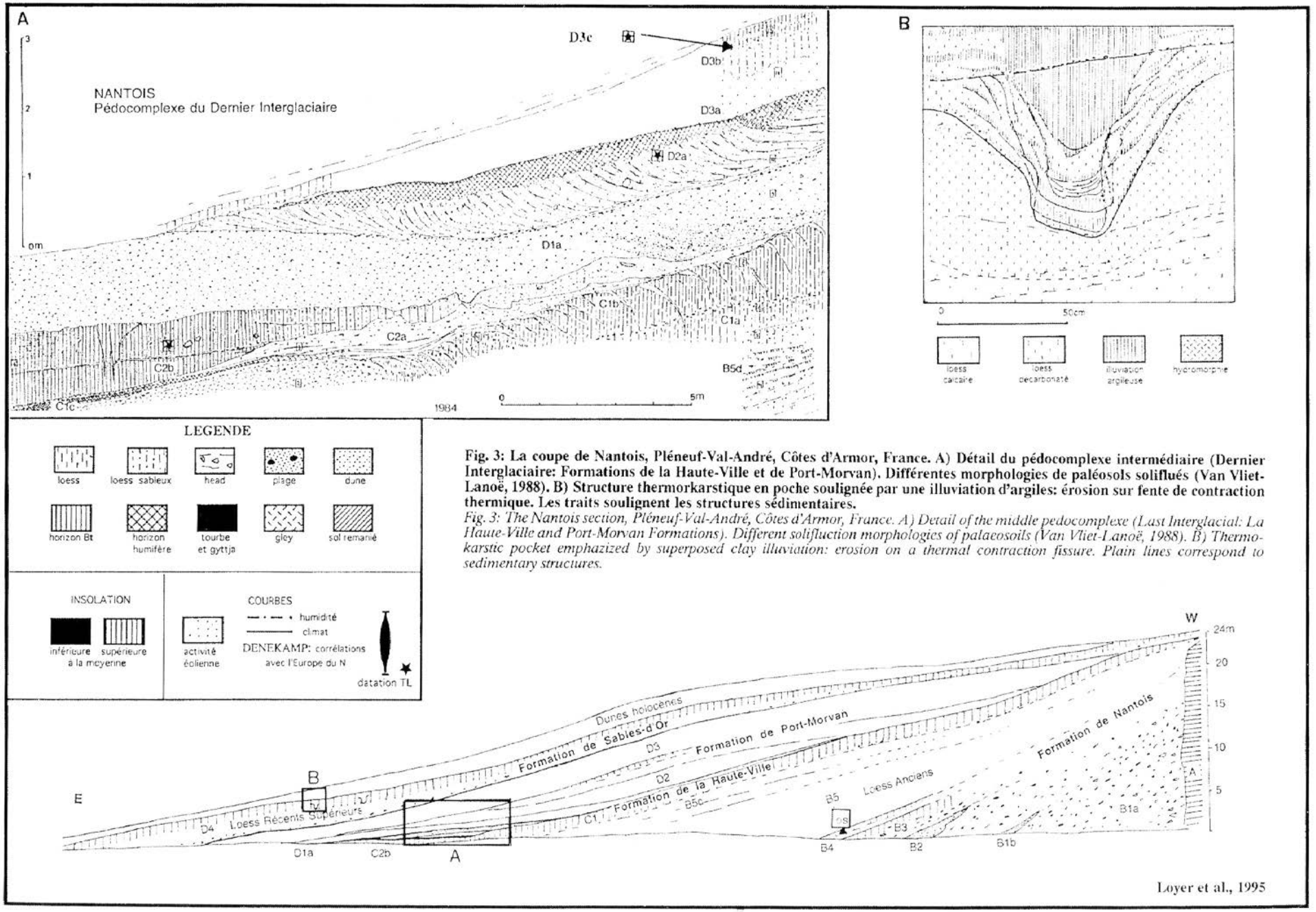

Fig. 3: La coupe de Nantois, Pléneuf-Val-André, Côtes d'Armor, France. A) Détail du pédocomplexe intermédiaire (Dernier Interglaciaire: Formations de la Haute-Ville et de Port-Morvan). Différentes morphologies de paléosols soliflués (Van Vliet-Lanoë, 1988). B) Structure thermorkarstique en poche soulignée par une illuviation d'argiles: érosion sur fente de contraction thermique. Les traits soulignent les structures sédimentaires.

Fig. 3: The Nantois section, Pléneuf-Val-André, Côtes d'Armor, France. A) Detail of the middle pedocomplexe (Last Interglacial: La Haute-Ville and Port-Morvan Formations). Different solifluction morphologies of palaeosoils (Van Vliet-Lanoë, 1988). B) Thermokarstic pocket emphazized by superposed clay illuviation: erosion on a thermal contraction fissure. Plain lines correspond to sedimentary structures.

Loyer et al., 1995

The older pedogenesis was formed over a loamy head deposit reworking the top of an old loess. It corresponds with a brownish-yellowish B3t horizon with polyedric structures well developed with a small hydromorphy at the end observed as isolated spots (figure 3-1) associated with ferruginous deposits.

Always in the same type of sediment a second washed complex developed (figure 3-2). A B3t with a thick coating of iron-poor clay characterizes it at the base. Upwards it is rapidly disturbed by sol fluxion, probably after mixing with marine clay (existence of smectite). A second washed soil looking like a Bt horizon with « glosses » and thin angular polyedrique structures exists. It is compact and well developed (figure 3-3). A strong hydromorphy occurred latter probably at the same time as a marsh developed behind a dune belt (figure 3-4) when the sea level was slightly lower than nowadays. This very complex paleosoil passes on the side and at a lower altitude with a "gley" soil with peat levels (gytja).
The second washed complex of Nantois is disturbed and covered by a thin loamy head but presenting traces of solifluxion incorporating 1% of marine sands (perhaps originating in dunes?) (figure 3-5).

Above all emplaced a marine sand, thick, argillaceous and moderately oxydized. This marine or littoral sand (figure 3-6) is in place. It partly eroded the head and is free of the loamy-stony sediments, which characterize the slope. The soil is very « illuviated » because of its topographic position and its mineralogy (smectite); the presence of goethite could correspond with some drying episode of the climate. As a matter of fact this pedogenesis affects the lower disturbed « glossic » soil showing a clay-humus-rich tendency similar to a forest soil (thin section), which confirms the dry aspect observed in the dune.

The Port Morvan Formation. (figure 3 level 7 and 9) (not seen)

The Port-Morvan section will not be visited itself but it is present in Nantois above the median pedo-complex. But here it is unfortunately not complete. From the bottom to the top we can observe:
-The « Nantois colluvion » originating in mud flows secondary reworked by « cryoreptation » with deep (figure 3-7) ice segregation. At the lowest part some hydromorphy may be seen as well as ice cracks affecting also the lower sand and clay horizon.
-carbonated loamy sands with « bioturbations » and continental mollusk shells (*Trichia hispida,Vallonia pulchella,Vallonia costata,Pupilla muscorum...)* with a small humus-rich horizon on top (arctic meadow with calcareous « mull »), deformed by « cryoreptation » with deep ice segregation (figure 3-8).
-calcareous sandy loams terminated by a Bt horizon coming from a « gelifluxed » calcareous brown soil now strongly decalcified and by a weak argillaceous coating (figure 3-9).
- Sheeted sandy loams and regularly deposited stones very much developed at Nantois because of their position at the lowest part of the slope (figure 1,C.7-12).
We must note the appearance of chlorite in the clay fraction when we reach the sandy loams with shells (layer 20; figure 3-8).

The recent loess (lithostratigraphy and sedimentology).

The loess with sandy beds and the upper homogeneous loess are only present in Nantois (see the Sables-d'or-les-Pins formation). Thin eolian sands locally terminate them. The whole section is eroded by running waters (figure 5) all along the slope.
Recent loess is carbonated (16%). They are typical and very well sorted. Median is 33,5 microns.
The terminating thin sands are decarbonated. They present a typical eolian granulometry. Median range between 50 and 60 microns. The heavy minerals are typical loess (hornblende-epidote-garnet association).
The presence of eolian sands at the end of the loess deposits witnesses the existence of a rising sea level.
The erode gullies correspond with an erosional feature well known during the Postglacial. They are filled by loess and thin sands colluvions. Like in most sites of littoral Brittany the section ends by an Holocene pedogenesis with deep illuvions stripes (which must not be confused with « twinned » loams structures.
Chronostratigraphy.

The lower sequence (carbonated sandy loams, lower pedocomplex, head, older loess) corresponds with the Nantois formation and can be attributed to the Penultimate glaciation (Saalian) and to its median interglacial (-200 000 BP?).
The median pedocomplex (La Haute Ville Formation) corresponds with the Last Interglacial (Eemian s.s.) and at the beginning of the Last Interglacial (Older Weichselan) (125 000 to 75 000).
The Port Morvan Formation corresponds with the Lower and Middle Pleniglacial of the Weichselian.

The recent loess (Sables d'or les Pins *pro pate*) corresponds with the Upper Pleniglacial.

The Uppermost thin sands are probably Tardiglacial.

The Nantois site delivered artifacts of the lithic industry and bones corresponding with different stratigraphic positions.

-A piece of cut flint in layer 38 (beach at the beginning of the saalian deposits)
-A rough tool in layer 27 (top of saalian deposits, lower part of the median pedocomplex)
- Some pieces of flint and tools associated with bison bones found in place under the actual beach and stratigraphically associate with the lower carbonated sandy loams (layers 34 to 35, at the base of the saalian deposits).

Fig. 1. — Profil général de la falaise de Port-Morvan et position de la coupe étudiée.
Fig. 1. — General contour of the cliff of Port-Morvan and localization of the studied section.

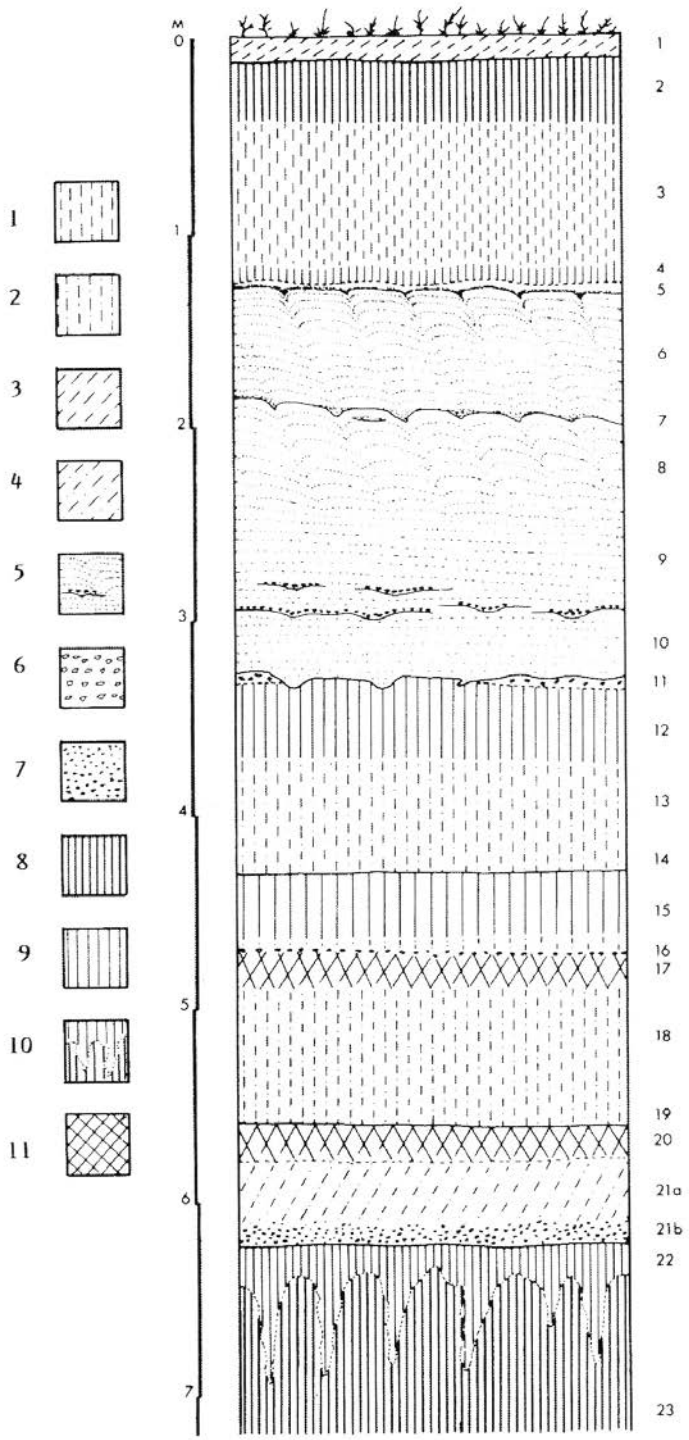

Fig. 2. — Coupe schématique de la partie supérieure de la falaise de Port-Morvan.

1 : loess; 2 : limons sableux carbonatés; 3 : limon soliflué ou colluvié; 4 : limon sableux soliflué ou colluvié; 5 : loess à lits sableux cryoturbés et à lentilles de graviers; 6 : cailloutis; 7 : horizon à graviers et concrétions; 8 : horizon B de sol brun lessivé; 9 : horizon B de sol brun calcique; 10 : horizon glossique; 11 : horizon humifère (sol isohumique). Les numéros à droite du profil correspondent aux couches décrites dans le texte.

Fig. 2. — Schematic section of the upper part of the cliff of Port-Morvan.

1 : loess; 2 : calcareous sandy loams; 3 : soliflucted or colluviated loam; 4 : soliflucted or colluviated sandy loam; 5 : loess with cryoturbated sandy layers and with gravelly pods; 6 : stoneline; 7 : horizon with gravels and concretions; 8 : B horizon of brown leached soil; 9 : B horizon of calcic brown soil; 10 : glossic horizon; 11 : humic horizon (isohumic soil). The numbers at the right of the section refer to the described layers in the text.

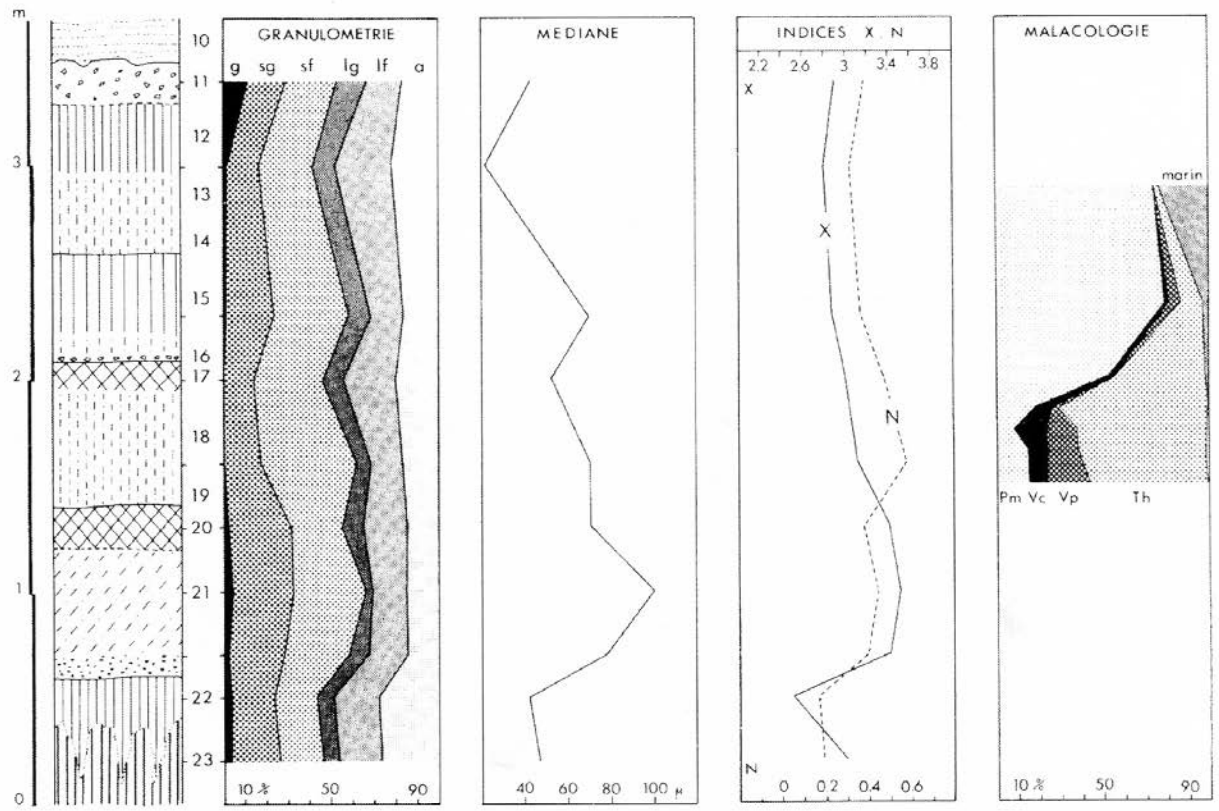

Fig. 3. — Formation de Port-Morvan : diagrammes granulométriques et malacologiques.

Granulométrie globale : g = graviers, sg = sable grossier, sf = sable fin, lg = limon grossier, lf = limon fin, a = argile. Malacologie : Pm = *Pupilla muscorum*, Vc = *Vallonia costata*, Vp = *Vallonia pulchella*, Th = *Trichia hispida*.

Fig. 3. — Formation of Port-Morvan : granulometric and malacologic diagrams.

Global granulometry : g = gravels, sg = coarse sand, sf = fine sand, lg = coarse loam, lf = fine loam, a = clay. Malacology : Pm = Pupilla muscorum, *Vc =* Vallonia costata, *Vp =* Vallonia pulchella, *Th =* Trichia hispida.

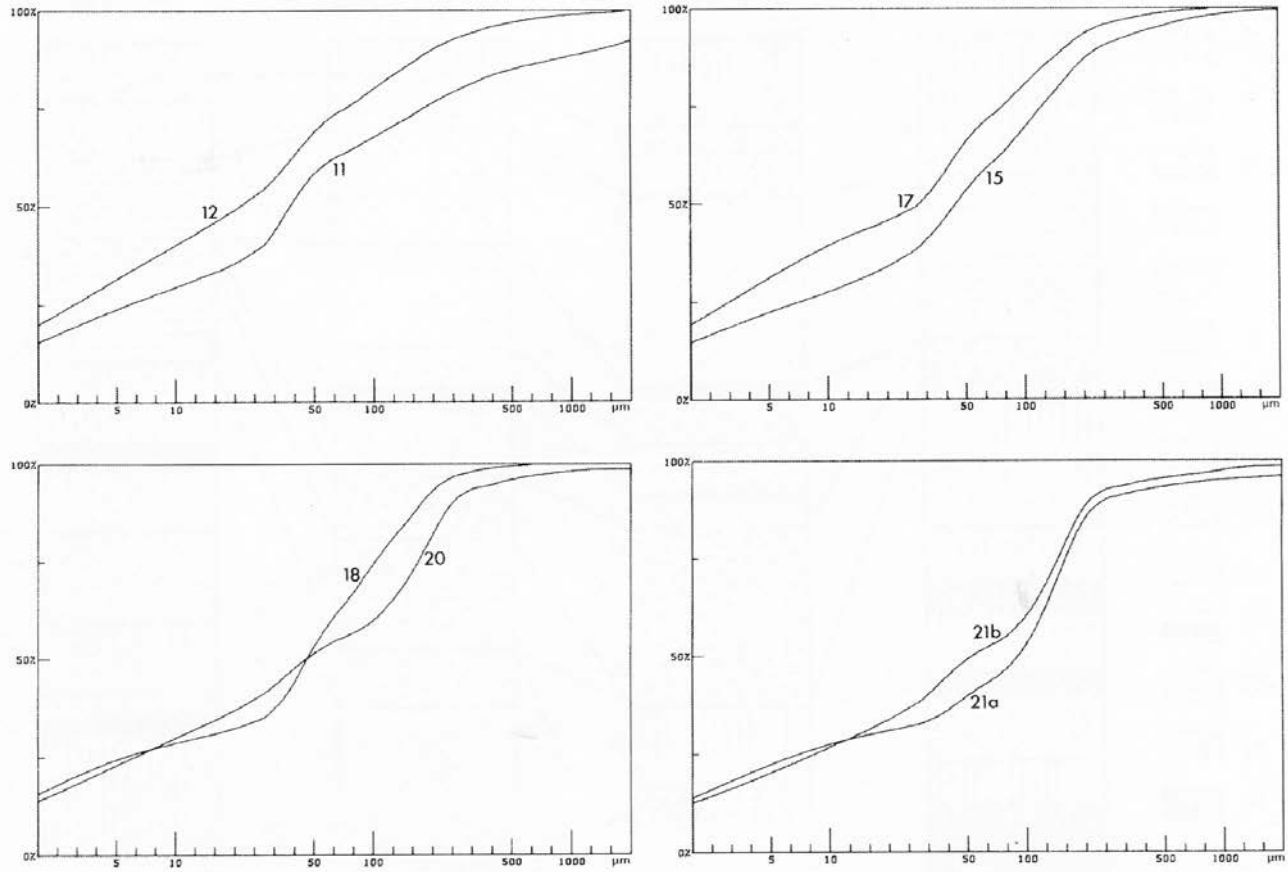

Fig. 4. — Formation de Port-Morvan : courbes granulométriques cumulatives semi-logarithmiques (Pipette d'Andreasen + tamisages). Les numéros renvoient aux couches décrites.

Fig. 4. — Formation of Port-Morvan : semi-logarithmic, cumulative granulometric curves (Pipette of Andreasen + sifting). The numbers refer to the described layers.

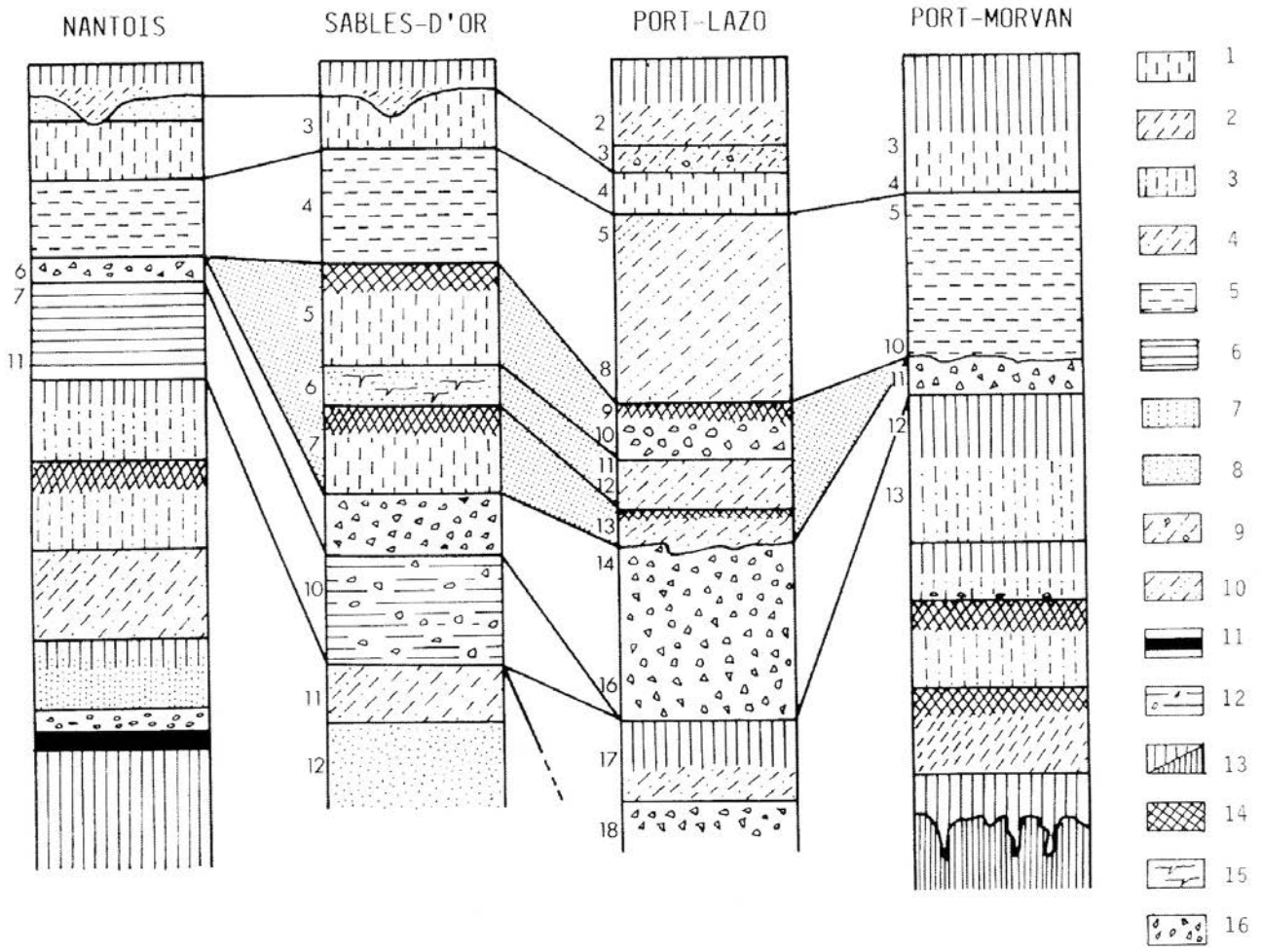

Fig. 5. — Corrélations lithostratigraphiques et pédostratigraphiques entre les coupes de Nantois, Sables-d'Or, Port-Lazo et Port-Morvan. 1 : loess massif; 2 : limon soliflué ou colluvié; 3 : limon sableux; 4 : limon sableux soliflué ou colluvié; 5 : loess lité; 6 : limon feuilleté; 7 : sable de dune oxydé; 8 : sable dunaire; 9 : limon sableux soliflué avec cailloux et graviers; 10 : limon et sables lités soliflués; 11 : dépôt organique de marécage; 12 : limon feuilleté avec lits d'arène et de cailloux; 13 : horizons respectivement peu lessivés et très lessivés; 14 : horizons humifiés; 15 : cryoturbations, fentes de gel; 16 : head.

Fig. 5. — Lithostratigraphic and pedostratigraphic correlations between the sections of Nantois, Sables-d'Or, Port-Lazo and Port-Morvan. *1 : massive loess; 2 : soliflucted or colluviated loam; 3 : sandy loam; 4 : soliflucted or colluviated sandy loam; 5 : bedded loess; 6 : foliated loam; 7 : leached dune sand; 8 : dune sand; 9 : soliflucted sandy loam with pebbles and gravels; 10 : soliflucted interbedded loam and sand; 11 : peaty deposit; 12 : foliated loam with arenaceous beds and pebbles; 13 : respectively little leached and very leached soils; 14 : humic soils; 15 : cryoturbations, frost wedges; 16 : head.*

General références

AUGUSTE P., CLIQUET D., HERVIEU G., LIOUVILLE M., LOUGUET S., MONNIER J.L. & RORIVE S., 2003 – Stratégies de subsistance dans l'Ouest de la France au Pléistocène moyen et supérieur : acquisition et traitement des matières premières d'origines minérale et animale à Piégu (Côtes-d'Armor), Ranville (Calvados) et au Mont-Dol (Ille-et-Vilaine). BAR International Series 1364, 2005, 519-532.

AUGUSTE P., MONCEL M.H., PATOU-MATHIS M., 1998 – Chasse ou "charognage" : acquisition et traitement des rhinocéros au Paléolithique moyen en Europe occidentale. In : Economie préhistorique : les comportements de subsistance au Paléolithique, 13èmes Rencontres Internationales d'Archéologie et d'Histoire d'Antibes, Juan-les-Pins, APDCA, p. 133-151.

BIGOT B., 1986 – Essai de modélisation de l'(apport loessique en Bretagne (France). C.R. Acad. Sc. Paris, t. 303, Série II, n°10, p. 919-921.

BIGOT B. 1987. - Le site Paléolithique moyen de la Pointe de la Heussaye (Erquy, Côtes-du-Nord). Rev. archéol. Ouest, 4, p. 29-33.

BIGOT B. & MONNIER J.L., 1987 - Stratigraphie et sédimentologie des loess récents du nord de la Bretagne. Données nouvelles d'après l'étude des coupes de Sables-d'Or-les-Pins et de Port-Lazo (Côtes-du-Nord, France). Bull. Asso. franç. Et. Quaternaire, 1987, p. 27-36.

CHALINE J. & MONNIER J.L., 1976 - Une faune à lagurus d'âge post-Brörup dans le site moustérien du Mont-Dol (Ille-et-Vilaine). Bull. Asso. franç. Et. Quaternaire, 1976, 47, p. 95-98.

HALLEGOUET B., MONNIER J.L. & GAGNEPAIN J., 1993 - Le site Paléolithique moyen de Piégu en Pléneuf-Val-André. Mém. Soc. Emul. Côtes-d'Armor, t. 121, p. 3-17.

LOYER S., MONNIER J.L., VAN VLIET-LANOE B., HALLEGOUET B. & MERCIER N., 1995 - La coupe de Nantois (Baie de Saint-Brieuc, France): datations par thermoluminescence (TL) et données paléoenvironnementales nouvelles pour le Pléistocène de Bretagne. Quaternaire, 1995, 6, 1, 21-33.

MONNIER J.L., 1973 - Contribution à l'étude des dépôts quaternaires de la région de Saint-Brieuc. Stratigraphie et sédimentologie des limons, des plages et des sols anciens (Thèse troisième cycle). Trav. Labo. Anthropologie, Rennes, 260 p.

MONNIER, J.L., 1980 - Le Paléolithique de la Bretagne dans son cadre géologique. Travaux du Laboratoire d'Anthropologie, Rennes, 1980, 607 p.

MONNIER J.L., 1985 - Données nouvelles sur le gisement paléolithique moyen de Piégu (Pléneuf-Val-André, Côtes-du-Nord). Rev. archéol. Ouest, 1985, 2, 7-21.

MONNIER J.L., 1986 - Le gisement paléolithique moyen de Nantois, Pléneuf (Côtes-du-Nord). Bull. Soc. préhist. française, 1986, 83, 146-150.

MONNIER J.L., 1991 - La préhistoire de Bretagne et d'Armorique. Les Universels Gisserot, Editions Jean-Paul Gisserot, Paris, 121 p.

MONNIER J.L., 1998 - Les premiers groupes humains en Armorique, des origines au cinquième millénaire. In : Giot, Monnier & L'Helgouach, Préhistoire de la Bretagne, Editions Ouest-France, col. Université, 1998, p. 39-87.

MONNIER J.L. & BIGOT B., 1987 - Stratigraphie des dépôts pléistocènes du nord de la Bretagne (France). Les Formations de Port-Morvan et de La Haute-Ville. Bull. Asso. franç. Et. Quaternaire, 1987, p.93-103.

MONNIER J.L., CLIQUET D., HALLEGOUET B., VAN VLIET-LANOE B. & MOLINES N., 1997 - Stratigraphie, paléoenvironnement et occupations humaines durant le dernier interglaciaire dans l'Ouest de la France (Massif Armoricain). Comparaison avec l'interglaciaire précédent. Actes de la table ronde INQUA d'Amiens, in : Le dernier Interglaciaire et les occupations humaines du Paléolithique moyen (Dir. A. Tuffreau & W. Roebroeks), Publications du CERP, Lille, n°8, 2002 : 115-141.

MONNIER J.L., FALGUERES C., LAURENT M., BAHAIN J.J., MORZADEC-KERFOURN M.T. & SIMONET P., 1995 - Analyse des données anciennes et contributions nouvelles à la connaissance et à la datation du gisement moustérien de Mont-Dol (Ille-et-Vilaine). In: Baie du Mont-Saint-Michel et Marais de Dol, milieux naturels et peuplements dans le passé (L. Langouët & M.T. Morzadec-Kerfourn, dir.), Les Dossiers du Centre régional d'Archéologie d'Alet, Saint-Malo, 1995, supplém. R, p.3-26.

MONNIER J.L. & VAN VLIET-LANOE B., 1986 - Les oscillations climatiques entre 125000 ans et le maximum glaciaire d'après l'étude des coupes littorales de la Baie de Saint-Brieuc. Apport de la lithologie, de la pédologie et de la malacologie. Bull. Asso. franç. Et. Quaternaire, 1986, 119-126.

SIMONET, P. & MONNIER, J.L., 1991 - Approche paléo-écologique et taphonomique de la grande faune du gisement moustérien du Mont-Dol (Ille-et-Vilaine, France). Quaternaire, t. 2, p. 5-15.

- DAY THREE -

Scientific excursion to the Quaternary of Normandy

Friday, 26 September 2008

Leaders: Dominique CLIQUET and Jean-Pierre LAUTRIDOU

Route which will be followed between St Lo and St Pierre des Elbeufs. Note the night in Cléon.

NOTICE

The following text is in French but all the necessary explanations will be given in English.
The text and the compilation have been made by Dominique Cliquet, Jean-Pierre Lautridou, Michel Lamothe, Mathieu Leroyer, Nicole Limondin-Lozouet and Norbert Mercier.

LE SITE DE SAINT-PIERRE-LES-ELBEUF: UN GISEMENT DE REFERENCE POUR LA CHRONOLOGIE DU PLEISTOCENE MOYEN ET SUPERIEUR ET POUR SES IMPLANTATIONS ANTHROPIQUES

Présentation du site

Le stratotype de Saint-Pierre-les-Elbeuf se situe a l'est d'Elbeuf, a la confluence de la Seine et d'une petite riviere l'Oison. L'enregistrement stratigraphique correspond aux depots lœssiques du Pleistocene moyen et superieur. L'epaisseur exceptionnelle de lœss ancien s'explique par la presence d'une falaise fossile elevee, associee a la terrasse moyenne dite de 30 m, et qui a protege le limon de l'erosion.

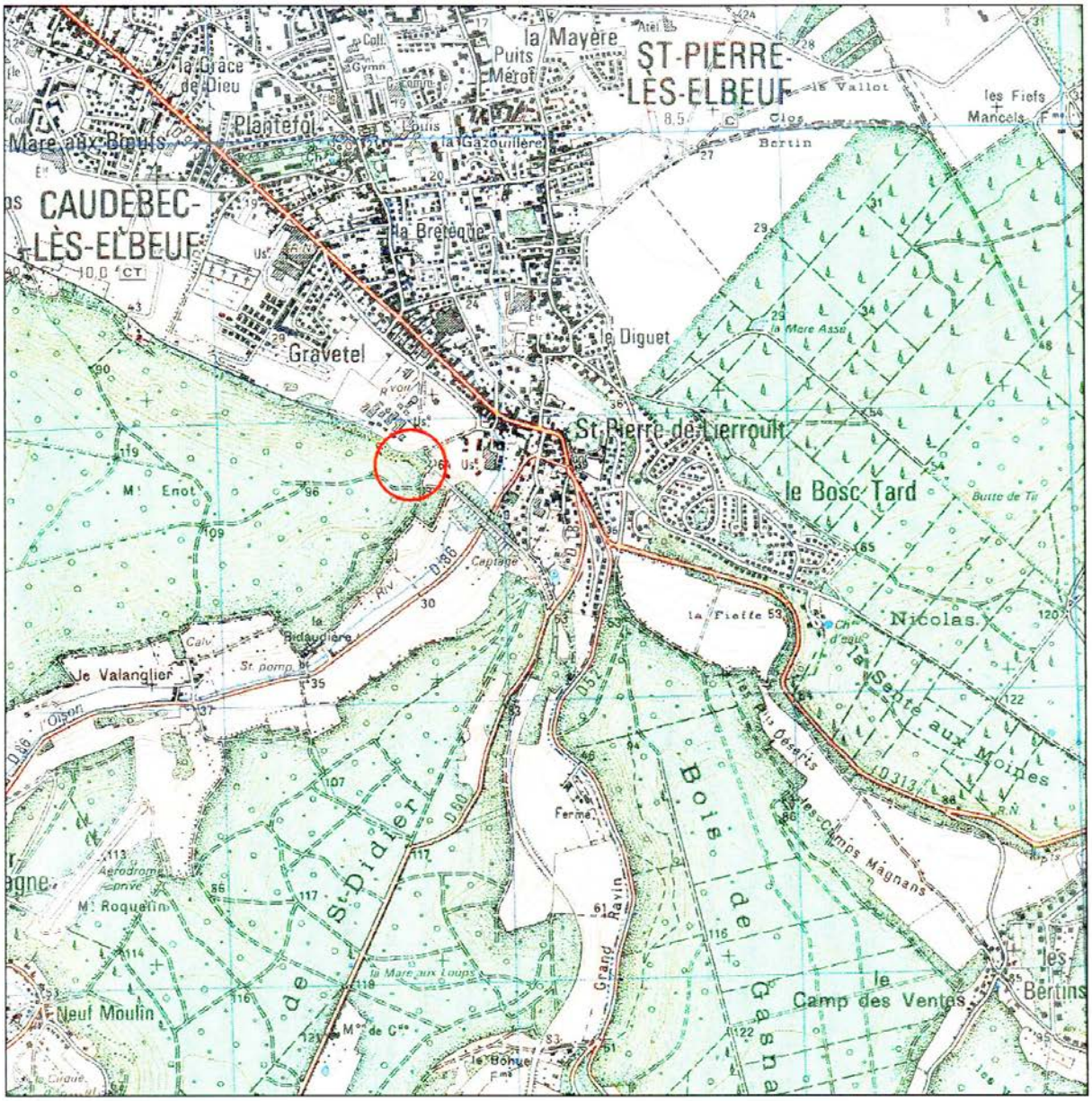

FIG. 1: LOCALISATION DES SITES DE SAINT-PIERRE-LES-ELBEUF

En 2004, d'importants travaux de nettoyage du site classé ont été effectués et ont motivé un ré-examen du site. L'opération a été soutenue par le S.R.A. de Haute-Normandie, Rouen (G. San Juan), la commune de Saint-Pierre-lès-Elbeuf et le projet collectif de recherche "Les premiers hommes en Normandie" (D. Cliquet).

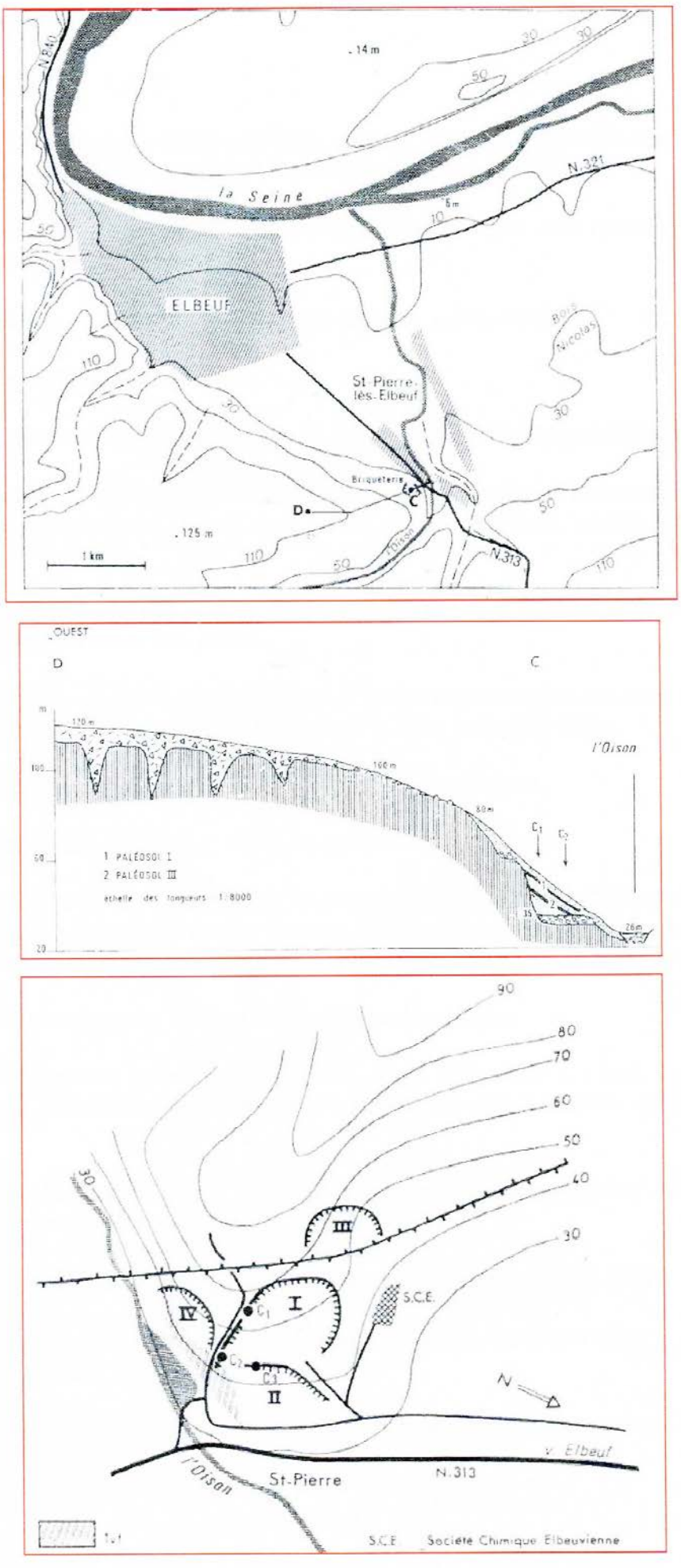

FIG. 2. SAINT-PIERRE-LES-ELBEUF: CROQUIS DE LOCALISATION ET PROFIL DU VERSANT

I - Données stratigraphiques

1 - les coupes 1 et 1 bis (fig. 3 et 4)

La coupe 1 - 2004 est immediatement a cote de la coupe 1 levee en 1969-1970 (fig. 1, 3 et 4). Il manque le sol brun lessive de surface visible en 1970 et observe dans la coupe iv (fig. 1).

1 – 0-90 cm: lœss calcaire jaunâtre, pseudo-mycelium, petites concrétions calcaires, rares points noirs ferro-manganiques.

2 – 90-250: lœss calcaire de couleur plus ocre, plus argileux, moins calcaire.

3 – 250-290: limon gris-brun, sol humifere.

4 – 290-330: cailloutis de petits silex gelifractes (1 a 2 cm) dans un limon gris clair (sol gris forestier).

5 – 330-450: horizon bt de sol brun lessive, structure polyedrique fine et prismatique, revetements argileux, enduits noirs ferro-manganiques (parois des fentes de dessiccation), couleur brun-rouge (7,5 yr 5/8) ***Paleosol Elbeuf I***

6 – 450-520: limon brun-jaune (10 yr 5/8), lite, a lits gris et bruns (0,3 à 2 cm), disloques, a contacts nets entre les lits, structure plus floue vers le bas.

7 – 520-560: limon a gros doublets ondules marron et gris, a contact moins net entre les lits (limon a doublets normand) qu'en 6, epaisseur des bandes de 1 a 5 cm; a la base, cailloutis diffus.

8 – 560-572: bande de limon gris jaunatre, a filaments obliques marron.

9 – 572: ligne de petits silex (1 a 5 cm): cailloutis mince.

10 - 572-690: horizon bt de sol brun lessive identique a celui situe entre 330 et 450 cm (elbeuf i), moins fendille et avec peu d'enduits noirs sur les fissures, structure polyedrique moyenne, revetements argileux, quelques concretions noires ferro- manganiques, couleur brun-rouge (7,5 yr 5/8) ***Paleosol Elbeuf II***

11 – 690-735: limon brun-marron, horizon b/c du paleosol sus jacent.

12 – 735-810: limon sableux brunatre (10 yr 6/6), litage diffus (0,2 a 1 cm), brun et gris, presence de quelques petits silex, points noirs quelques lits gris diffus sont casses comme entre 450 et 520 cm mais en moins net.

13 – 810-848: limon brunatre a points noirs, homogene puis a trainees grises diffuses de 835 a 848 cm, presence de quelques petits silex.

14 – 848-890: limon un peu plus argileux, légèrement plus brun (10 yr 5/8).

15 – 890-930: limon brun-gris a litage flou tres irregulier, lits de 1 a 2 mm bruns et grisatres, fines tubulures noires ferro-manganiques.

16 – 930-990: cailloutis de petits silex disperses dans un limon brun tirant sur le gris.

17 – 990-1020: limon brun, legerement fonce, assez argileux.

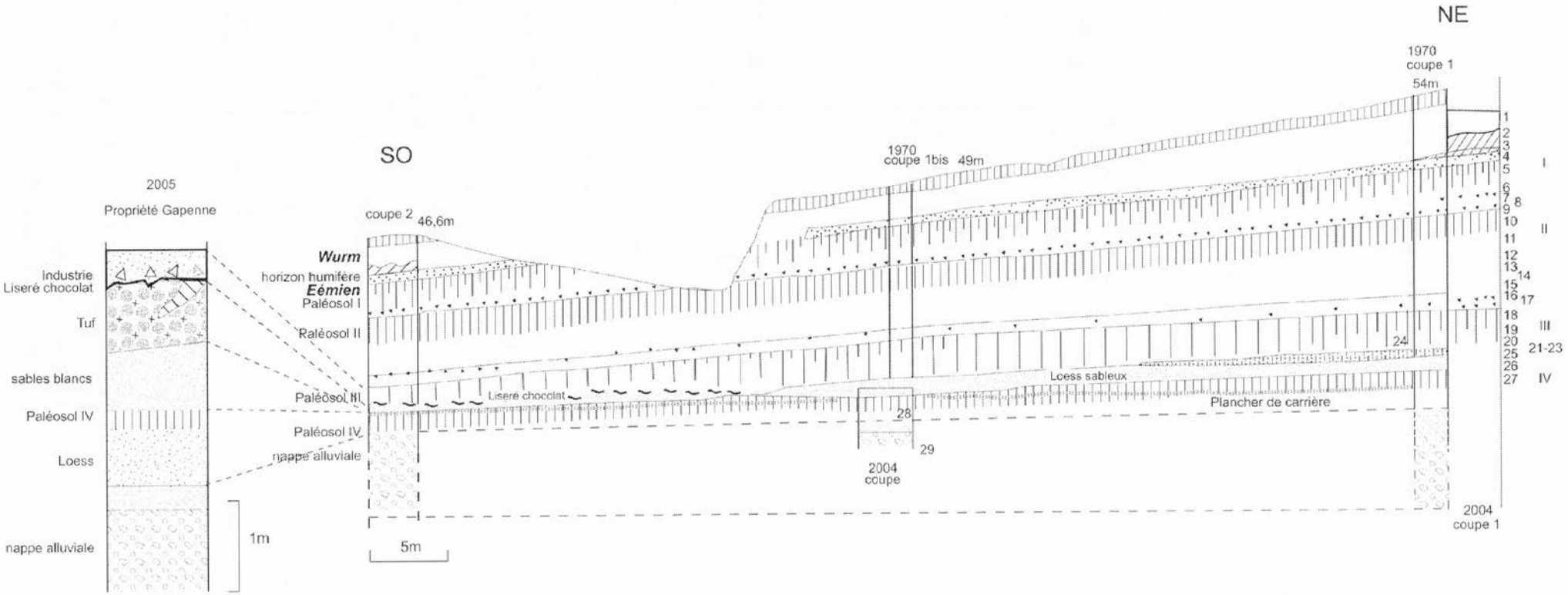

Fig. 3 - Site classique. Profil de la paroi lœssique des coupes 1 à 2 et coupe de la « propriété Gapenne/Michel».

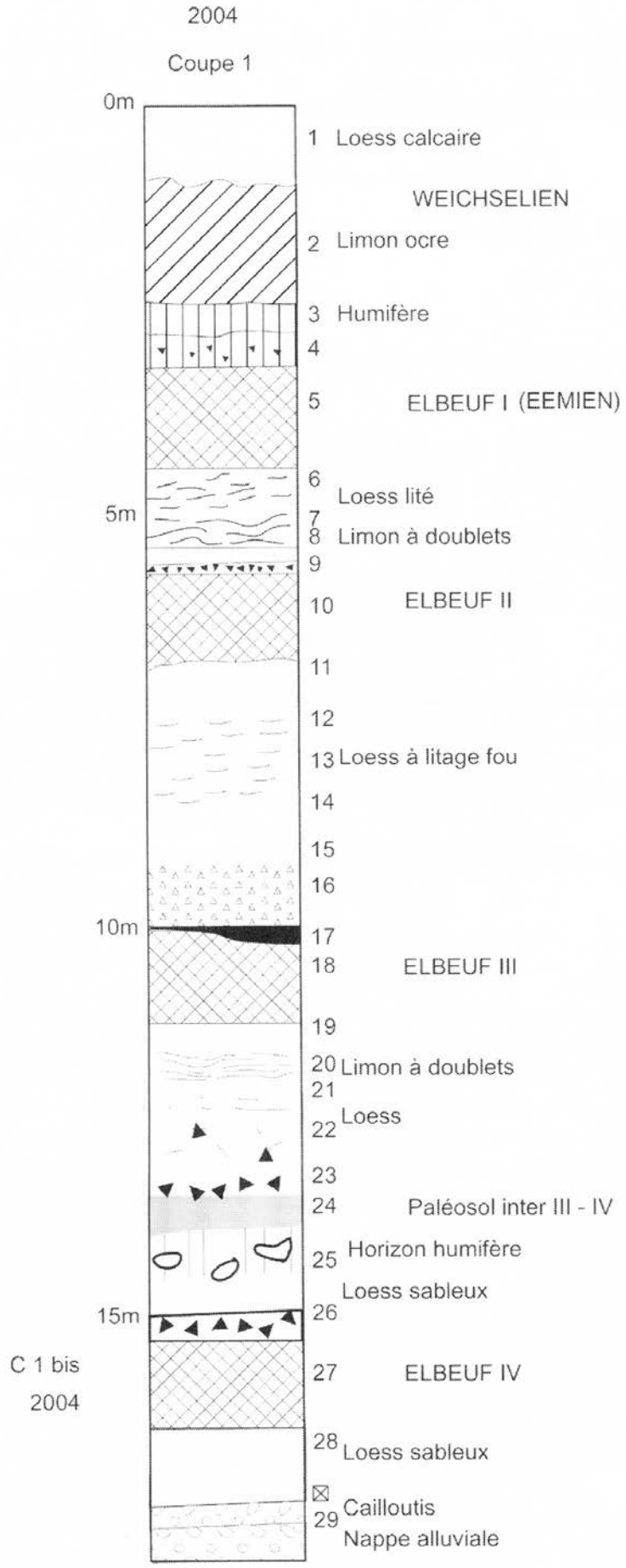

Figure 4 - Coupe 1 complétée par la coupe 1 bis.

18 – 1020-1120: horizon Bt de sol brun lessivé, brun-rouge (7,5 YR 5/8), fendillé, à revêtements argileux, à enduits noirs peu nombreux (fissures) ***Paléosol Elbeuf III***

19 – 1120-1160: limon brun (10 YR 5/8), quelques revêtements argileux, horizon B/C du Paléosol Elbeuf III.

20 - 1160-1200 : limon brun, à fin litage (0,3 à 1 cm), à nombreux points noirs.

21 - 1200-1240 : limon brun à taches grises diffuses.

22 - 1240-1340 : limon brun-jaune, à points noirs, à petits silex dispersés.

23 - 1340 : cailloutis de petits silex.

24 - 1340-1390 : limon brun, assez argileux, formant un horizon plus sombre, bien distinct, visible aussi en coupe 1 bis.

25 - 1390-1490 : limon brun clair (10 YR 5/8), paléosol à terriers de crotovines, à points noirs, devenant grisâtre vers le bas et plus sableux, légèrement humifère.

26 - 1490-1520 : limon grisâtre à taches gris clair, sableux, à nombreux petits silex (cailloutis).

Le prolongement vers le bas n'a pas pu être étudié dans la suite de la coupe 1, comme en 1970, mais a été levé dans la coupe 1 bis.

27 - 1520-1620 : horizon Bt de sol brun lessivé, limon argileux, brun-rouge (entre 5 YR et 7,5 YR 5/8), à structure polyédrique et à revêtements argileux ***Paléosol Elbeuf IV***

28 - 1620-1720 : limon sableux vers le bas, brun-jaune (10 YR 5/8), à points noirs.

29 - 1720-1800 : sommet de la terrasse alluviale, sables, graviers et galets de silex émoussés, gélifractés entre 1720 et 1750 cm, non pédogénéisés.

Conclusion

Sur la nappe alluviale d'Elbeuf (n° 29) retouchée au sommet (silex gélifractés), épaisse selon les sondages, de cinq mètres, on observe cinq lœss séparés par des horizons Bt de sols bruns lessivés, peu différents de celui du sol de surface, manquant dans la coupe 1 - 2004, dénommés : Elbeuf I, II, III et IV et de type interglaciaire. Le complexe de lœss sommital (nos 1 à 4) a été décrit en plus dilaté dans la coupe IV située dans l'enceinte de la société IFRACHEM ex WITCO (Lautridou, 1974). C'est la séquence séquanienne comportant de bas en haut, au-dessus du paléosol interglaciaire Elbeuf I (n°5), un cailloutis de petits silex gélifractés (4), deux paléosols humifères (3) gris-noir (sol gris forestier, sol isohumique), un limon assez argileux, brun orangé (2) légèrement carbonaté et un lœss calcaire gris-jaune (1). Cette séquence séquanienne différente de la séquence normande (Epouville) est donc définie (Lautridou, 1985) par : un cailloutis de base, Début Weichsélien, un complexe de sols noirs, très souvent érodés et constituant un marqueur dans le Bassin parisien (Antoine *et al.,* 1998) du Weichsélien ancien, un limon brunifié attribué au complexe de Saint-Acheul (Cliquet et Lautridou, 2005) c'est-à-dire au Pléniglaciaire moyen et le lœss récent supérieur (1) post horizon de Nagelbeek. Comme très souvent en Normandie, il manque le lœss récent inférieur (22 à 35 Ka).

Les lœss deviennent de moins en moins épais et les paléosols I à IV sont plus tronqués surtout Elbeuf III et Elbeuf IV très résiduels en coupe 2.

Le fait nouveau est la présence de sables limoneux gris-blanc comportant quelques gravillons anguleux ou sub-émoussés de silex. Fins (médiane 0,06 mm), à courbe granulométrique cumulative parabolique (Lautridou, 1985), à grains quartzeux essentiellement (80 %), sub-émoussés mats, ils ont été interprétés comme des sables fluviatiles d'une petite rivière, l'Oison, qui vient confluer avec la Seine (fig. 2).

Dans la coupe 2, quelques granules calcaires sont repérables. Ils jalonnent l'extrémité ouest du tuf calcaire, cartographié par Chédeville (fig. 2), qui contient la célèbre faune malacologique. Juste au-dessus, un limon argileux de couleur marron foncé, à faces de glissement (slickensides), appelé "liseré chocolat", de 1 à 5 cm d'épaisseur, est interprété comme un horizon B bêta ; les argiles d'illuviation liées à la pédogenèse lessivante d'Elbeuf III, immédiatement au-dessus, se bloquent sur un horizon carbonaté dont il ne subsiste ici que quelques traces. Le tuf a été observé dans une fosse, à 10 mètres de la coupe 2, mais son épaisseur limitée, 5 cm, nous a amené à l'étudier dans la propriété Gapenne/Michel (ancienne carrière IV, fig. 2), où son épaisseur peut atteindre un mètre. Après les prélèvements de J.-J. Puisségur (Lautridou et al., 1974), une fosse a été creusée en 2004 avec P. Antoine et N. Limondin, puis un chantier archéologique a été ouvert en 2005 sous la direction de D. Cliquet. On retrouve exactement la même stratigraphie qu'en coupe 2 sauf que le tuf y est épais de 0,1 à 1 mètre. Le sommet du tuf est affecté de petites dépressions qui évoquent des marmites formées par des tourbillons de l'Oison (fig. 6). Cette caractéristique, ainsi que la forme allongée du dépôt, font plus penser à un tuf de bras de rivière qu'à celui d'une mare alimentée par des sources (hypothèse de J.-J. Puisségur, voir infra). Le paléosol Elbeuf III ; très tronqué, a affecté le lœss sus-jacent au tuf 5 (couches 19 à 22 de la coupe 1) et comme dans la coupe 2 du site classé, l'illuviation s'est bloquée sur le tuf calcaire (liseré chocolat).
L'industrie préhistorique se situe au-dessus du liseré chocolat dans le lœss postérieurement affecté par la pédogenèse Elbeuf III (fig. 2).

Bibliographie

ANTOINE P., LAUTRIDOU J.-P., SOMMé J., AUGUSTE P., AUFFRET J.-P., BAIZE S.,CLET-PELLERIN M., COUTARD J.-P., DEWOLF Y., DUGUé O., JOLY F., LAIGNIEL B., LAURENT M., LAVOLLé M., LEBRET P., LéCOLLE F., LEFEBVRE D., LIMONDIN-LOZOUET N., MUNAUT A. V., Ozouf J.-C., QUESNEL F. et ROUSSEAU D.-D., 1998 - Les formations quaternaires de la France du Nord-Ouest. Quaternaire, 9, (3), 227-241.

CLIQUET D. et LAUTRIDOU J.-P., 2005 - Chronostratigraphie des formations du Pléistocène moyen et supérieur et sites associés en Normandie. In Molines N., Moncel M.-H., Monnier J.-L. (dir.), Les premiers peuplements en Europe. (Actes du colloque international de Rennes, 2003), Oxford, Hadrian Books (BAR International Series ; 1364), 53-62.

LAUTRIDOU J.-P., 1974 - La séquence loessique séquanienne du Wurm à Saint-Pierre-lès-Elbeuf. Bulletin de l'Association Française pour l'étude du Quaternaire, 3-4, 242-243.

LAUTRIDOU J.-P., 1985 - Le cycle périglaciaire pléistocène en Europe du Nord-Ouest et plus particulièrement en Normandie. Thèse, Centre de Géomorphologie du CNRS éd., 907 p.

LAUTRIDOU J.-P., MARTIN P. et PUISSéGUR J.-J., 1974 - Lœss, heads, nappes alluviales et niveaux marins dans la Basse-Seine ; essais de corrélation entre les coupes de Saint-Romain, de Tancarville, de Cléon et de Saint-Pierre-lès-Elbeuf. Bulletin de la Société géologique de Normandie, 3-4, 208-211.

LAUTRIDOU J.P., MASSON M., PAEPE R., PUISSEGUR J.J., VERRON G., 1974. Lœss, nappes alluviales et tuf de Saint-Pierre-lès-Elbeuf, près de Rouen ; les terrasses de la Seine de Muids à Caudebec. Bulletin de l'Association française pour l'Etude du Quaternaire, 40-41 (3-4), 193-201.

LAUTRIDOU J.-P. et PUISSéGUR J.-J., 1977 - Données nouvelles sur les microfaunes malacologiques et sur les rongeurs du Pléistocène continental de la Basse-Seine. Bulletin de la Société géologique de Normandie, tome LXIV, fasc. 4, 119-128.

LAUTRIDOU J.-P. et VERRON G., 1970 - Paléosols et lœss de Saint-Pierre-lès-Elbeuf. Bulletin de l'Association Française pour l'étude du Quaternaire, 2, 145-165.